The effect of observation errors on parameter estimates applied to seismic hazard and insurance risk modelling

by

Samantha Pretorius

Submitted in partial fulfilment of the requirements for the degree MSc Actuarial Science

in the Faculty of Natural and Agricultural Sciences

University of Pretoria

Pretoria

30 April 2014

Abstract

The research attempts to resolve which method of estimation is the most consistent for the parameters of the earthquake model, and how these different methods of estimation, as well as other changes, in the earthquake model parameters affect the damage estimates for a specific area. The research also investigates different methods of parameter estimation in the context of the log-linear relationship characterised by the Gutenberg-Richter relation. Traditional methods are compared to those methods that take uncertainty in the underlying data into account. Alternative methods based on Bayesian statistics are investigated briefly. The efficiency of the feasible methods is investigated by comparing the results for a large number of synthetic earthquake catalogues for which the parameters are known and errors have been incorporated into each observation. In the second part of the study, the effects of changes in key parameters of the earthquake model on damage estimates are investigated. This includes an investigation of the different methods of estimation and their effect on the damage estimates. It is found that parameter estimates are affected by observation errors. If errors are not included in the method of estimation, the estimate is subject to bias. The nature of the errors determines the level of bias. It is concluded that uncertainty in the data used in earthquake parameter estimates is largely a function of the quality of the data that is available. The inaccuracy of parameter estimates depends on the nature of the errors that are present in the data. In turn, the nature of the errors in an earthquake catalogue depends on the method of compilation of the catalogue and can vary from being negligible, for single source catalogues for an area with a sophisticated seismograph network, to fairly impactful, for historical earthquake catalogues that predate seismograph networks. Probabilistic seismic risk assessment is used as a catastrophe modelling tool to circumvent the problem of scarce loss data in areas of low seismicity and is applied in this study for the greater Cape Town region in South Africa. The results of the risk assessment demonstrate that seemingly small changes in underlying earthquake parameters as a result of the incorporation of errors can lead to significant changes in loss estimates for buildings in an area of low seismicity.

Keywords

Catastrophe modelling, parameter estimates, earthquake risk, Gutenberg-Richter, probabilistic seismic risk assessment, Cape Town, South Africa, property insurance, errors, uncertainties

Acknowledgements

I would like to thank Professor Andrzej Kijko and Dr Conrad Beyers for their support in this research; my husband, Roland, for his continued patience, encouragement and support; and my family for their encouragement and support.

Declaration

I, Samantha Pretorius, declare that the dissertation, which I hereby submit for the degree MSc Actuarial Science at the University of Pretoria, is my own work and has not previously been submitted by me for a degree at this or any other institution.

Signature: _____

Date: _____

Contents

List of Figures

List of Tables

1 Introduction

1.1 Background

Increasing global urbanisation means that the potential impact of a catastrophic event, such as an earthquake, is increasing. To this end, insurers are taking a more comprehensive view of managing and understanding risk. This means that catastrophe models are becoming more sophisticated and the importance of accurate input data is becoming increasingly important (Grossi and Zoback, 2009). As an example, Figure 1.1 depicts the effects of a recent seismic event in Christchurch, New Zealand; the estimated insurance claims triggered by the event were in excess of US$ 12 billion (Booker, 2012).

This event was by far one of the most costly for insurers in the past decade, (Booker, 2012). Concerns arise when we consider that the same kinds of losses can occur due to similar seismic events in the near future. By increasing the accuracy of the input parameters for earthquake recurrence, it is possible that ultimate insurance loss forecasts will be more accurate and more prudent. More accurate and prudent earthquake damage forecasts will help to minimise the financial and social impact of earthquake, by assisting insurers in the risk management process.

Figure 1.1: The effects of the 7.1 magnitude earthquake in Christchurch, New Zealand in 2011 as well as the subsequent aftershock of magnitude 6.7 (news.com.au)

To draw some conclusions about events that may happen in the future, real-life phenomena are observed in order to collect data and to ascertain what is already known about these events. This data is then used to draw some inference from the behaviour of the past events to that of possible future events.

These observations are not always perfect, and usually contain some form of error. Observation errors impact a wide range of problems. This includes categories as diverse as biological sciences (population estimation models), seismology (earthquake prediction models) and finance (equity pricing models). Any field in which estimates or predictions are made based on observations is subject to distortion of the results if some observational error exists. Since any data that is observed by individuals is likely to contain some form of subjectivity, observation errors are present in most types of data.

The level of accuracy required when implementing models varies depending on the context in which the results will be used. However, increased accuracy clearly implies better results which will lead to better decision-making. In particular, accuracy in predicting seismic activity is of very high importance when dealing with highly populated areas or modern critical structures like nuclear power plants.

Seismic activity in South Africa is of particular concern when it comes to the accuracy of forecasting damage caused by seismic events. The area is characterised by few damage-inducing seismic events which means that the data used for forecasting is scarce. It is worrying, when it is considered that the only natural seismicity of damage causing intensity has taken place in an area that contains the only nuclear power station in the country. Further concerns arise when considering that the deepest underground mining activity in the world takes place within several hundred kilometres of the financial hub of Southern Africa. Induced seismicity, particularly if caused by underground mining activity, alters the seismicity of a particular area. Therefore a clearer view of the seismic activity and possible losses connected thereto in the area needs to be established.

1.2 Research problem

Uncertainty in data leads to inaccurate parameter estimates for the models which describe the data. The effect of these inaccuracies in the context of the extent of estimated damage suffered by buildings due to earthquakes in areas of low seismic activity is largely unknown. Earthquake magnitude data for those earthquakes that cause notable damage is scarce and

several methods of estimation are used for the parameters involved in earthquake models. The research endeavours to answer how uncertainty in earthquake magnitude data affect parameter estimates in models that estimate damage in an area of low seismic activity such as the greater Cape Town area in South Africa.

1.3 Research objectives

The research attempts to resolve the problem in two parts, namely, which method of estimation is the most consistent for the parameters of the earthquake model, and how these different methods of estimation, as well as other changes, in the earthquake model parameters affect the damage estimates for a specific area.

The research investigates different methods of parameter estimation in the context of the log-linear relationship characterised by the Gutenberg-Richter relation. Traditional methods are compared to those methods that take uncertainty in the underlying data into account. Alternatives based on Bayesian statistics are also investigated briefly. The efficiency of the feasible methods is investigated by comparing their results for a large number of synthetic earthquake catalogues for which the parameters are known and errors have been incorporated into each observation.

In the second part of the study, the effects of changes in key parameters of the earthquake model on damage estimates are investigated. This includes an investigation of the different methods of estimation and their effect on the damage estimates. Probabilistic seismic risk assessments are utilised as a catastrophe modelling tool in order to achieve this.

2 Literature Study

2.1 Earthquake magnitude and uncertainty

2.1.1 The Gutenberg-Richter relation

The Gutenberg-Richter relation (Gutenberg and Richter, 1954) describes the relationship between the number of earthquakes and their associated magnitudes for a variety of tectonic settings and is defined as:

$$\log N = a - bM \tag{1.1.1}$$

where N is the number of earthquakes associated with seismic events of magnitude M and a and b are suitable parameters. The importance of the Gutenberg-Richter relation and its applications to a range of industries that are concerned with earthquake recurrence forecasting, for example, engineering, insurance and reinsurance companies as well as disaster management, further emphasises the importance of accurate forecasting.

The occurrence of major catastrophic earthquakes (i.e. where more than 50 000 deaths occur) have been few and far between, but seem to be becoming more frequent (see Table 2.1). The increasing population density in earthquake prone areas is cause for concern that the destructive power of future earthquakes, particularly near heavily populated areas, will increase greatly (Grossi *et al.*, 2005).

2.2 Measures of earthquake magnitude and intensity

Magnitude is the most well-known measure of the "size" of an earthquake and was introduced by Charles Richter and Beno Gutenberg during the 1930s. There are several different types of magnitude which are based on different characteristics of earthquake seismic waves, as measured by seismographs (Werner and Sornette, 2008).

The original Richter magnitude is defined as:

"The magnitude of any shock is taken as the logarithm of the maximum trace amplitude, expressed in microns, with which the standard short-period torsion seismometer would register that shock at an epicentral distance of 100 kilometres." (Richter, 1935)

Table 2.1: Most destructive earthquakes, in terms of number of deaths

Date	Location	Deaths	Magnitude
856/12/22	Iran, Damghan	200000	
893/03/23	Iran, Ardabil	150000	
1138/08/09	Syria, Aleppo	230000	
1268	Asia Minor, Silicia	60000	
1290/09/27	China, Chihli	100000	
1556/01/23	Shaanxi (Shensi), China	830000	8
1667/11/	Caucasia, Shemakha	80000	
1693/01/11	Italy, Sicily	60000	7.5
1727/11/18	Iran, Tabriz	77000	
1755/11/01	Portugal, Lisbon	70000	8.7
1783/02/04	Italy, Calabria	50000	
1908/12/28	Messina, Italy	72000	7.2
1920/12/16	Haiyuan, Ningxia (Ning-hsia), China	200000	7.8
1923/09/01	Kanto (Kwanto), Japan	142800	7.9
1948/10/05	Ashgabat (Ashkhabad), Turkmenistan (Turkmeniya, USSR)	110000	7.3
1970/05/31	Chimbote, Peru	70000	7.9
1976/07/27	Tangshan, China	242769	7.5
1990/06/20	Western Iran	50000	7.4
2004/12/26	Sumatra	227898	9.1
2005/10/08	Pakistan	86000	7.6
2008/05/12	Eastern Sichuan, China	87587	7.9
2010/01/12	Haiti region	316000	7.0

(U.S. Geological Survey, 2012)

This is not the only definition of magnitude that is used. Several other definitions that include body wave magnitudes, surface wave magnitudes and moment magnitudes (Werner and Sornette, 2008) are used, sometimes in the same catalogue. One notable exception that uses uniform magnitude types is the (Harvard) Centroid Moment Tensor (CMT) catalogue. Naturally, there exist some differences in the different measures of magnitude for a particular event, which will result in uncertainties of a particular magnitude estimate

compared to a magnitude that best forecasts future events, provided the latter exists (Werner and Sornette, 2008). This was termed the inter-magnitude uncertainty by Werner and Sornette (2008).

Of particular interest is the uncertainty that arises for individual magnitude observations. Several contributing factors add to the errors that are inherent in an observed magnitude. These factors include, but are not limited to, the effects of discretization of media and equations, the measurement precision of seismometers, the assumed velocity and attenuation models of the Earth, the resolution of the inversion algorithm, and, most particularly, the definition of an earthquake event (Werner and Sornette, 2008).

The magnitude of an earthquake is never accurately known. Unit accuracy ranges from 0.1 units for recent magnitudes, to 0.25 units for older magnitudes and up to 0.6 units for historic and paleoseismic earthquakes (Kijko, 1988). Historic earthquakes refer to those earthquakes that are recovered from historical records and are not directly observed with the help of modern instruments. Paleoseismic earthquakes refer to those earthquakes that are estimated by investigation of sediment and rocks. The unit accuracy clearly indicates that modern earthquake catalogues contain fewer errors than historical and paleoseismic studies, but the additional factors described above still mean that some uncertainty is still present (Werner & Sornette, 2008).

Additionally, for the purposes of assessing losses that can be attributed to seismic events, we need to measure the strength of a seismic event at a given site in terms of the resultant structural damage to buildings. A well-known measure is the Modified Mercalli (MM) intensity scale. A summary of each intensity measure is outlined in Table 2.2 and a full summary is provided in Appendix A. Since the scale is, for the most part, subjective, further uncertainty persists, especially where eye-witness accounts make up the majority of the body of evidence to determine the magnitude of a particular event (Davies and Kijko, 2003).

Table 2.2: A summary of the Modified Mercalli Intensity scale

Scale	Description
I	Not felt except by a very few under especially favourable conditions
II	Felt only by a few persons at rest, especially on upper floors of buildings
III	Felt quite noticeably by persons indoors, especially on upper floors of buildings. Many people do not recognize it as an earthquake. Parked motor cars may rock slightly. Vibrations similar to the passing of a truck. Duration estimated.
IV	Felt indoors by many, outdoors by few during the day. At night, some woke up. Dishes, windows, doors disturbed; walls make cracking sound. Sensation like heavy truck striking building. Parked motor cars rocked noticeably.
V	Felt by nearly everyone; many woke up. Some dishes, windows broken. Unstable objects overturned. Pendulum clocks may stop.
VI	Felt by all, many frightened. Some heavy furniture moved; a few instances of fallen plaster. Damage slight.
VII	Damage negligible in buildings of good design and construction; slight to moderate in well-built ordinary structures; considerable damage in poorly built or badly designed structures; some chimneys broken.
VIII	Damage slight in specially designed structures; considerable damage in ordinary substantial buildings with partial collapse. Damage great in poorly built structures. Fall of chimneys, factory stacks, columns, monuments, walls. Heavy furniture overturned.
IX	Damage considerable in specially designed structures; well-designed frame structures thrown out of plumb. Damage great in substantial buildings, with partial collapse. Buildings shifted off foundations.
X	Some well-built wooden structures destroyed; most masonry and frame structures destroyed with foundations. Rails bent.
XI	Few, if any (masonry) structures remain standing. Bridges destroyed. Rails bent extensively.
XII	Damage total. Lines of sight and level are distorted Objects thrown into the air

(U.S. Geological Survey, 1989)

2.2.1 Estimating the Gutenberg-Richter parameters

Estimation of the parameters of the Gutenberg-Richter relation is of particular importance and an extensive body of work exists on the subject. The *a* parameter is a measure of the level, or rate, of seismicity and the *b* value describes the proportion of seismic events with different magnitudes or the relationship between the number of small and large seismic events (Kijko and Smit, 2012a; Bengoubou-Valérius and Gilbert, 2013). For global seismicity, the *b* value is approximately 1 (Kagan, 1999), but has been shown to vary significantly between regions (Wiemer and Benoit, 1996; Ayele and Kulhánek, 1997; Wiemer *et al*., 1998; Gerstenberger *et al*., 2001; Schorlemmer *et al*., 2003).

Prior to 1964, the parameters of the Gutenberg-Richter relation (1.1.1) were estimated by the traditional least squares method (Aki, 1965). This method is based on the principle of least squares, which minimises the sum of the squared deviations from the fitted line (Engelhardt and Bain, 1992*)*. Consequent investigations indicate that the least squares technique is by far the most inaccurate means of estimating the *b*-value of the Gutenberg-Richter relation (Sandri and Marzocchi, 2006). Additionally, the least squares method of estimation does not have any statistical foundation for this particular case (Page, 1968; Bender and Bannert, 1983).

In 1964, two Japanese seismologists, K. Aki and T. Utsu, working independently, proposed the new formula: (Aki, 1965; Utsu 1965)

$$\hat{b} = \frac{\log_{10} e}{\bar{m} - M_{\min}} \,, \tag{1.1.2}$$

which is both the moment and maximum likelihood estimator of the *b* value. In (1.1.2) , which is sometimes called the Aki-Utsu or classical estimator, $M_{\min}$ denotes the level of completeness of the catalogue. Since we are dealing with real world phenomena, the observed events in an actual catalogue may not always follow the Gutenberg-Richter relation exactly.

Some of the deviation from the Gutenberg-Richter relation can be attributed to a small number of events with large magnitude taking place or from incompleteness of the catalogue at small magnitudes. This incompleteness arises as a result of a detection threshold (Rydelek and Sacks, 1989). This threshold could possibly exist because below a certain magnitude

only a portion of events that occur are recorded because they are too small to be recorded by enough stations in a seismograph network (Woessner and Wiemer, 2005).

Alternatively, network operators could decide not to record seismic events below a certain magnitude since smaller events are of little interest to them (Woessner and Wiemer, 2005). Specifically, for the former problem, seismographs have difficulty recording events with small magnitudes due to background noise caused by cultural activity, surface temperature and winds (Rydelek and Sacks, 1989). This noise also varies according to the time of day and some earthquake below a certain magnitude will only be recorded at night (Rydelek and Sacks, 1989). The level of completeness is then defined as the magnitude above which all of the events within a specific area and timeframe are detected (Rydelek and Sacks, 1989).

Several methods for evaluating completeness have been proposed (Rydelek and Sacks, 1989; Woessner and Wiemer, 2005), but for the purposes of this study it is assumed that the level of magnitude below which no damage to buildings occur (Davies and Kijko, 2003) would be chosen. This is generally accepted as a magnitude of 4.0, however, in areas where buildings are not specifically designed to withstand seismic activity, magnitudes as low as 3.8 can cause notable damage.

From the maximum likelihood estimator (1.1.2) we can infer that the probability distribution function of earthquake magnitude is:

$$f_M(m) = \beta e^{-\beta(m-M_{\min})} \quad for \quad m \geq M_{\min} \tag{1.1.3}$$

and that the parameters of the Gutenberg-Richter relation are related to the above by:

$$a = \log \lambda + bM_{\min} \tag{1.1.4}$$

where $b = \beta \log(e)$ and λ is the mean activity rate which is defined as the number of earthquakes in the catalogue that exceed $M_{\min}$ divided by the time interval under investigation (Kijko, 2011).

It is notable that the Aki-Utsu or classical estimator (1.1.2) does not include magnitude uncertainty. The effects of magnitude uncertainties in the data used to estimate the *b* value and consequently seismic hazard and risk remained largely unexplored for some time. However, this oversight has since been corrected by several others (Shi and Bolt, 1982; Tinti

and Mulargia, 1985; Kijko, 1988; Rhoades, 1996; Dowrick and Rhoades, 2000; and Marzocchi and Sandri, 2003).

In general, uncertainties can be divided into two main categories, namely aleatory and epistemic uncertainty. Aleatory uncertainties "*are those uncertainties that for all practical purposes cannot be known in detail or cannot be reduced*" (Budnitz, 1997), this is also referred to as systematic uncertainty (Ku, 1969), and is uncertainty that can be measured (Bommer, 2003). Epistemic uncertainties, however, are those uncertainties that arise from a "lack of knowledge", for the present (Budnitz, 1997). Therefore, epistemic uncertainties can be reduced by more adequate models or by better measurement techniques. This type of uncertainty is also referred to as random error (Ku, 1969) and is the main type of uncertainty that affects magnitude observations (Kijko, 1988).

A discussion by Bommer (2003) indicates that the use of the terms aleatory and epistemic uncertainty are an improvement on the concepts of uncertainty and randomness in that it may add to the use of unambiguous terminology. The problem with seismic risk assessment is that almost all of it involves a multitude of disciplines, including physicists, seismologists, geologists, engineers of various backgrounds and actuaries when the scope is extended to damage and loss assessments. This multidisciplinary field calls for unambiguous terminology.

While the uncertainty in the model can be explicitly allowed for, the uncertainty of the underlying data is seldom included in the analysis of uncertainty (Dowrick and Rhoades, 2000). What this study is primarily concerned with is the uncertainty in the underlying data, which is in this case, the seismic catalogue. It is notable that data and parameter uncertainty should be treated differently (Dowrick and Rhoades, 2000). We can isolate the effect of data uncertainties by assuming that noisy estimates use the parameters as the "true" rate (Werner and Sornette, 2008). This assumption means that we can ignore parameter uncertainty, and focus on data uncertainty when conducting an investigation.

Furthermore the Aki-Utsu estimator (1.1.2) does not include the upper bound for the magnitudes, M_{max}. Several methods exist to estimate M_{max} (Kijko and Graham, 1998), including deterministic and probabilistic methods. Deterministic methods lead to high levels of uncertainty. Extreme value theory applied to the maximum values of an earthquake indicates that the number of earthquakes can be determined by a Poisson process and that

their magnitudes follow the Gutenberg-Richter relation (Kijko and Dessokey, 1987; Kijko and Graham, 1998).

An estimator for the maximum possible magnitude proposed by Kijko and Graham (1998):

$$\begin{aligned}\hat{M}_{\max} &= M_{\max}^{obs} + \int_{M_{\min}}^{M_{\max}^{obs}} \left[F_M\left(m \middle| M_{\max}^{obs}\right)\right]^n dm \\ &= M_{\max}^{obs} + \int_{M_{\min}}^{M_{\max}^{obs}} \left[\frac{1-e^{-\beta m}}{e^{-\beta M_{\min}} - e^{\beta M_m^{obs}}} \right]^n dm.\end{aligned} \tag{1.1.5}$$

The calculation of (1.1.5) is not of particular concern for this study and the formula is noted here for completeness. For the purposes of further study an assumption about the value of $M_{\max}$ is made using past available experience for the area under investigation, and sensitivity testing is conducted in order examine the effect of changes in the maximum magnitude for a specific area on estimates of the parameters of the Gutenberg Richter relation and on loss estimates (Kijko *et al.*, 2002).

In order to include this upper bound for the magnitudes in estimates of the parameters, we truncate the exponential distribution of the magnitudes at $M_{\min}$ and $M_{\max}$ in order to arrive at a probability distribution function

$$f_M(m) = \frac{\beta}{e^{-\beta M_{\min}} - e^{-\beta M_{\max}}} e^{-\beta m} \quad for \quad M_{\min} \le m \le M_{\max} \ . \tag{1.1.6}$$

An estimator that includes this upper bound is Page's relation (Page, 1968):

$$\frac{1}{\hat{\beta}} - \bar{m} + M_{\min} + \frac{\left(M_{\max} - M_{\min}\right) e^{-\hat{\beta}\left(M_{\max} - M_{\min}\right)}}{1 - e^{-\hat{\beta}\left(M_{\max} - M_{\min}\right)}} = 0 \ , \tag{1.1.7}$$

which is equivalent to the maximum likelihood estimator for the double truncated exponential distribution and can also be written as

$$\left(\frac{1}{\hat{\beta}} - \bar{m} + \frac{\left(M_{\max} e^{\hat{\beta} M_{\min}} - M_{\min} e^{\hat{\beta} M_{\max}}\right)}{\left(e^{\hat{\beta} M_{\min}} - e^{\hat{\beta} M_{\max}}\right)} \right) = 0 \ . \tag{1.1.8}$$

Note that $\hat{\beta}$ denotes an estimator of the parameter β .

The first mention of potential bias in the *a* and *b* parameters of Gutenberg-Richter relation (1.1.1) due to magnitude uncertainty is made by Tinti and Mulargia (1985). In this particular paper, the authors propose an improved estimate for parameters *a* and *b*, by treating the observed magnitudes as random variables with normally distributed observational errors. The findings of this paper are reiterated by Marzocchi and Sandri (2003). The studies show that magnitude errors do not cause significant bias in the estimation of the *b* parameter if the same degree of earthquake magnitude uncertainty (standard deviation) applies to all the magnitudes (Tinti and Mulargia, 1985). It must be noted that this study only considered the first iteration of the estimation procedure applied to determine the value of *b*.

The assumption that the errors follow a Gaussian distribution has been widely accepted for some time. It has been shown that empirical distributions of errors in observation are well approximated by the Gaussian distribution (Mertikas, 1985). The assumption implies that errors are symmetrical about zero, which means that they are equally likely to be positive or negative and that the distribution tails off at higher error values which means that extremely high or low error values become very unlikely. Both these assumptions make intuitive sense because of what we understand to be true about errors. Significant errors will most likely be indicated in data checks and these unlikely observations are usually excluded from the data set.

Research by Werner and Sornette (2008) found that, in case of large magnitude uncertainties, the double-exponential (Laplace) distribution might be another good approximation of the distribution of the errors. The use of the Laplace (or double exponential) distribution increases the possibility of the occurrence of large error outliers (Werner and Sornette, 2008). Consequently, this assumption could lead to more conservative assumptions regarding the influence of errors, but not necessarily more accurate. The properties that are most desirable for error distributions, namely symmetry and low probabilities for absolute large values, are also satisfied by the Laplace distribution.

The most likely use for the Laplace assumption would be for catalogues where the data is fairly uncertain, such as historic catalogues that predate sophisticated seismograph networks and where earthquake magnitudes are estimated from eye-witness accounts, geological survey and photographs or artworks of the damage caused. It is also very likely that only those earthquakes that are large enough to cause significant damage would be included in these types of catalogues.

When we compare the Laplace and Normal error distributions as in Figure 2.1, it can be seen that the Laplace distribution has much higher kurtosis than the normal distribution and has marginally thicker tails. This means that we are taking a higher probability of larger errors into account.

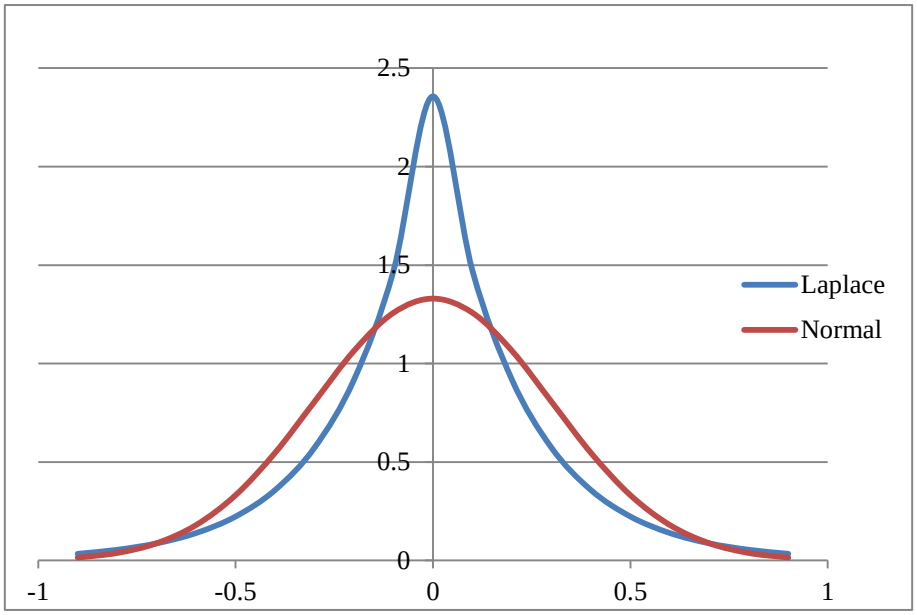

Figure 2.1: Comparing Laplace and Normal Distributions with mean 0 and standard deviation 0.3

Measurement uncertainty has been reduced over time due to the introduction of higher-quality instrumentation (Rhoades, 1996), which would again lead to the fact that uncertainties in magnitude determination are not the same for whole earthquake catalogues that stretch over considerable periods of time. Some studies have attempted to provide improved estimates for the *b* value by taking uncertainties into account (Rhoades, 1996, Kijko, 1988). It is notable, however, that the moment magnitude is believed to be the most stable with uncertainties around 0.1 (Werner and Sornette, 2008; Kijko, 1988).

The approach by Rhoades (1996) proposes a probability distribution of magnitudes of earthquakes in a catalogue as the sum of a uniform random variable and a normal random variable with mean $y-\sigma^2\beta$ and variance, σ^2. Thus the paper proposes an adjustment to each observed magnitude of $(-\sigma^2\beta)$, although it is shown that often this provides an over-correction to the bias (Rhoades, 1996). Kijko's (1988) approach is based on the assumption

that the observed magnitudes are each from a uniformly distributed interval and proceeds to calculate a maximum likelihood estimate.

The latter two approaches should succeed in calculating more accurate estimates for the *b* value, but can be too dependent on the quality of the data. A method proposed by Kijko and Dessokey (1987) solves the problem of changes in data quality within a particular catalogue. The method is particularly good when dealing with catalogues that stretch over long periods of time where improvements in instrumentation or the seismograph network in a particular area have led to changes in the quality of data. The method proposed offers maximum likelihood estimates of the activity rate, λ, and the value of β by taking advantage of extreme distribution theory. By assuming that earthquake occurrence follows a Poisson process with parameter (λT) where T is a particular time interval and that the magnitudes are distributed according to the double truncated exponential distribution as before, we can find a distribution for the largest possible earthquake, X, in a time interval T:

$$F_X\left(x \mid T\right) = \exp\left[-\lambda T \frac{e^{-\beta M_{\max}} - e^{-\beta x}}{e^{-\beta M_{\max}} - e^{-\beta M_{\min}}}\right] \tag{1.1.9}$$

By applying the maximum likelihood methodology, we find that

$$\frac{1}{\lambda} = \frac{\sum_{i=1}^{N} T_i\left(e^{-\beta M_{\max}} - e^{-\beta X_i}\right)}{N\left(e^{-\beta M_{\max}} - e^{-\beta M_{\min}}\right)} \tag{1.1.10}$$

and

$$\frac{1}{\beta} = \frac{\sum_{i=1}^{N} X_i}{N} - \frac{M_{\max} e^{-\beta M_{\max}} \sum_{i=1}^{N} T_i - \sum_{i=1}^{N} T_i X_i e^{-\beta X_i}}{\sum_{i=1}^{N} T_i\left(e^{-\beta M_{\max}} - e^{-\beta X_i}\right)} \tag{1.1.11}$$

where $\vec{X} = (X_1,...,X_N)$ is a sequence of the largest earthquake magnitudes selected from the corresponding consecutive time intervals $\vec{T} = (\mathrm{T}_1,...,\mathrm{T}_N)$. The understanding is that higher quality data will use shorter time intervals to draw the maximum magnitudes from than lower quality data (Kijko and Dessokey, 1987).

The technique is useful for catalogues with differing quality, but still does not include observation error. It is also particularly difficult to establish the time intervals to consider when you have a lot of data available but little knowledge of the actual quality of the data (Kijko and Dessokey, 1987).

There is an apparent need for an approach that will be less onerous to implement and could possibly lead to equally accurate, if not more accurate, assumptions of the *b* value.

The definition of λ makes it simple to estimate. Areas of concern arise when we consider the choice of the level of completeness and the assumption that earthquake recurrence follows a Poisson distribution, however, these assumptions were not investigated further in this study. The effect of observation errors on the activity rate are discussed in much detail in previous publications and it was found that errors lead to overestimation of the activity rate (Tinti and Mulargia, 1985, McGuire, 2001).

2.3 Earthquakes and the Insurance Industry

2.3.1 Background

Insurers are able to accept risks that individuals or companies cannot retain because they exploit the concept of pooling risks. The law of large numbers dictates that the average of a large number of homogeneous, independent risks will tend towards the expected value (Engelhardt and Bain, 1992). This implies that long-term average results will be fairly stable, meaning that insurers will have a better idea of their expected average risk than individuals or companies.

Additionally, the central limit theorem also exploits the concept of pooling homogeneous, independent risks, since the theorem states that the arithmetic mean of these risks will be approximately normally distributed (Engelhardt and Bain, 1992). This means that insurers can also formulate an idea of the variance of the risk if they pool a sufficiently large number of similar, independent risks together. This implies that insurance companies can reduce their uncertainty about specific risks to an extent that is not possible for individual entities.

Catastrophes pose a threat to the assumptions underlying the principle of risk pooling. Catastrophes remove the independence assumption from the equation. Insurers then have to

employ risk management tools that are at their disposal to remove risks that arise from catastrophes such as overexposure and concentration risk. They can do so by several methods, including reinsurance or alternative risk transfer products such as catastrophe bonds. Additionally, insurers can avoid these risks by ensuring that their portfolios are diverse enough to withstand catastrophic shocks by means of spreading of risk in terms of geographical location or by means of portfolio swaps with other insurers.

Traditionally, reinsurers supply indemnity contracts against unforeseen or extraordinary losses to insurers. In terms of earthquakes, reinsurers usually write catastrophe excess of loss reinsurance. This is a non-proportional type of reinsurance that protects the reinsured against potential aggregation or accumulation of losses that might arise as a result of natural perils. For an excess of loss reinsurance product the insured covers all losses up to, and including, a fixed monetary amount and the reinsurer pays amounts in excess of this figure up to a further identified amount or limit of the layer. A reinsured may purchase several “layers” of excess of loss reinsurance from different reinsurers (Paine, 2004).

For a risk to be insurable several criteria need to be satisfied:

- the policyholder must have an interest in the risk being insured,
- a risk must be of a financial and reasonably quantifiable nature, and
- the amount payable in the event of a claim must bear some relationship to the financial loss

(Acted, 2013).

The main issue when considering earthquake risk, in terms of property insurance, is setting the premiums for a particular risk, since we cannot rely solely on past loss data as with other risks because it is insufficient.

Insurers consider many issues when setting premiums for a particular risk - this process is also called ratemaking. While a good understanding of the possible losses that can be attributed to a risk event, insurers will also have to consider other issues such as:

- Are the premiums sufficient to cover the expenses of administering the policy and running the business?
- Will the premiums deliver an acceptable level of profit with an acceptable level of confidence? Conversely, does the product avoid an unacceptable level of loss?

- Are regulatory standards being met by the particular product?

(Acted, 2013; Grossi *et al.*, 2005).

Traditionally insurers use actuarial modelling to determine the quantifiable nature of a particular risk. For example, for motor vehicle policies insurers can use past accident and claim data to determine the appropriate rates to charge for different types of policyholders. This means that young drivers of sporty vehicles will pay higher motor vehicle insurance premiums than a middle aged policyholder with young children and stable employment.

Traditional actuarial approaches, where statistical inference of loss data is heavily relied upon, to managing risk is useful for pricing different types of risk, but fail when applied to low probability, high severity events like earthquakes (Grossi and Zoback, 2009). For these situations, catastrophe modelling is a much more effective solution. The claims data for catastrophe insurance is a lot more limited than other areas of insurance and actuarial modelling, whereby past loss data is used to infer probable future losses, is no longer an effective tool. This is why catastrophe models are used widely by modern insurers in the ratemaking and risk management processes that consider the effects of catastrophes (Grossi *et al.*, 2005).

2.3.2 Catastrophe models

A catastrophe model aims to maximise the use of available information on a particular risk. It also allows insurers and other stakeholders to estimate the potential impact from events that might occur in the future. It does this by combining the hazard and risk of an event to get some idea of the vulnerability of the portfolio under investigation. The hazard will be the loss-causing event and the risk will be the possible losses incurred by the hazard, if and when it occurs. In turn, this vulnerability is used to evaluate potential losses for a portfolio of risks (Grossi *et al.*, 2005).

The hazard is the loss-causing event and can be defined as the size and location of a catastrophic event as well as other defining characteristics. In the case of an earthquake the magnitude would be a measure of the size of an event and would define the earthquake hazard. The risk considers the particular portfolio that is exposed to the risk of loss when an event occurs. In the case of an earthquake, when considering property insurance, the location and building type as well as its age will characterise the risk for a particular policy. The

entire portfolio will have to be broken down in this manner to establish the losses possible (Grossi *et al.*, 2005).

In order to determine the effects that an earthquake can have on a particular area, we need to determine the adverse consequences of a seismic event. Generally, it is also useful to estimate the probabilities associated with these consequences. Catastrophe models that fulfil these criteria, built exclusively for the insurance industry, first emerged in the 1980s. For earthquake hazard, the models have been mainly focused on risks in the United States (Grossi and Zoback, 2009). Natural hazards are problematic for insurers and reinsurers since they involve potentially high losses that are extremely uncertain (Grossi *et al.*, 2005).

When modelling catastrophes, there are three elements to consider: the most likely locations of the future events, their frequency of occurrence and their severity (Grossi *et al.*, 2005). By taking these elements into account, insurers can forecast future losses and attach a probability of occurrence to the losses. By multiplying the potential loss of an event by the probability of occurrence of said event, reinsurers can price products accurately and can also limit their exposure in areas where substantial, regular losses are forecast (Paine, 2004). While the potential losses can be estimated for natural disasters of a given size, the probability of occurrence is of importance since it is usually more difficult to calculate.

For a seismic event the location is important since the soil conditions will determine the rate at which ground motion attenuates, which will determine the extent of the area that needs to be modelled (Grossi *et al.*, 2005). The frequency is easily approximated by a Poisson Process with the activity rate as parameter (Kijko, 2011). Finally, the severity is characterised by the magnitude, focal depth and various fault-rupture characteristics such as peak ground acceleration (Grossi *et al.*, 2005). For this part of the modelling process the expertise of seismologists and other seismic experts is heavily relied upon.

Similarly, the risk can be determined by the possible damage that earthquakes can inflict on buildings. Construction type is the main driving factor when determining building damage. The location of the building in relation to the epicentre of the earthquake will also assist to determine the likely level of damage (Liechti *et al.*, 2000; Grossi *et al.*, 2005).

In terms of errors, it is extremely difficult to differentiate between aleatory and epistemic uncertainty within a catastrophe model (Hanks and Cornell, 1994). This is because the types of uncertainty vary drastically between models. Aleatory uncertainty in one model can easily

be classified as epistemic uncertainty in another, or even a later version of the original model and vice versa.

Aleatory uncertainty is taken into account in the probability distributions underlying the model. Where it is felt the simple distributions do not adequately reflect the uncertainty an additional error term can be incorporated. Epistemic uncertainty is constantly reduced as more information becomes available over time. In the meantime, we account for the effects of epistemic uncertainty by assuming that our estimates of the parameters reflect the true values underlying the model (Werner and Sornette, 2008) and by making an assumption of the variance about this estimate and incorporating this into our model (Davies and Kijko, 2003).

By improving the accuracy or information generated by a catastrophe model, or at the very least the accuracy of the elements that make up the model, insurers will be able to make better risk management decisions, which will ultimately lead to better preparedness for catastrophic events. It is also wise to be cautious of an overreliance on catastrophe models alone. They should be viewed as a tool that can be employed in the risk management process rather than a definitive picture of the risk.

2.3.3 Probabilistic Seismic Risk Analysis

In order to assess the impact of changes in the Gutenberg-Richter relation's parameters (1.1.1) we need to use a seismic risk model to assess the possible losses for different scenarios. To this end, probabilistic seismic risk assessments (PSRAs) are conducted for different parameter values.

Deterministic studies are used frequently in the insurance industry and are also known as probable maximum loss calculations. The deterministic approach only considers the worst case scenario earthquake. The probabilistic approach used here and outlined by Davies and Kijko (2003) not only includes the most severe seismic event, but looks at the range of events that are likely to occur over a particular time period. For insurance purposes, a time interval of one year is sufficient since most cover is reviewed annually.

It must be noted that the deterministic and probabilistic approaches should be considered together since this considers the problem of seismic risk holistically. Following a deterministic or probabilistic approach is not mutually exclusive. In some cases more weight

is just given to an approach that suits the purposes of the application of the study better (McGuire, 2001). Insurance decisions are highly quantitative and require thorough analysis of all the possible scenarios; this means that a probabilistic approach will be favoured in this kind of environment (McGuire, 2001).

It is, however, difficult to classify models in this area of investigation as purely deterministic since they will most likely contain some probabilistic elements (Davies and Kijko, 2003). Probabilistic models are used extensively to estimate possible losses in seismic risk analysis (Cornell, 1968; Shah and Dong, 1991; Schmid and Schaad, 1995).

One of the main components of seismic risk analysis, attenuation functions, is complemented by earthquake occurrence models. Of the earthquake occurrence models in use, most are based on the Gutenberg-Richer relation (Liechti *et al*., 2000). What follows is a summary of the probabilistic seismic risk analysis procedure described by Davies and Kijko (2003).

In order to assess the seismic risk for a particular area, we first need to conduct a probabilistic seismic hazard assessment (PSHA). According to Davies and Kijko (2003) seismic hazard is:

> "…the probability of occurrence, within a specified period of time, of a seismic event that could damage buildings or objects."

The results of the PSHA are used to estimate seismic risk by translating probabilistic estimates of ground motion into damage via ground-motion-damage relationships. Earthquakes cause the ground to vibrate, meaning that any motion will not be constant. In order to assess the movement of the ground we examine the peak ground acceleration (PGA), *a'*, which is the maximum value of the acceleration recorded at a particular site during an event. The PGA is characterised by the following attenuation function:

$$\ln(a') = c_1 + c_2 m + c_3 R + c_4 \ln(R) + \varepsilon \qquad (2.3.1)$$

where c_1, c_2, c_3, c_4 are empirical constants, m is the Richter magnitude of the earthquake, R is the distance from the epicentre and ε is a random error, assumed to follow a Gaussian distribution with a mean of zero and a standard deviation of $\sigma_{a'}$ (Boore and Joyner, 1982; Ambraseys, 1995).

To connect hazard and risk, some kind of connection between seismic parameters and damages and losses is required. The PSRA under discussion suggests the use of the work of Whitman *et al* (1973). The damage probability matrix (DPM) divides the extent of damage into different states (Table 2.3) and by a range of damage factors or damage expressed as a percentage of the total replacement value of the structure.

A typical DPM for a particular building class is represented in Table 2.4. DPM's for different building types are given in Appendix B. The fraction of buildings in a particular damage state is given in the DPM matrix, for each modified Mercalli intensity, or MM intensity. The damage state describes the extent of damage in both words and in terms of the actual damage as a percentage of the total replacement value of the structure (Davies and Kijko. 2003).

Table 2.3: Description of damage factors

Damage Factor	Damage Factor Name	Description	Damage Factor Range (%)	Central Damage Factor (%)
1	None	No damage	0	0
2	Slight	Limited localised minor damage not requiring repair	0-1	0.5
3	Light	Significant localised damage of some components generally not requiring repair	1-10	5
4	Moderate	Significant localised damage of many components warranting repair	10-30	20
5	Heavy	Extensive damage requiring major repairs	30-60	45
6	Major	Widespread damage that may result in the facility being razed	60-100	80
7	Destroyed	Total destruction of the majority of the facility	100	100

(Whitman *et al.*, 1973)

Table 2.4: Example of a DPM for a particular building type

Damage Factor	Damage Factor Range (%)	Central Damage Factor (%)	Probability of damage (%) by MM intensity and damage state				
			VI	VII	VIII	IX	X
1	0	0.0	95.0	49.0	30.0	14.0	3.0
2	0-1	0.5	3.0	38.0	40.0	30.0	10.0
3	1-10	5.0	1.5	8.0	16.0	24.0	30.0
4	10-30	20.0	0.4	2.0	8.0	16.0	26.0
5	30-60	45.0	0.1	1.5	3.0	10.0	18.0
6	60-100	80.0	0.0	1.0	2.0	4.0	10.0
7	100	100.0	0.0	0.5	1.0	2.0	3.0

(Panel on Earthquake Loss Estimation Methodology, 1989: 82)

As mentioned, each DPM uses the MM intensity as a measure of the strength of a seismic event at a given site in terms of the resultant structural damage to buildings. The MM intensity scale is discussed in Table 2.2 and outlined fully in Appendix A.

As stated by Freeman (1932) and Davies and Kijko (2003), losses attributable to a particular seismic event vary, from very little to substantial damage. Additionally, substantial damage and the resultant losses, monetary or otherwise, are usually limited to a small proportion of structures. The general public perception is that damage is absolute across the board when a seismic event is particularly damaging, when this is, in fact, not the case (Freeman, 1932). This expectation is perpetuated by media coverage of buildings that suffer extensive damage and the negligence to mention buildings that are left with little or no damage (Freeman, 1932). DPM's ensure that damage is considered across an entire area for several building types.

Due to the nature of the South African seismic landscape, which has not suffered much damage in recent history, the data required to compile a complete vulnerability assessment is

somewhat limited. There are several ways in which damage curves of particular types of buildings can be established. Some procedures that can be considered are statistical analysis, such as Markov chains, subjective expert opinion or detailed analytical tools, such as a combination of systems theory, neural networks and fuzzy logic (Thiel and Zsutty, 1987; Sanchez-Silva and Garcia, 2001; Kijko and Smit, 2012a).

A good source of damage probability matrices is ATC-13 and is widely applied in South African studies of seismic hazard. ATC-13 is a seismic risk study that was conducted by the Applied Technology Council in 1985. The Earthquake Damage Evaluation Data for California report was prepared as a result thereof (ATC-13, 1985). DPM's are central to the ATC-13 framework as well as to those damage assessment criteria used in other areas of the United States, China, Russia and the former Soviet Union, New Zealand (Davies and Kijko, 2003). This is why the ATC-13 framework is could be a good option to borrow concepts from in order to apply to the South African seismic landscape. While ATC-13 was used in the current study, alternative studies can be considered. In recent years, there has been a shift by many European countries from ATC-13 to the European Macroseismic Scale (EMS) (EMS, 1998, Spence *et al.*, 2003, Solares and Arroyo, 2004).

The 12 building classes as defined in ATC-13 and applicable to South Africa are described in Table 2.5. Four of the building classes represent the most prevalent structures in South Africa. These are

- Unreinforced masonry, with load bearing wall, low rise (Class 3),
- Reinforced concrete shear wall without moment resisting frame, high rise (Class 7),
- Reinforced concrete shear wall without moment resisting frame, medium rise (Class 8), and
- Reinforced concrete shear wall without moment resisting frame, high rise (Class 9).

Rough estimates imply that these four classes represent over 80% of all South African urban buildings (Davies and Kijko, 2003). Figures 2.2 to 2.5 represent examples of these buildings.

Table 2.5: Classification of building classes

Description of Class of Building	Ref. No.
Wood Frame, Low rise	**1**
Light Metal, Low Rise	**2**
Unreinforced Masonry, Bearing Wall, Low Rise	**3**
Unreinforced Masonry, Load Bearing, Frame, Low Rise	**4**
Unreinforced Masonry, Load Bearing, Frame, Medium Rise	**5**
Reinforced Concrete Shear Wall with Moment-Resisting Frame, Medium Rise	**6**
Reinforced Concrete Shear Wall with Moment-Resisting Frame, High Rise	**7**
Reinforced Concrete Shear Wall without Moment-Resisting Frame, Medium Rise	**8**
Reinforced Concrete Shear Wall without Moment-Resisting Frame, High Rise	**9**
Braced Steel Frame, Low Rise	**10**
Precast Concrete, Low Rise	**11**
Long Span, Low Rise	**12**

(ATC-13, 1985)

Figure 2.2: Building class 3, unreinforced masonry, with load bearing wall, low rise (EMS, 1998)

Figure 2.3: Building class 7, reinforced concrete shear wall, with moment resisting frame, high rise (panoramio.com, 2008)

Figure 2.4: Building class 8, reinforced concrete shear wall, without moment resisting frame, medium rise (EMS, 1998)

Figure 2.5: Building class 9, reinforced concrete shear wall, without moment resisting frame, high rise (EMS, 1998)

For the purposes of the PSRA we define seismic hazard, $H(a';T)$, as "the probability that a certain level of ground shaking characterised by PGA, will be exceeded at least once within the specified time interval, T" (Davies and Kijko 2003) and is given by

$$H(a';T) = 1 - F_{A'}^{MAX}(a';T) \tag{2.3.2}$$

where $F_{A'}^{MAX}(a';T)$ is the cumulative distribution function of the PGA in the specified time interval. For insurance purposes we use durations of 1 year. This is because most structural insurance policies are sold, or re-rated, on an annual basis. We can then easily define $f_{A'}^{MAX}(a';T) = -\frac{d}{da}\left[H(a';T)\right]$.

There is no direct link between PGA and seismic risk for insurance purposes, so the assessment model links PGA with damage via MM intensity as follows:

$$p_D(d;T) = \int_{d}^{d_{\max}} \int_{i_{\min}}^{i_{\max}} \int_{a_{\min}}^{a_{\max}} f_D(\tilde{d} \mid i)\, f_I(i \mid a')\, f_{A'}^{MAX}(a';T)\, \mathrm{d}a'\, \mathrm{d}i\, \mathrm{d}\tilde{d} \tag{2.3.3}$$

with $f_I(i \mid a')$ being the conditional probability distribution function for the MM intensity, given by I given the PGA, a' and $f_D(d \mid i)$ being the conditional probability distribution function for the damage, D, for a given MM intensity, i. The damage d is substituted in the integral by the variable $\tilde{d}$ in order to use the variable d as a bound for the integral. Additionally $i_{\min}$ and $i_{\max}$ are the minimum and maximum levels of intensity respectively; $a'_{\min}$ and $a'_{\max}$ are the minimum and maximum levels of PGA respectively and $d_{\max}$ is the maximum level of possible damage.

The bounds for the integrals are determined. The minimum PGA should be the PGA above which damage to infrastructure is likely to result, also termed the PGA of engineering interest. This is usually $0.05g$, where g is the acceleration due to gravity. The maximum PGA is the maximum possible at the site being investigated. The intensity is determined as the scales for the MM intensity which range from IV to XII, since, for scales less than IV, no damage results.

In the vulnerability curves that the PSRA produces, damage values for the MM intensity values in the range IV to VI are obtained by linear extrapolation since the derived central

damage factors are not available for intensity levels less than VI. As stated previously, any intensity level less than IV implies zero damage. An example of a vulnerability curve is shown in Figure 2.6. The maximum possible damage is 100% of the total replacement value of the building.

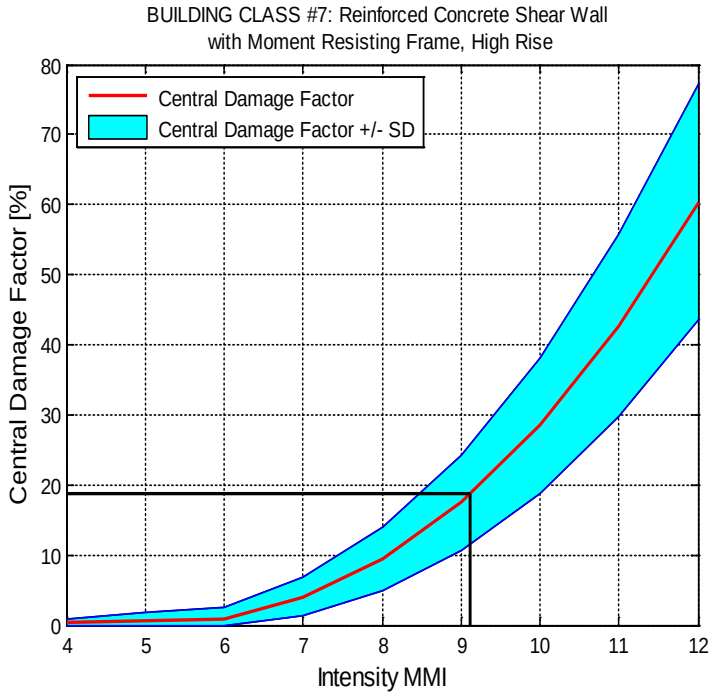

Figure 2.6: Vulnerability curve for a specific building class

In terms of an insurance application, we are interested in the expected damage over a particular period of time:

$$E\left[D(t)\right] = \int_{d_{\min}}^{d_{\max}} \int_{i_{\min}}^{i_{\max}} \int_{a'_{\min}}^{a'_{\max}} d\, f_D(d \mid i)\, f_I(i \mid a')\, f_{A'}^{MAX}(a';T)\,\mathrm{d}a'\,\mathrm{d}i\,\mathrm{d}d$$
$$= \int_{i_{\min}}^{i_{\max}} \int_{a'_{\min}}^{a'_{\max}} E\left[D \mid i\right] f_I(i \mid a')\, f_{A'}^{MAX}(a';T)\,\mathrm{d}a'\,\mathrm{d}i \qquad (2.3.4)$$

where

$$E\left[D \mid i\right] = \int_{d_{\min}}^{d_{\max}} d\, f_D(d \mid i)\,\mathrm{d}d \ . \qquad (2.3.5)$$

When the mean expected damage for a given intensity is plotted against intensity we obtain a vulnerability curve. The conditional probability distribution functions are given in the form of a DPM. In ATC-13 there are seven damage states and seven MM intensity levels and by considering the central damage factors (CDF) we can replace the integral with a summation:

$$E\left[D \mid i\right] = \sum_{j=1}^{7} CDF_j \, DPM_{ij} \tag{2.3.6}$$

over the 7 possible central damage factors denoted by subscript *j* and the level of intensity, *i*, implying that the entries in the column of the DPM corresponding to that intensity need to be taken into account in the calculation. As an example, with reference to the DPM given Table 2.4 we can calculate the expected damage for an event of MM intensity VI as follows:

$$\begin{aligned} E\left[D \mid i = VI\right] &= 0 \times 0.95 + 0.005 \times 0.03 + 0.05 \times 0.015 \\ &\quad + 0.2 \times 0.004 + 0.45 \times 0.001 + 0.8 \times 0 + 1 \times 0 \\ &= 0.00215 \\ &= 0.215\% \end{aligned} \tag{2.3.7}$$

So this implies that an earthquake of MM intensity level VI will result in an expected level of damage of 0.215% of the total value of the building. Next, we need to define the remaining conditional probability distribution functions. For the intensity given PGA, we assume that intensity follows a Gaussian distribution (Davies and Kijko, 2003):

$$f_I\left(i \mid a'\right) = \frac{1}{\sigma_I \sqrt{2\pi}} \exp\left\{ -\frac{\left(i - E\left[I \mid a'\right]\right)^2}{2\sigma_I^2} \right\} \tag{2.3.8}$$

where $E\left[I \mid a'\right] = 10.5 + 1.48 \ln a'$ (Trifunac and Brady, 1975) and $\sigma_I = 0.75$ (McGuire, 2001; Cao *et al.*, 1999).

Finally, we have to specify the probability distribution function of the seismic hazard. Engineering seismologists usually assume that the occurrence of events with a PGA larger than the minimum PGA of engineering interest follows a Poisson distribution. This assumption is based on the common assumption made in engineering seismology (Davies and Kijko, 2003). The cumulative distribution of the largest PGA recorded at the site and is then characterised by a truncated exponential distribution and is given by

$$F_{A'}^{MAX}(a';T)=\begin{cases}0 & for \quad a'<a'_{\min}\\ \dfrac{\exp\left\{-\nu T\left[1-F_{A'}(a')\right]\right\}-\exp(-\nu T)}{1-\exp(-\nu T)} & for \quad a'_{\min}\le a'\le a'_{\max}\\ 1 & for \quad a'>a'_{\max}\end{cases} \quad (2.3.9)$$

where $F_{A'}(a')$ is the cumulative distribution of the PGA and follows the truncated Pareto distribution (Davies and Kijko, 2003). The truncated Pareto distribution is then given by

$$F_{A'}(a')=\begin{cases}0 & for \quad a'<a'_{\min}\\ \dfrac{a'^{-\gamma}_{\min}-a'^{-\gamma}}{a'^{-\gamma}_{\min}-a'^{-\gamma}_{\max}} & for \quad a'_{\min}\le a'\le a'_{\max}\\ 1 & for \quad a'>a'_{\max}\end{cases}. \quad (2.3.10)$$

It then follows, by differentiating $F_{A'}^{MAX}(a';T)$ with respect to a' that

$$f_{A'}^{MAX}(a';T)=\nu T\, f_{A'}(a')F_{A'}^{MAX}(a';T)\frac{\exp\left\{-\nu T\left[1-F_{A'}(a')\right]\right\}}{\exp\left\{-\nu T\left[1-F_{A'}(a')\right]\right\}-\exp(-\nu T)} \quad (2.3.11)$$

where ν and γ are parameters that are estimated according to the maximum likelihood procedure in the assessment where $f_{A'}(a')$ denotes the probability density function of the PGA at the site (Davies and Kijko, 2003).

We derive Equation (2.3.11) by first defining a cumulative distribution function for the maximum possible earthquake magnitude within a specific time period was developed by Kijko and Graham (1999):

$$F_M^{\max}(m\,|\,m_0,m_{\max},\mathrm{t})=\frac{\exp\left\{-\lambda_0 t\left[1-F_M(m\,|\,m_0,m_{\max})\right]\right\}-\exp\left[-\lambda_0 t\right]}{1-\exp\left[-\lambda_0 t\right]} \quad (2.3.12)$$

where $\lambda_0=\lambda(m_0)=\lambda\left[1-F(m_0\,|\,m_{\min},m_{\max})\right]$ is the mean activity rate of earthquake occurrence within the specified area with magnitude m_0 and above. In the case under discussion, $m_0=m_{\min}$.

We can then define the probability that the PGA meets or exceeds a certain level as

$$P\left[PGA \geq a'\right] = \frac{\exp\left(-\beta m_{\max}\right) - y\exp\left(\frac{-\beta\left(x-c_1\right)}{c_2}\right)}{\exp\left(-\beta m_{\max}\right) - \exp\left(-\beta m_{\min}\right)} \tag{2.3.13}$$

where $x = \ln\left(a'\right)$ and $y\left(.\right)$ is a function of the form

$$\int_{r_{\min}}^{r_{\max}} \exp\left[\beta \frac{c_3 r + c_4 \ln\left(r\right)}{c_2}\right] f_R\left(r\right) dr \tag{2.3.14}$$

where, $r_{\min}$ and $r_{\max}$ are the minimum and maximum distances for the epicentre of the earthquake under consideration and for each site, the value of $y\left(.\right)$ is a constant (Kijko and Graham, 1999).

From the probability of exceedance of the PGA as characterised above, it follows that $X = \ln\left(A'\right)$ is distributed in the same manner as earthquake magnitudes:

$$F_X\left(x \mid x_{\min}, x_{\max}\right) = \frac{\exp\left(-\gamma x_{\min}\right) - \exp\left(-\gamma x\right)}{\exp\left(-\gamma x_{\min}\right) - \exp\left(-\gamma x_{\max}\right)} \tag{2.3.15}$$

where $\gamma = \frac{\beta}{c_2}$, $x_{\min} = \ln\left(a'_{\min}\right)$, $x_{\max} = \ln\left(a'_{\max}\right)$, $a'_{\min}$ is the lowest ground acceleration of engineering interest and $a'_{\max}$ is the highest possible ground acceleration for the area under consideration (Kijko and Graham, 1999). This also leads to the conclusion that the distribution of the log of peak ground acceleration, $F_X^{\max}$, is analogous to the distribution of the maximum magnitude $F_M^{\max}$. This means that

$$F_X^{\max}\left(x \mid x_{\min}, x_{\max}, t\right) = \frac{\exp\left\{-\nu t\left[1 - F_X\left(x \mid x_{\min}, x_{\max}\right)\right]\right\} - \exp\left(-\nu t\right)}{1 - \exp\left(-\nu t\right)} \tag{2.3.16}$$

where ν is the mean activity rate of the selected ground motion parameter experienced at the site and needs to be estimated (Kijko and Graham, 1999). It then follows that

$$f_X^{\max}\left(x \mid x_{\min}, x_{\max}, t\right) = \nu t F_X^{\max}\left(x \mid x_{\min}, x_{\max}, t\right) f_x\left(x \mid x_{\min}, x_{\max}\right) \tag{2.3.17}$$

where

$$f_X\left(x \mid x_{\min}, x_{\max}\right) = \frac{\gamma \exp\left(-\gamma x\right)}{\exp\left(-\gamma x_{\min}\right) - \exp\left(-\gamma x_{\max}\right)} \tag{2.3.18}$$

where γ is an unknown parameter that needs to be estimated (Kijko and Graham, 1999). Since $X = \ln\left(A'\right)$ it follows that A' follows the double truncated Pareto distribution with parameter γ:

$$F_{A'}\left(a' \mid a'_{\min}, a'_{\max}\right) = \frac{a'^{-\gamma}_{\min} - a'^{-\gamma}}{a'^{-\gamma}_{\min} - a'^{-\gamma}_{\max}} \quad \text{for} \quad a'_{\min} \le a' \le a'_{\max} \ . \tag{2.3.19}$$

Now we can find the distribution of the peak ground acceleration over a period of time by the relationship between X and A' given by

$$P\left(A' < a'\right) = P\left(e^X < a'\right) = P\left(X < \ln a'\right) = P\left(X < x\right) \tag{2.3.20}$$

which implies that:

$$F^{\max}_{A'}\left(a' \mid a'_{\min}, a'_{\max}, t\right) = F^{\max}_{X}\left(x \mid x_{\min}, x_{\max}, t\right) \tag{2.3.21}$$

or:

$$F^{MAX}_{A'}\left(a';T\right) = \begin{cases} 0 & \text{for} \quad a' < a'_{\min} \\ \dfrac{\exp\left\{-\nu \mathrm{T}\left[1 - F_{A'}\left(a'\right)\right]\right\} - \exp\left(-\nu \mathrm{T}\right)}{1 - \exp\left(-\nu \mathrm{T}\right)} & \text{for} \quad a'_{\min} \le a' \le a'_{\max} \\ 1 & \text{for} \quad a' > a'_{\max} \end{cases} \tag{2.3.22}$$

It then follows, by differentiating $F^{MAX}_{A'}\left(a';T\right)$ with respect to a' that equation (2.3.11) holds (Davies and Kijko, 2003).

In order to summarise the results of the PSRA effectively, some curves are examined. The basic seismic hazard curve combines the estimated distribution of the PGA and the relationship between the PGA and MM intensities. By averaging the distribution of the PGA over the distance and magnitude we obtain the hazard curve that, in turn, can be used to obtain the damage curve. Seismic risk curves can be created detailing the annual probabilities of exceedance of given values of damage. This is done by combining the seismic hazard curve with the vulnerability curves (Davies and Kijko, 2003).

The tool used most by insurers in catastrophe modelling is the exceedance probability curve. This is a graphical representation of the probability that a certain level of loss will be surpassed in a given time period, usually one year. The curve helps insurers when deciding in which buildings to insure, in terms of type and location, what kind of coverage to offer, which premiums to charge and what percentage of risk to transfer (Grossi *et al.*, 2005).

The concept of a return period is also closely linked to annual exceedance probabilities. The return period is the inverse of an annual probability of exceedance. For example, a 1 in 250 year return period is equivalent to a 0.4% probability of exceedance (Grossi *et al.*, 2005). It is important to note that return periods are just probabilities stated in a different way. The 1 year in 250 could very well be the current year or the next; therefore the measure should be treated with caution.

Several similar PSRA's can be compared, by varying only a single variable at a time, it is possible to draw inferences about the way in which certain parameters affect the damage estimates for certain areas.

2.3.4 Linking risk assessments and insurance

One of the main goals of an insurance company is to increase expected profits while maintaining an acceptable level of risk. Most insurers take a threefold approach when attempting to meet this goal. Insurers focus on ratemaking, portfolio management and risk financing. Catastrophe modelling is one of the tools the insurer uses to meet its goals but is used in conjunction with tools such as capital allocation and enterprise risk management (Grossi *et al.*, 2005).

The ratemaking process aims to ensure that expected annual losses as well as expenses are covered while still making an acceptable level of profit. Premiums are a function of supply and demand, and these forces should also be taken into account when setting rates. When taking catastrophes into account, insurers have the option of increasing premiums in order to cover the additional risk, or to decrease their exposure by increasing excesses payable or by ceding risks above a certain threshold to a reinsurer. Additionally regulation concerning ratemaking must be taken into account (Acted, 2013; Grossi *et al.*, 2005).

Regulation in terms of catastrophes can be a lot more onerous in areas where catastrophes have a tendency to occur on a regular basis. In areas of low seismicity it is very likely that regulation may not sufficiently allow for the risk under consideration (Grossi *et al.*, 2005).

Portfolio management is the process whereby insurers actively manage and monitor the risk in the existing portfolio of business and aim to apply measures to mitigate or transfer undesirable risks. For catastrophes the main issue can arise when there is a geographical concentration of risk in one specific disaster-prone area. This is also sometimes referred to as accumulation of risk (Acted, 2013). Insurers can mitigate this risk by spreading their policies over a wider geographical area or by arranging a swap with an insurer whose risks are a good diversification of the company's current risks. Insurers must also consider risk financing. If their exposure to risk is too high they can cede some risk to a reinsurer or make use of alternative risk transfer (ART) tools such as discounted covers, integrated risk covers, securitisation, insurance derivatives or swaps (Acted, 2013). Catastrophe bonds are an ART tool that is increasing in relevance and popularity and particularly relevant to the topic under investigation.

Finally there are other risks that the company will have to take into account but decisions made regarding these risks are not directly impacted by the catastrophe models, although they could be a helpful auxiliary source of information. The other significant risk that is exacerbated by catastrophes is liquidity risk, which is the risk that a company does not have enough liquid assets to meet its short term obligations or can only secure these assets at an exorbitant cost. Other risks that should be considered are:

- Credit risk: the risk that third parties default on their debt.
- Insurance risk: the risk that claims are higher than expected.
- Exposure risk: the risk that damage is underestimated.
- Expense risk: the risk that expenses are not adequately allowed for.
- Reinsurance risk: the risk that reinsurance is insufficient, inadequate, incorrectly priced or not available.

In summary, an insurer will have to work closely with experts in other fields to understand the inner workings of a catastrophe model. The results of the model however, can be used for a range of applications within the insurance company. It is therefore important to examine the effects of changes in the underlying parameters of the model on the results that are obtained.

3 Methodology Part 1: Estimators

3.1 Background: Methods of estimation

There are several ways in which observation errors can be taken into account (Shi and Bolt, 1982; Tinti and Mulargia, 1985; Kijko, 1988; Rhoades, 1996; Dowrick and Rhoades 2000; and Marzocchi and Sandri, 2003, Werner and Sornette, 2008), two of which will be discussed in this section. The first method will be examined in detail for estimating the parameters of the Gutenberg-Richter relation, whereas the second will be discussed generally. The first method, which is a method well-described by Marzocchi and Sandri (2003), involves the classical assumption that the real observation $\tilde{Y}$ is a sum of two random variables, namely, the actual observation Y and some error ε. This paper (Marzocchi and Sandri, 2003) specifically discusses observation errors for the Gutenberg-Richter relation for earthquake magnitude predictions and its effect on the *b* value of this relation.

Alternative estimates are then derived for the parameters of the model by deriving a distribution for the real observations and obtaining a maximum likelihood estimate from the distribution. The assumption that errors follow a Gaussian distribution is investigated (Tinti and Mulargia, 1985) and a second assumption, that the errors follow a Laplace distribution (Werner and Sornette, 2008) is also investigated. The second method which is an application of Bayes' Theorem for the multivariate case is examined further for both distribution types considered in the first method, Gaussian (Tinti and Mulargia, 1985) and Laplace (Werner and Sornette, 2008), and its possibilities are discussed.

The estimators that are deemed fit for application are then tested against two other estimates that do not incorporate the errors in the observed magnitudes, such as the Aki-Utsu estimator (Aki, 1965; Utsu 1965) and Page's relation (Page, 1968), in order to examine the possible implications of using different methods. A probabilistic approach is used to determine the effect of the different estimators on an area of low seismicity. Sensitivity tests are then conducted to establish the extent to which the different estimators compare under different scenarios.

The study only refers to the effect of changes in the activity rate as a means of testing the sensitivity of the models. The *b* value estimation is slightly more complex and previous investigation has not been as extensive. The *a* value is dependent on the *b* value and on λ

and the assumptions for the latter parameter are not considered explicitly in this study. This research therefore focuses on the estimation of the *b* value.

3.2 Traditional method

In order to take the measurement errors into account, consider the apparent magnitude, M, as the sum of two independent random variables (Tinti and Mulargia, 1985), this can also be viewed as a perturbation of the real magnitudes by independent error (Werner and Sornette, 2008), i.e.

$$M = M_R + \varepsilon \ , \tag{3.2.1}$$

where M_R is the real magnitude and ε is the measurement error. As stated previously, we do not differentiate between the two distinct types of error at this level of investigation. We can isolate the effect of data uncertainties by assuming that noisy estimates use the parameters as the "true" rate (Werner and Sornette, 2008). This assumption means that we can ignore parameter uncertainty, and focus on data uncertainty when conducting an investigation.

3.2.1 Assumption 1: Errors follow a Gaussian distribution

We have to make assumptions about the distributions of the real magnitudes and the errors or noise that are added to them. For the first estimator, we will assume that the real magnitudes follow the double truncated exponential distribution as the underlying properties of the Gutenberg-Richter relation suggest and that the errors follow the Gaussian or normal distribution with a zero mean and some standard deviation.

Since we will most likely have some knowledge of the standard deviation of an earthquake catalogue, we will probably not need to estimate the standard deviation of the errors. As stated previously, errors in catalogues are acknowledged and are usually stated as an approximation in the catalogue at the outset.

The real magnitudes are then assumed to have the following probability distribution function, (Aki, 1965; Page, 1968):

$$f_{M_R}(m_R) = \frac{1}{\left(e^{-\beta M_{\min}} - e^{-\beta M_{\max}}\right)} \beta e^{-\beta m_R} \quad M_{\min} \le m_R \le M_{\max} \tag{3.2.2}$$

and the errors are assumed to have the following probability distribution function:

$$f_{\mathrm{E}}(\varepsilon) = \frac{1}{\sigma\sqrt{2\pi}} e^{\frac{-\varepsilon^2}{2\sigma^2}} \qquad \varepsilon \in \mathbb{R} \tag{3.2.3}$$

(Abramowitz and Stegun, 1972).

We can then find the probability distribution function for M by finding the convolution $M_R * \varepsilon$ of M_R and ε. Since the random variables are independent their convolution is given by the density of their sum, namely

$$f_M(m) = \left(f_{M_R} * f_{\mathrm{E}}\right)(m) = \int_{-\infty}^{\infty} f_{\mathrm{E}}(m - m_R)\, f_{M_R}(m_R)\, dm_R \ . \tag{3.2.4}$$

It then follows that:

$$\begin{aligned}
f_M(m) &= \int_{M_{\min}}^{M_{\max}} \frac{1}{\sigma\sqrt{2\pi}\left(e^{-\beta M_{\min}} - e^{-\beta M_{\max}}\right)} \exp\left[\frac{-(m - m_R)^2}{2\sigma^2}\right] \beta e^{-\beta m_R} dm_R \\
&= \frac{\beta}{\sigma\sqrt{2\pi}\left(e^{-\beta M_{\min}} - e^{-\beta M_{\max}}\right)} \int_{M_{\min}}^{M_{\max}} \exp\left[\frac{1}{2\sigma^2}\left(-m^2 + 2m.m_R - {m_R}^2 - 2\beta\sigma^2 m_R\right)\right] dm_R \\
&= \left(\frac{\beta}{\sigma\sqrt{2\pi}\left(e^{-\beta M_{\min}} - e^{-\beta M_{\max}}\right)}\right) \exp\left[-\frac{1}{2\sigma^2}\left(m^2\right)\right] \int_{M_{\min}}^{M_{\max}} \exp\left[-\frac{1}{2\sigma^2}\left(m_R^2 - 2m.m_R + 2\beta\sigma^2 m_R\right)\right] dm_R \\
&= \left(\frac{\beta}{\sigma\sqrt{2\pi}\left(e^{-\beta M_{\min}} - e^{-\beta M_{\max}}\right)}\right) \exp\left[-\frac{1}{2\sigma^2}\left(m^2 - \left(m - \beta\sigma^2\right)^2\right)\right] \\
&\qquad \int_{M_{\min}}^{M_{\max}} \exp\left[-\frac{1}{2\sigma^2}\left(m_R - \left(m - \beta\sigma^2\right)\right)^2\right] dm_R .
\end{aligned} \tag{3.2.5}$$

In order to evaluate the integral we consider the error function $erf(z)$ which is encountered when integrating the normal distribution and is defined as

$$erf(z) = \frac{2}{\sqrt{\pi}} \int_0^z e^{-t^2} dt \tag{3.2.6}$$

(Abramovitz and Stegun, 1972).

Consider the integral:

$$\begin{aligned}
&\int_{M_{\min}}^{M_{\max}} \exp\left[-\frac{1}{2\sigma^2} \left(m_R - \left(m - \beta\sigma^2 \right) \right)^2 \right] dm_R \\
&= \int_{M_{\min}}^{M_{\max}} \exp\left[-\left(\frac{m_R - \left(m - \beta\sigma^2 \right)}{\sqrt{2}\sigma} \right)^2 \right] dm_R \\
&= \int_0^{M_{\max}} \exp\left[-\left(\frac{m_R - \left(m - \beta\sigma^2 \right)}{\sqrt{2}\sigma} \right)^2 \right] dm_R - \int_0^{M_{\min}} \exp\left[-\left(\frac{m_R - \left(m - \beta\sigma^2 \right)}{\sqrt{2}\sigma} \right)^2 \right] dm_R .
\end{aligned} \tag{3.2.7}$$

Then we let $u = \dfrac{m_R - \left(m - \beta\sigma^2 \right)}{\sqrt{2}\sigma}$ and it follows that $du = \dfrac{dm_R}{\sqrt{2}\sigma}$, which implies that

$$\begin{aligned}
&\int_0^{M_{\max}} \exp\left[-\left(\frac{m_R - \left(m - \beta\sigma^2 \right)}{\sqrt{2}\sigma} \right)^2 \right] dm_R - \int_0^{M_{\min}} \exp\left[-\left(\frac{m_R - \left(m - \beta\sigma^2 \right)}{\sqrt{2}\sigma} \right)^2 \right] dm_R \\
&= \left(\sqrt{2}\sigma \right) \left(\frac{\sqrt{\pi}}{2} \right) \left(\frac{2}{\sqrt{\pi}} \right) \left\{ \int_0^{\frac{M_{\max} - \left(m - \beta\sigma^2 \right)}{\sqrt{2}\sigma}} e^{-u^2} du - \int_0^{\frac{M_{\min} - \left(m - \beta\sigma^2 \right)}{\sqrt{2}\sigma}} e^{-u^2} du \right\} \\
&= \frac{\sigma\sqrt{2\pi}}{2} \left[erf\left(\frac{M_{\max} - \left(m - \beta\sigma^2 \right)}{\sqrt{2}\sigma} \right) - erf\left(\frac{M_{\min} - \left(m - \beta\sigma^2 \right)}{\sqrt{2}\sigma} \right) \right]
\end{aligned} \tag{3.2.8}$$

and it follows that

$$f_M(m) = \left(\frac{\beta}{\sigma\sqrt{2\pi}\left(e^{-\beta M_{\min}} - e^{-\beta M_{\max}}\right)}\right)\exp\left[-\frac{1}{2\sigma^2}\left(m^2 - m^2 + 2m\beta\sigma^2 - \left(\beta\sigma^2\right)^2\right)\right]\left(\frac{\sigma\sqrt{2\pi}}{2}\right)$$
$$\left\{erf\left[\frac{M_{\max} - \left(m - \beta\sigma^2\right)}{\sqrt{2}\sigma}\right] - erf\left[\frac{M_{\min} - \left(m - \beta\sigma^2\right)}{\sqrt{2}\sigma}\right]\right\}$$
$$= \frac{\beta}{2\left(e^{-\beta M_{\min}} - e^{-\beta M_{\max}}\right)} e^{-\frac{\beta}{2}\left(2m - \beta\sigma^2\right)}\left\{erf\left(\frac{M_{\max} - \left(m - \beta\sigma^2\right)}{\sqrt{2}\sigma}\right) - erf\left(\frac{M_{\min} - \left(m - \beta\sigma^2\right)}{\sqrt{2}\sigma}\right)\right\}, \tag{3.2.9}$$

which is the joint probability distribution function of the apparent magnitude.

By applying the maximum likelihood methodology (Engelhardt and Bain, 1992), we first need to find the joint probability distribution function, $L(\beta) = \prod_{i=1}^{n} f_{M_i}(m_i)$, of the apparent magnitudes $(M_1, M_2, ..., M_n)$ for a given set of observations $(m_1, m_2, ..., m_n)$:

$$L(\beta) = \prod_{i=1}^{n} \frac{\beta}{2\left(e^{-\beta M_{\min}} - e^{-\beta M_{\max}}\right)} e^{-\frac{\beta}{2}\left(2m_i - \beta\sigma^2\right)}\left\{erf\left(\frac{M_{\max} - \left(m_i - \beta\sigma^2\right)}{\sqrt{2}\sigma}\right) - erf\left(\frac{M_{\min} - \left(m_i - \beta\ \sigma^2\right)}{\sqrt{2}\sigma}\right)\right\}$$
$$= \frac{\beta^n}{2^n\left(e^{-\beta M_{\min}} - e^{-\beta M_{\max}}\right)^n} e^{-\frac{\beta}{2}\sum_{i=1}^{n}\left(2m_i - \beta\sigma^2\right)} \prod_{I=1}^{n}\left\{erf\left(\frac{M_{\max} - \left(m_i - \beta\sigma^2\right)}{\sqrt{2}\sigma}\right) - erf\left(\frac{M_{\min} - \left(m_i - \beta\sigma^2\right)}{\sqrt{2}\sigma}\right)\right\}. \tag{3.2.10}$$

The assumption that the observed magnitudes are independent from one another is made, since earthquake catalogues list distinct seismic events. We can find a maximum likelihood estimator for β by solving the following equation:

$$\frac{\partial}{\partial\beta}\ln L(\beta) = 0 \tag{3.2.11}$$

It follows that

$$\ln L(\beta) = n\ln\beta - n\ln 2 - n\ln\left(e^{-\beta M_{\min}} - e^{-\beta M_{\max}}\right) - \frac{\beta}{2}\sum_{i=1}^{n}\left(2m_i - \beta\sigma^2\right) + \sum_{i=1}^{n}\ln\left\{\left[erf\left(\frac{M_{\max} - \left(m_i - \beta\sigma^2\right)}{\sqrt{2}\sigma}\right)\right] - \left[erf\left(\frac{M_{\min} - \left(m_i - \beta\sigma^2\right)}{\sqrt{2}\sigma}\right)\right]\right\} \quad (3.2.12)$$

and

$$\frac{\partial}{\partial\beta}\ln L(\beta) = \frac{n}{\beta} + n\frac{\left(M_{\max}e^{\beta M_{\min}} - M_{\min}e^{\beta M_{\max}}\right)}{\left(e^{\beta M_{\min}} - e^{\beta M_{\max}}\right)} - \sum_{i=1}^{n} m_i + n\beta\sigma^2 + \sum_{i=1}^{n}\frac{\sqrt{2}\sigma\left(e^{-\frac{\left(M_{\max}+\beta\sigma^2-m_i\right)^2}{2\sigma^2}} - e^{-\frac{\left(M_{\min}+\beta\sigma^2-m_i\right)^2}{2\sigma^2}}\right)}{\sqrt{\pi}\left[erf\left(\frac{M_{\max}+\beta\sigma^2-m_i}{\sqrt{2}\sigma}\right) - erf\left(\frac{M_{\min}+\beta\sigma^2-m_i}{\sqrt{2}\sigma}\right)\right]}. \quad (3.2.13)$$

It is beneficial to consider $\frac{\partial}{\partial\beta}\ln\left(e^{-\beta M_{\min}} - e^{-\beta M_{\max}}\right)$ in more detail since it is not a straightforward result.

If we use the chain rule $\frac{\partial}{\partial\beta}\ln\left(e^{-\beta M_{\min}} - e^{-\beta M_{\max}}\right) = \frac{d\log(u)}{du}\frac{du}{dx}$ where $u = \left(e^{-\beta M_{\min}} - e^{-\beta M_{\max}}\right)$ and $\frac{d}{du}\log(u) = \frac{1}{u}$ then

$$\frac{\partial}{\partial\beta}\ln\left(e^{-\beta M_{\min}} - e^{-\beta M_{\max}}\right) = \frac{\frac{\partial}{\partial\beta}\left(e^{-\beta M_{\min}} - e^{-\beta M_{\max}}\right)}{\left(e^{-\beta M_{\min}} - e^{-\beta M_{\max}}\right)}. \quad (3.2.14)$$

Now we have to use the chain rule on both terms in the numerator to differentiate the numerator:

Firstly the rule $\frac{d}{d\beta}\left(e^{-\beta M_{\min}}\right) = \frac{de^u}{du}\frac{du}{d\beta}$ with $u = -\beta M_{\min}$ and $\frac{d}{du}\left(e^u\right) = e^u$

$$\frac{\partial}{\partial\beta}\ln\left(e^{-\beta M_{\min}}-e^{-\beta M_{\max}}\right)=\frac{-\frac{\partial}{\partial\beta}\left(e^{-\beta M_{\max}}\right)+\frac{\partial}{\partial\beta}\left(-\beta M_{\min}\right)e^{-\beta M_{\min}}}{\left(e^{-\beta M_{\min}}-e^{-\beta M_{\max}}\right)}$$
$$=\frac{-\frac{\partial}{\partial\beta}\left(e^{-\beta M_{\max}}\right)-M_{\min}e^{-\beta M_{\min}}}{\left(e^{-\beta M_{\min}}-e^{-\beta M_{\max}}\right)} \quad . \qquad (3.2.15)$$

Similarly for $\frac{d}{d\beta}\left(e^{-\beta M_{\max}}\right)=\frac{de^u}{du}\frac{du}{d\beta}$ with $u=-\beta M_{\max}$ and $\frac{d}{du}\left(e^u\right)=e^u$:

$$\frac{\partial}{\partial\beta}\ln\left(e^{-\beta M_{\min}}-e^{-\beta M_{\max}}\right)=\frac{-\frac{\partial}{\partial\beta}\left(-\beta M_{\max}\right)e^{-\beta M_{\max}}-M_{\min}e^{-\beta M_{\min}}}{\left(e^{-\beta M_{\min}}-e^{-\beta M_{\max}}\right)}$$
$$=\frac{M_{\max}e^{-\beta M_{\max}}-M_{\min}e^{-\beta M_{\min}}}{\left(e^{-\beta M_{\min}}-e^{-\beta M_{\max}}\right)} \quad . \qquad (3.2.16)$$

If we multiply Equation (3.2.16) by $\frac{e^{\beta M_{\max}+\beta M_{\min}}}{e^{\beta M_{\max}+\beta M_{\min}}}$ and swop terms around in the denominator we find:

$$\frac{\partial}{\partial\beta}\ln\left(e^{-\beta M_{\min}}-e^{-\beta M_{\max}}\right)=-\frac{M_{\max}e^{\beta M_{\min}}-M_{\min}e^{\beta M_{\max}}}{\left(e^{\beta M_{\min}}-e^{\beta M_{\max}}\right)}$$
$$=-M_{\min}-\frac{\left(M_{\max}-M_{\min}\right)e^{-\beta\left(M_{\max}-M_{\min}\right)}}{1-e^{-\beta\left(M_{\max}-M_{\min}\right)}} \quad . \qquad (3.2.17)$$

We equate the above partial derivative (3.2.13) to zero and divide by n to find an expression to evaluate the maximum likelihood estimate for β:

$$\left(\frac{1}{\hat{\beta}}-\overline{m}+\frac{\left(M_{\max}e^{\hat{\beta}M_{\min}}-M_{\min}e^{\hat{\beta}M_{\max}}\right)}{\left(e^{\hat{\beta}M_{\min}}-e^{\hat{\beta}M_{\max}}\right)}\right)+$$
$$\left(\hat{\beta}\sigma^2+\frac{1}{n}\sum_{i=1}^{n}\frac{\sqrt{2}\sigma\left(e^{-\frac{\left(M_{\max}+\hat{\beta}\sigma^2-m_i\right)^2}{2\sigma^2}}-e^{-\frac{\left(M_{\min}+\hat{\beta}\sigma^2-m_i\right)^2}{2\sigma^2}}\right)}{\sqrt{\pi}\left[erf\left(\frac{M_{\max}+\hat{\beta}\sigma^2-m_i}{\sqrt{2}\sigma}\right)-erf\left(\frac{M_{\min}+\hat{\beta}\sigma^2-m_i}{\sqrt{2}\sigma}\right)\right]}\right)=0 \qquad (3.2.18)$$

where $\bar{m} = \frac{1}{n}\sum_{i=1}^{n} m_i$. If we let the variance of the error term tend to zero we find that

$$\left(\frac{1}{\hat{\beta}} - \bar{m} + \frac{\left(M_{\max} e^{\hat{\beta} M_{\min}} - M_{\min} e^{\hat{\beta} M_{\max}} \right)}{\left(e^{\hat{\beta} M_{\min}} - e^{\hat{\beta} M_{\max}} \right)} \right) = 0 \qquad (3.2.19)$$

which is the maximum likelihood estimator for the bounded magnitude distribution.

Furthermore, if we let the maximum possible magnitude tend to infinity, we find:

$$\begin{aligned}
&\lim_{M_{msax} \to \infty} \left(\frac{1}{\hat{\beta}} - \bar{m} + \frac{\left(M_{\max} e^{\hat{\beta} M_{\min}} - M_{\min} e^{\hat{\beta} M_{\max}} \right)}{\left(e^{\hat{\beta} M_{\min}} - e^{\hat{\beta} M_{\max}} \right)} \right) \\
&= \lim_{M_{msax} \to \infty} \left(\frac{1}{\hat{\beta}} - \bar{m} + M_{\min} + \frac{\left(M_{\max} - M_{\min} \right) e^{-\hat{\beta}\left(M_{\max} - M_{\min} \right)}}{1 - e^{-\hat{\beta}\left(M_{\max} - M_{\min} \right)}} \right) \\
&= \frac{1}{\hat{\beta}} - \bar{m} + M_{\min} + \lim_{M_{msax} \to \infty} \left(\frac{(\infty) e^{-\infty}}{1 - e^{-\infty}} \right) \\
&= \frac{1}{\hat{\beta}} - \bar{m} + M_{\min} \qquad \text{since } e^{-\infty} = 0 \text{ and approaches zero faster than } M_{\max} \text{ approaches infinity}
\end{aligned} \qquad (3.2.20)$$

and which is the Aki-Utsu (1965) maximum likelihood estimate of β.

3.2.2 Assumption 2: Errors follow a Laplace distribution

We can vary the assumption about the errors that perturb the actual magnitudes. An alternative distribution that can be considered is the Laplace, or double exponential, distribution (Werner and Sornette, 2008) with a zero mean and some standard deviation. In order to keep some consistency between the estimators we will use the same standard deviation for both assumptions in our further investigations. As with the Gaussian distribution, this distribution is symmetrical about the mean. We will, once again, assume that the real magnitudes follow the double truncated exponential distribution as the underlying properties of the Gutenberg-Richter relation suggests.

The real magnitudes will then have the following probability distribution function, (Aki, 1965):

$$f_{M_R}(m_R) = \frac{1}{\left(e^{-\beta M_{\min}} - e^{-\beta M_{\max}}\right)} \beta e^{-\beta m_R} \quad M_{\min} \le m_R \le M_{\max} \tag{3.2.21}$$

and the errors will have the following probability distribution function:

$$f_{\mathrm{E}}(\varepsilon) = \frac{1}{2\nu_c} e^{\frac{-|\varepsilon|}{\nu_c}} \qquad \varepsilon \in \mathbb{R} \tag{3.2.22}$$

where ν_c is both the scale and shift parameters. The relationship between the standard deviation and the scale and shift parameter is $\sigma^2 = 2\nu_c^2$, which implies that no further assumptions are required if the standard deviation has already been estimated. We can then find the probability distribution function for M by finding the convolution $M_R * \varepsilon$ of M_R and ε.

Since the random variables are independent their convolution is given by the density of their sum:

$$f_M(m) = \left(f_{M_R} * f_{\mathrm{E}}\right)(m) = \int_{-\infty}^{\infty} f_{\mathrm{E}}(m - m_R)\, f_{M_R}(m_R)\, dm_R \ . \tag{3.2.23}$$

It then follows that

$$f_M(m) = \int_{M_{\min}}^{M_{\max}} \frac{1}{2\nu_c} e^{\frac{-1}{\nu_c}|m_R - m|} \frac{1}{\left(e^{-\beta M_{\min}} - e^{-\beta M_{\max}}\right)} \beta e^{-\beta m_R} dm_R \ \text{for}\ M_{\min} \le m \le M_{\max} \ . \tag{3.2.24}$$

We need to investigate this problem in terms of the possible values within the absolute value, i.e. the case where the absolute value exceeds zero and the case where the absolute value is less than zero.

Let $Y_1 = m_R$ and $Y_2 = m_R + \varepsilon = m$ then we can find the marginal distribution of m by using the convolution formula. However, since we have an absolute value in our formula, we need to consider where $m > m_R$ and where $m < m_R$ since this will dictate which formula we will need to integrate over the interval $(M_{\min}, M_{\max})$, the area over which m_R is defined. Figure 3.1 shows where the probability distribution function is defined (the shaded areas which

continue to infinity both positive and negative) and which integral should be considered under which circumstances as indicated by the legend.

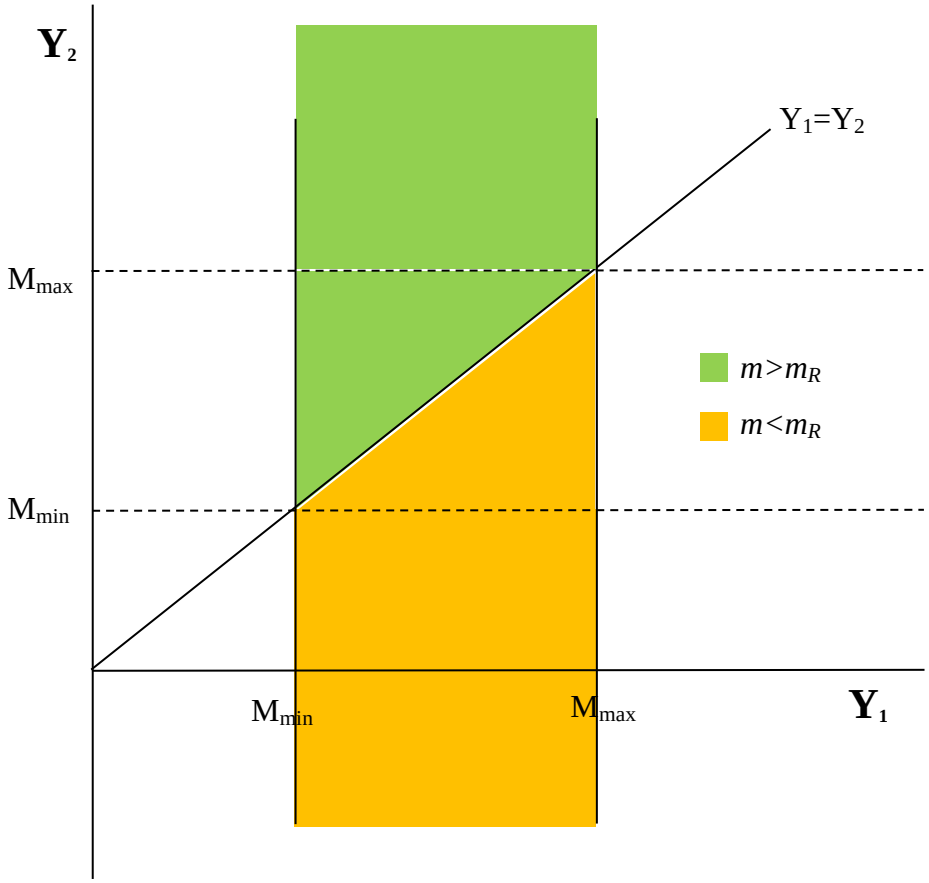

Figure 3.1: Region over which the probability distribution function for *m* is defined

According to Figure 3.1, we can see that we will define the probability distribution function as follows:

$$f_M(m)=\begin{cases}\displaystyle\int_{M_{\min}}^{M_{\max}}\frac{1}{2\nu_c}e^{-\frac{(m-m_R)}{\nu_c}}\frac{1}{\left(e^{-\beta M_{\min}}-e^{-\beta M_{\max}}\right)}e^{-\beta m_R}dm_R & \text{for} \quad M_{\max}<m<\infty \\ \displaystyle\int_{M_{\min}}^{m}\frac{1}{2\nu_c}e^{-\frac{(m-m_R)}{\nu_c}}\frac{1}{\left(e^{-\beta M_{\min}}-e^{-\beta M_{\max}}\right)}e^{-\beta m_R}dm_R + & \\ \displaystyle\int_{m}^{M_{\max}}\frac{1}{2\nu_c}e^{-\frac{(m_R-m)}{\nu_c}}\frac{1}{\left(e^{-\beta M_{\min}}-e^{-\beta M_{\max}}\right)}e^{-\beta m_R}dm_R & \text{for} \quad M_{\min}\le m\le M_{\max} \\ \displaystyle\int_{M_{\min}}^{M_{\max}}\frac{1}{2\nu_c}e^{-\frac{(m_R-m)}{\nu_c}}\frac{1}{\left(e^{-\beta M_{\min}}-e^{-\beta M_{\max}}\right)}e^{-\beta m_R}dm_R & \text{for} \quad -\infty<m<M_{\min}\end{cases} \tag{3.2.25}$$

Since our definition of earthquake catalogue entries determines that $M_{\min}\le m\le M_{\max}$, we will only consider this case. Further in depth investigation of inclusion of the magnitudes outside these bounds could yield interesting results but were beyond the scope of the simplifying assumptions made here. So we consider the part of the probability distribution function as follows:

$$f_M(m)=\int_{m}^{M_{\max}}\frac{1}{2\nu_c}e^{\frac{-(m_R-m)}{\nu_c}}\frac{1}{\left(e^{-\beta M_{\min}}-e^{-\beta M_{\max}}\right)}\beta e^{-\beta m_R}dm_R + \int_{M_{\min}}^{m}\frac{1}{2\nu_c}e^{\frac{-(m-m_R)}{\nu_c}}\frac{1}{\left(e^{-\beta M_{\min}}-e^{-\beta M_{\max}}\right)}\beta e^{-\beta m_R}dm_R . \tag{3.2.26}$$

Then

$$\begin{aligned}f_M^{+}(m)&=\int_{m}^{M_{\max}}\frac{1}{2\nu_c}e^{\frac{-(m_R-m)}{\nu_c}}\frac{1}{\left(e^{-\beta M_{\min}}-e^{-\beta M_{\max}}\right)}\beta e^{-\beta m_R}dm_R \\ &=\frac{-\beta}{2\nu_c\left(e^{-\beta M_{\min}}-e^{-\beta M_{\max}}\right)}\int_{m}^{M_{\max}}e^{-\beta m_R-\frac{m_R-m}{\nu_c}}dm_R \\ &=\frac{\beta e^{-\beta m}}{2\left(e^{-\beta M_{\min}}-e^{-\beta M_{\max}}\right)(\beta\nu_c+1)}\left[1-e^{\frac{(m-M_{\max})(\beta\nu_c+1)}{\nu_c}}\right]\end{aligned} \tag{3.2.27}$$

and

$$f_M^-(m) = \int_{M_{\min}}^{m} \frac{1}{2\nu_c} e^{\frac{-(m-m_R)}{\nu_c}} \frac{1}{\left(e^{-\beta M_{\min}} - e^{-\beta M_{\max}}\right)} \beta e^{-\beta m_R} dm_R$$

$$= \frac{-\beta}{2\nu_c\left(e^{-\beta M_{\min}} - e^{-\beta M_{\max}}\right)} \int_{M_{\min}}^{m} e^{-\beta m_R - \frac{m-m_R}{\nu_c}} dm_R \qquad (3.2.28)$$

$$= \frac{\beta e^{-\beta m}}{2\left(e^{-\beta M_{\min}} - e^{-\beta M_{\max}}\right)(\beta\nu_c - 1)}\left[e^{\frac{(m-M_{\min})(\beta\nu_c - 1)}{\nu_c}} - 1\right].$$

Therefore:

$$f_M(m) = f_M^+(m) + f_M^-(m)$$

$$= \frac{\beta e^{-\beta m}}{2\left(e^{-\beta M_{\min}} - e^{-\beta M_{\max}}\right)\left(\beta^2\nu_c^2 - 1\right)}\left\{(\beta\nu_c - 1)\left[1 - e^{\frac{(m-M_{\max})(\beta\nu_c + 1)}{\nu_c}}\right] - (\beta\nu_c + 1)\left[e^{\frac{(m-M_{\min})(\beta\nu_c - 1)}{\nu_c}} - 1\right]\right\}$$

$$= \frac{\beta e^{-\beta m}}{2\left(e^{-\beta M_{\min}} - e^{-\beta M_{\max}}\right)\left(\beta^2\nu_c^2 - 1\right)}\left\{(\beta\nu_c + 1)\left[e^{\frac{(m-M_{\min})(\beta\nu_c - 1)}{\nu_c}}\right] - (\beta\nu_c - 1)\left[e^{\frac{(M_{\max}-m)(\beta\nu_c + 1)}{\nu_c}}\right] - 2\right\}, \qquad (3.2.29)$$

which is the joint probability distribution function of the apparent magnitude.

Then by applying the maximum likelihood methodology (Engelhardt and Bain, 1992), we first need to find the joint probability distribution function, $L(\beta) = \prod_{i=1}^{n} f_{M_i}(m_i)$, of the apparent magnitudes $(M_1, M_2, ..., M_n)$ for a given set of observations $(m_1, m_2, ..., m_n)$:

$$L(\beta) = \left\{\prod_{i=1}^{n} \frac{\beta e^{-\beta m_i}}{2\left(e^{-\beta M_{\min}} - e^{-\beta M_{\max}}\right)\left(\beta^2\nu_c^2 - 1\right)}\left\{(\beta\nu_c + 1)\left[e^{\frac{(m_i - M_{\min})(\beta\nu_c - 1)}{\nu_c}}\right] - (\beta\nu_c - 1)\left[e^{\frac{(M_{\max}-m_i)(\beta\nu_c + 1)}{\nu_c}}\right] - 2\right\}\right\}$$

$$= \frac{\beta^n}{2^n\left(e^{-\beta M_{\min}} - e^{-\beta M_{\max}}\right)^n\left(\beta^2\nu_c^2 - 1\right)^n} e^{-\beta\sum_{i=1}^{n} m_i} \times$$

$$\prod_{i=1}^{n}\left\{(\beta\nu_c + 1)\left[e^{\frac{(m_i - M_{\min})(\beta\nu_c - 1)}{\nu_c}}\right] - (\beta\nu_c - 1)\left[e^{\frac{(m_i - M_{\max})(\beta\nu_c + 1)}{\nu_c}}\right] - 2\right\}. \qquad (3.2.30)$$

We assume that the observed magnitudes are independent form one another, since earthquake catalogues list distinct seismic events. We can find a maximum likelihood estimator for β by solving the following equation

$$\frac{\partial}{\partial\beta}\ln L(\beta)=0 \tag{3.2.31}$$

It follows that

$$\begin{aligned}\ln L(\beta) &= n\ln\beta - n\ln 2 - n\ln\left(e^{-\beta M_{\min}} - e^{-\beta M_{\max}}\right) - n\ln\left(\beta^2\nu_c^2 - 1\right) - \beta\sum_{i=1}^{n} m_i \\ &+\sum_{i=1}^{n}\ln\left\{(\beta\nu_c+1)\left[e^{\frac{(m_i-M_{\min})(\beta\nu_c-1)}{\nu_c}}\right] - (\beta\nu_c-1)\left[e^{\frac{(m_i-M_{\max})(\beta\nu_c+1)}{\nu_c}}\right] - 2\right\}\end{aligned} \tag{3.2.32}$$

and

$$\begin{aligned}\frac{\partial}{\partial\beta}\ln L(\beta) &= \frac{n}{\beta} - \sum_{i=1}^{n} m_i + \frac{n\left(M_{\max}e^{\beta M_{\min}} - M_{\min}e^{\beta M_{\max}}\right)}{\left(e^{\beta M_{\min}} - e^{\beta M_{\max}}\right)} + \frac{n2\nu_c^2\beta}{\left(\nu_c^2\beta^2-1\right)} \\ &+\sum_{i=1}^{n}\left\{\frac{\left(\nu_c+(m_i-M_{\min})(\beta\nu_c+1)\right)\left[e^{\frac{(m_i-M_{\min})(\beta\nu_c-1)}{\nu_c}}\right] - \left(\nu_c+(m_i-M_{\max})(\beta\nu_c-1)\right)\left[e^{\frac{(m_i-M_{\max})(\beta\nu_c+1)}{\nu_c}}\right]}{(\beta\nu_c-1)\left[e^{\frac{(m_i-M_{\max})(\beta\nu_c+1)}{\nu_c}}\right] - (\beta\nu_c+1)\left[e^{\frac{(m_i-M_{\min})(\beta\nu_c-1)}{\nu_c}}\right] + 2}\right\} \\ &= 0.\end{aligned} \tag{3.2.33}$$

If we equate the above partial derivative to zero and divide by n to find an expression to evaluate the maximum likelihood estimate for β:

$$\left(\frac{1}{\hat{\beta}}-\bar{m}+\frac{\left(M_{\max}e^{\hat{\beta}M_{\min}}-M_{\min}e^{\hat{\beta}M_{\max}}\right)}{\left(e^{\hat{\beta}M_{\min}}-e^{\hat{\beta}M_{\max}}\right)}\right)+$$

$$+\left\{\frac{2\nu_c^2\hat{\beta}}{\left(\nu_c^2\hat{\beta}^2-1\right)}+\right.$$

$$\left.\frac{1}{n}\sum_{i=1}^{n}\left\{\frac{\left(\nu_c+\left(m_i-M_{\min}\right)\left(\hat{\beta}\nu_c+1\right)\right)\left[e^{\frac{\left(m_i-M_{\min}\right)\left(\hat{\beta}\nu_c-1\right)}{\nu_c}}\right]-\left(\nu_c+\left(m_i-M_{\max}\right)\left(\hat{\beta}\nu_c-1\right)\right)\left[e^{\frac{\left(m_i-M_{\max}\right)\left(\hat{\beta}\nu_c+1\right)}{\nu_c}}\right]}{\left(\hat{\beta}\nu_c-1\right)\left[e^{\frac{\left(m_i-M_{\max}\right)\left(\hat{\beta}\nu_c+1\right)}{\nu_c}}\right]-\left(\hat{\beta}\nu_c+1\right)\left[e^{\frac{\left(m_i-M_{\min}\right)\left(\hat{\beta}\nu_c-1\right)}{\nu_c}}\right]+2}\right\}\right\}$$

$$=0,\qquad(3.2.34)$$

where $\bar{m}=\frac{1}{n}\sum_{i=1}^{n}m_i$. If we let the variance of the error term tend to zero, and subsequently the scale and shift parameter since they are directly proportional to one another, we find:

$$\left(\frac{1}{\hat{\beta}}-\bar{m}+\frac{\left(M_{\max}e^{\hat{\beta}M_{\min}}-M_{\min}e^{\hat{\beta}M_{\max}}\right)}{\left(e^{\hat{\beta}M_{\min}}-e^{\hat{\beta}M_{\max}}\right)}\right)=0,\qquad(3.2.35)$$

which is the maximum likelihood estimator for the bounded magnitude distribution. Furthermore, if we let the maximum possible magnitude tend to infinity, we find:

$$\frac{1}{\hat{\beta}}-\bar{m}+M_{\min}=0\ ,\qquad(3.2.36)$$

which is the Aki-Utsu (1965) maximum likelihood estimate of β, as given by equation (1.1.2) and the derivation is as shown in equation (3.2.20).

We are now able to compare the results of these estimators with more traditional estimators in order to draw inferences about their accuracy and usefulness. Before this comparison is made, an alternative investigation is discussed.

3.3 Alternative method

A possible alternative approach is investigated in which the magnitude errors are incorporated into the parameter estimate, by means of an adaptation of the multivariate case

of Bayes' theorem. This approach has been rejected on several grounds and is discussed in this section.

If we assume that the magnitudes $\left(m_i \ \forall \ i=1,2,...,n\right)$ are observations from populations that follow a Gaussian distribution with means μ_i and the same standard deviation, σ_m, across all populations.

Bayes' Theorem states that:

$$f_X\left[x \mid Y=y\right]=\frac{f_X\left[X\right] f_Y\left[y \mid X=x\right]}{f_Y\left[y\right]} \tag{3.3.1}$$

Where X and Y are random variables with probability distribution functions $f_X\left(x\right)$ and $f_Y\left(y\right)$ respectively. This can easily be extended to the multivariate case by assuming that $X=\vec{X}=(X_1,...,X_n)$, $Y=\vec{Y}=(Y_1,...,Y_n)$, $x=\vec{x}=(x_1,...,x_n)$ and $y=\vec{y}=(y_1,...,y_n)$ or any other combination of single variable and multivariate distributions.

In terms of our assumptions, we have the following information:

$$f_{\vec{X}}\left[\vec{x}\right]=f_{M_1,...,M_n}\left(m_1,...,m_n\right)=\prod_{i=1}^{n}\phi\left(m_i\right)=\prod_{i=1}^{n}\frac{1}{\sqrt{2\pi}.\sigma}\exp\left(-\frac{\left(m_i-\mu_i\right)^2}{2\sigma^2}\right) \tag{3.3.2}$$

which is the joint probability distribution of the magnitudes.

$$f_Y\left[y \mid \vec{X}=\vec{x}\right]=f_\beta\left[\beta \mid M_1=m_1,...,M_n=m_n\right]=L\left(\beta\right)=\prod_{i=1}^{n}\frac{\beta}{\left(e^{-\beta M_{\min}}-e^{-\beta M_{\max}}\right)}e^{-\beta m_i} \tag{3.3.3}$$

which is the conditional distribution of β, given a set of magnitudes. And finally

$$f_Y\left[y\right]=\ell\left(\beta\right)=\int_{M_{\min}}^{M_{\max}}...\int_{M_{\min}}^{M_{\max}}L\left(\beta\right)\prod_{i=1}^{n}\phi\left(m_i\right)dm_1...dm_n \tag{3.3.4}$$

which is a marginal likelihood where the effects of the magnitudes have been removed from the distribution of β.

We can rearrange the joint probability distribution function of the magnitudes and the conditional distribution of the parameter β as follows:

$$L(\beta)=\prod_{i=1}^{n}\frac{\beta}{\left(e^{-\beta M_{\min}}-e^{-\beta M_{\max}}\right)}e^{-\beta m_i}=\prod_{i=1}^{n}\varphi(\beta) \tag{3.3.5}$$

$$\ell(\beta)=\prod_{i=1}^{n}\int_{M_{\min}}^{M_{\max}}\varphi(\beta)\phi(m_i)\,dm_i=\prod_{i=1}^{n}I(\beta) \tag{3.3.6}$$

By applying Bayes' Theorem using the above information, we can find the joint conditional distribution of the magnitudes, given a specific value for the parameter β, ensuring that the distribution is normalised to comply with the conditions of a probability distribution function:

$$\begin{aligned} f_{\vec{X}}\left(\vec{x}\,|\,Y=y\right)&=\varphi\left(m_1,\ldots,m_n\,|\,\beta=\hat{\beta}\right)\\ &=\frac{L(\beta)\prod_{i=1}^{n}\phi(m_i)}{\ell(\beta)}\\ &=\frac{f_{\beta}\left(\beta\,|\,M_1=m_1,\ldots,M_n=m_n\right)f_{M_1,\ldots,M_n}\left(m_1,\ldots,m_n\right)}{\ell(\beta)}\\ &=\prod_{i=1}^{n}\frac{\phi(m_i)\varphi(\beta)}{I(\beta)} \end{aligned} \tag{3.3.7}$$

and by applying the maximum likelihood methodology we can differentiate the log-likelihood function with respect to β and equate this to zero:

$$\begin{aligned} \ell(\beta)&=\frac{\partial}{\partial\beta}\ln\left(\prod_{i=1}^{n}\frac{\phi(m_i)\varphi(\beta)}{I(\beta)}\right)\\ &=\sum_{i=1}^{n}\frac{\partial}{\partial\beta}\ln\left(\phi(m_i)\right)+\sum_{i=1}^{n}\frac{\partial}{\partial\beta}\ln\left(\varphi(\beta)\right)-\sum_{i=1}^{n}\frac{\partial}{\partial\beta}\ln\left(I(\beta)\right)\\ &=\sum_{i=1}^{n}\frac{\partial}{\partial\beta}\ln\left(\varphi(\beta)\right)-\sum_{i=1}^{n}\frac{\partial}{\partial\beta}\ln\left(I(\beta)\right)\\ &=0 \end{aligned} \tag{3.3.8}$$

By applying the general methodology to the assumptions made regarding the distributions we find an expression for an estimate of β:

$$-\sum_{i=1}^{n} m_i - \sum_{i=1}^{n} \mu_i + n\sigma^2\beta + \sqrt{\frac{2}{\pi}}\left(\sum_{i=1}^{n_1} \frac{e^{-\left(\frac{\sigma^2\beta+\mu_i-M_{\max}}{\sqrt{2\sigma^2}}\right)^2}}{erf\left(\frac{\sigma^2\beta+\mu_i-M_{\max}}{\sqrt{2\sigma^2}}\right)} - \sum_{i=1}^{n_2} \frac{e^{-\left(\frac{\sigma^2\beta+\mu_i-M_{\min}}{\sqrt{2\sigma^2}}\right)^2}}{erf\left(\frac{\sigma^2\beta+\mu_i-M_{\min}}{\sqrt{2\sigma^2}}\right)} \right) = 0 \tag{3.3.9}$$

If we assume that the magnitudes are observations taken from Laplace-distributed populations with means μ_i and shift and scale parameter, ν_c, then we are assuming that:

$$\phi(m_i) = \frac{1}{2\nu_c} e^{\frac{-|m_i-\mu_i|}{\nu_c}} \qquad m_i \in \mathbb{R} \tag{3.3.10}$$

and we obtain another expression for β by solving for $\ell(\beta) = 0$ as above:

$$-\sum_{i=1}^{n} m_i + \sum_{i=1}^{n_1} m_i - \sum_{i=1}^{n_2} m_i - \frac{n_1\nu_c}{\beta\nu_c - 1} - \frac{n_2\nu_c}{\beta\nu_c + 1} = 0$$

where n_1 is the number of observations where the observed magnitude exceeds the mean magnitude and n_2 is the number of observed magnitudes where the observed magnitude is less than the mean magnitude.

Three problems become evident when the estimators derived using this reasoning are investigated. Firstly, all the terms that involve β are dependent on the standard deviation inherent in the distribution of the magnitudes. The normalisation constant has the effect of removing the terms in the expression that will enable us to draw conclusions about the estimators without the effect of the variance.

Furthermore, there is a fundamental issue with the assumption that the magnitudes are all taken from different populations with varying means. The underlying assumption is that each observation is taken from a different population with varying mean values and the same variance. The mean value for each population is not apparent from the data and we are essentially dealing with a sample size of 1 for each population. A possibility may be to look at intervals of magnitudes and estimate the mean as the centre of each of these intervals, however, the issue of the dependency on the variability still remains.

Lastly, when operating under the assumption that the magnitudes are taken from Laplace populations, the estimator excludes all those observations that exceed the mean magnitude, which seems nonsensical. In the light of all of the above problems, it has been decided that the method under investigation would be excluded from the applied tests.

4 Methodology Part 2: Comparing methods of estimation

4.1 Introduction

In order to compare the estimators derived by means of the traditional method with those derived by previous researchers, we need to generate a synthetic data set containing earthquake magnitudes and disturbed by a certain amount of noise in order to simulate the errors inherent in an actual earthquake catalogue.

Since the maximum likelihood estimators that are derived in the previous section have no theoretical solution but can be solved numerically using iterative methods, such as the Newton Raphson, Secant or *Regula Falsi* methods (Press *et al.*, 1992*;* Labuschagne *et al.*, 2006), a single solution of these estimators are only point estimates. This implies that we cannot compare these point estimates in terms of unbiasedness, uniformly minimum variance estimators, often abbreviated as UMVUE, or relative efficiency (Engelhardt and Bain, 1992).

We look at a number of point estimates in order to assess the asymptotic characteristics of these estimators. We compare simple consistency, asymptotic bias and mean squared error consistency in order to establish which method of estimation should be used to estimate β most accurately (Engelhardt and Bain, 1992).

Code has been compiled in Matlab to conduct the calculations described in this section and is included in Appendix C.

4.2 Generating a synthetic earthquake catalogue

A synthetic earthquake catalogue can be generated by means of Monte Carlo simulation. Deciding on the characteristics of a specific site are the primary inputs for the simulation. The inputs required are:

- $m_{\min}$: the smallest possible earthquake magnitude at the specific site
- $m_{\max}$: the largest possible earthquake magnitude at the specific site
- σ_m: the standard deviation of the errors for each observed magnitude
- b: the b value as defined under the Gutenberg-Richter relation

- λ: the activity rate, i.e. the number of earthquakes greater than $m_{\min}$ that occur per year

For the specific catalogue that have been generated, values specific to South African seismic activity are chosen. However sensitivity testing is conducted in Sections 4.5 and 4.7 to test the robustness of the estimators:

- $m_{\min} = 3.8$
- $m_{\max} = 7.0$
- $\sigma_m = 0.2$
- $b = 1$
- $\lambda = 7.0$

None of the earthquakes are expected to exceed magnitude 7. The largest seismic event in South Africa took place in the Ceres-Tulbagh region in 1969 which exhibited a local Richter magnitude of 6.3 (Kijko *et al.*, 2002). Note that the simulated catalogues include errors that follow either a Normal or Laplace distribution.

Errors should be truncated at a maximum of three standard deviations about the mean value of the error distribution, which is usually zero. The errors are truncated since outliers beyond three standard deviations from a specific magnitude are highly unlikely. Since we can quantify the magnitude of an earthquake by means other than a magnitude measurement on a seismograph, for example the Modified Mercalli Intensity Scale, errors will rarely be larger than 1 unit of magnitude, let alone infinite.

As an example, if we consider the damage caused by a magnitude 5 earthquake, as opposed to a magnitude 6 earthquake, under the same soil conditions, it is highly unlikely that a magnitude 5 earthquake will be mistaken for a magnitude 6 earthquake, and vice versa. Therefore we truncate the errors because we can quantify the effects of an earthquake which means we can quantify the limits of its magnitude.

The program then creates a loop for the time interval specified:

1. Firstly, a random number, u, is generated from a uniform distribution between 0 and 1.

2. Next, provided that the errors follow a Normal distribution, a random number from the standard normal distribution is generated and multiplied by the standard deviation of the errors to convert it to a random number from the distribution of the errors. Alternatively, if the errors follow a Laplace distribution, another random number from a uniform distribution between 0 and 1 is generated, say r , and reduced by 0.5 to obtain a random number from a uniform distribution between -0.5 and 0.5. A random number from a Laplace distribution is then generated by transforming r into *error* by means of $error = -\nu_c\left(\text{sgn}\left(r\right)\right)\ln\left(1-2\left|r\right|\right)$. It is also ensured that this number lies within three standard deviations about the mean, zero. Any error beyond three standard deviations is highly unlikely to occur in terms of the structure of a normal distribution and for practical reasons as discussed above.

3. The loop then proceeds to generate a magnitude for the seismic event by

$$m = \frac{1}{\beta}\left(-\ln\left(e^{-\beta m_{\min}} - u\left(e^{-\beta m_{\min}} - e^{-\beta m_{\max}}\right)\right)\right) + error \qquad (4.2.1)$$

where *error* is the random number generated in step 2 and $b = \beta \log_{10} e$ and which relates to the distribution of the magnitudes, which is assumed to follow a truncated exponential distribution as given in equation (1.1.6). The first term in equation (4.2.1) is found by isolating the unknown variable *m* in equation (4.2.2) and using the random uniformly distributed number between 0 and 1, *u*, that was generated in step 1, as a probability.

4. The time at which the earthquake is expected to have occurred is then generated, smaller time intervals are generated within each iteration of the loop at which seismic events are assumed to have occurred, which are created by using the activity rate parameter, λ . The number of earthquakes exceeding the activity rate parameter per year are assumed to follow a Poisson process and the time at which the i^{th} earthquake occurs, t_{m_i} , is generated by

$$t_{m_i} = t_{m_{i-1}} + \frac{\log\left(1-u\right)}{\lambda} \ . \qquad (4.2.2)$$

Since the waiting times of a Poisson process are exponentially distributed (Engelhardt and Bain, 1992). This ensures that the waiting times are consistent for the seismic catalogue. Equation (4.2.2) is derived in a similar way to equation (4.2.1)

Figure 4.1 shows a particular simulated catalogue as the number of earthquakes against their respective magnitudes. The noise that has been added to the magnitudes is visible. A total of 737 seismic events are generated for a single earthquake catalogue over 110 years in the catalogue depicted. Results for the additional 999 catalogues generated were fairly similar.

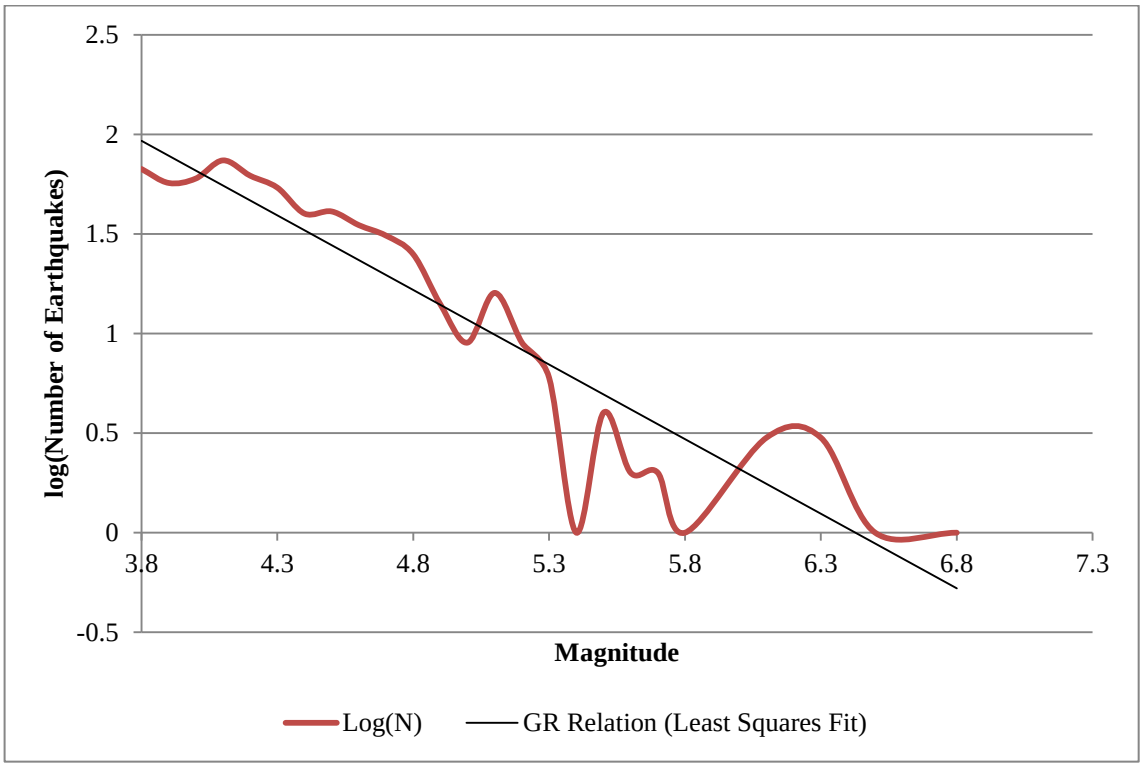

Figure 4.1: Example of a synthetic Earthquake Catalogue perturbed by Gaussian errors

4.3 Applying the formulae for the estimators

Since the maximum likelihood estimators that include errors cannot be solved theoretically, numerical methods have to be employed to establish the point estimates for β. Several numerical methods can be employed but we will consider the Newton Raphson, Secant and *Regula falsi* methods in turn (Labuschagne *et al.*, 2006).

The Newton Raphson method calculates iterations for a root of a function using

$$x_{k+1} = x_k - \frac{f(x_k)}{f'(x_k)}, \qquad k = 0,1,2,... \tag{4.3.1}$$

(Labuschagne *et al.*, 2006) .

Since the estimators are difficult to differentiate, due to the inclusion of the error function, *erf*, the Newton Raphson method is not the ideal method to calculate the point estimates.

The secant method does not require differentiation of the function under investigation, but rather uses the assumption that a derivative can be approximated by the divided difference of a function:

$$f'(x_n) \approx \frac{f(x_n) - f(x_{n-1})}{x_n - x_{n-1}} \tag{4.3.2}$$

(Labuschagne *et al.*, 2006).

The iterations for the secant method can then be calculated using

$$x_{n+1} = x_n - f(x_n)\frac{x_n - x_{n-1}}{f(x_n) - f(x_{n-1})} \tag{4.3.3}$$

which means that we will require two initial values instead of one as for the Newton Raphson method (Labuschagne *et al.*, 2006).

The *Regula falsi*, or false position method, is a refinement of the secant method since it adds the constraint that the function values for the original iteration values chosen must be of opposite sign (Labuschagne *et al.*, 2006). It is preferable since it will always converge and we have a good idea within which interval the root lies.

The false position method starts with two possible root values, a_0 and b_0, which will result in values of the function for which the root is required such that, $f(a_0)$ and $f(b_0)$ are of opposite signs. Therefore we know from the intermediate value theorem that the interval (a_0, b_0) contains a root of function $f(x)$. We can then find a closer approximation to the root by applying the secant method and calculating third value, c_0, by

$$c_0 = b_0 - \frac{f(b_0)(b_0 - a_0)}{f(b_0) - f(a_0)} \tag{4.3.4}$$

which is the root of the secant line through $(a_0, f(a_0))$ and $(b_0, f(b_0))$. The value of the function at c_0 is evaluated. If $f(c_0)$ and $f(a_0)$ are of the same sign then we let $a_1 = c_0$ and $b_1 = b_0$, otherwise $b_1 = c_0$ and $a_1 = a_0$. We repeat the process above using the next iterative approximation of the root until the value of $f(c_k)$ is sufficiently close to zero. It then follows that c_k is a good approximation of the root (Press, *et al.*, 1992, Labuschagne *et al.*, 2006).

Problems arise with the false position method when there is more than one root within the initial interval $[a_0, b_0]$. The equation will struggle to converge to the correct root. We can use the estimate found from the Aki-Utsu estimator, which does not require any iterative methods as an approximation of the root and choose small enough intervals around this estimated value where one value yields a positive function value and the other a negative function value.

4.4 Assessing the asymptotic properties of the methods of estimation when catalogues are generated with Gaussian errors

In order to compare the methods of estimation, the underlying distribution of each estimator had to be established. One thousand earthquake catalogues are generated using the same parameters, as described above. For each iteration the estimators for β are calculated using the different methods of estimation.

The various estimators are then used to calculate the sample mean and variance for each method. These sample estimates are then used to compare the methods in terms of the asymptotic properties of parameter estimates. The estimators themselves are described specifically in Table 4.1. In Figure 4.2, the mean of the estimates is plotted for each estimator over the number of catalogues generated and compared with one another as well as the actual value of β .

Table 4.1: Estimated results

Notation in Graphs	Description	Equation Number
β_1	Aki-Utsu / Classic estimator	(1.1.2)
β_2	Double bounded exponential distribution / Classic bounded estimator	(1.1.8)
β_3	Classic bounded estimator with normally distributed errors	(3.2.18)
β_4	Classic bounded estimator with Laplace distributed errors	(3.2.34)

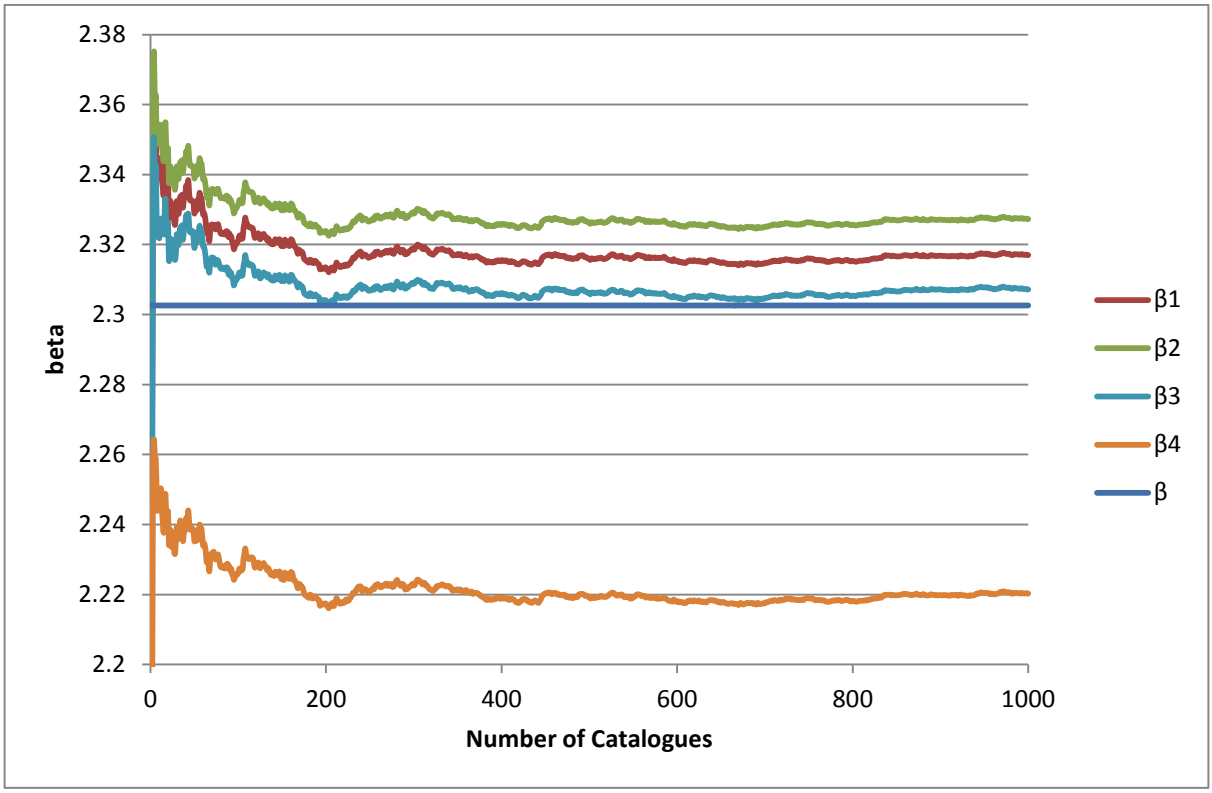

Figure 4.2: Average of estimators when catalogues are perturbed by Gaussian errors

Figure 4.2 demonstrates that there is very little difference between the estimators. It can also be seen that the estimator corrected for normal errors and the bounded classical estimator are closer to the actual value of β, on average. This is expected since the underlying data has been perturbed by normal errors and because the classical bounded estimator is the same estimator, without the perturbation of errors that are relatively small. The first three estimators indicate that on average, they overestimate the true value of β, and the final estimator, that takes Laplace error into account, underestimates the true value of β. It is also evident that the averages of the estimates follow the same pattern, which indicates that the estimates are sensitive to the underlying catalogues.

In order to establish the asymptotic properties of the estimators we first need to examine if the estimators are mean squared error consistent, if they are, it follows that such an estimator is also simply consistent and asymptotically unbiased (Engelhardt and Bain, 1992). The condition for mean squared error consistency is

$$\lim_{n\to\infty} E\left[\hat{\beta}_n - \beta\right]^2 = 0 \ . \tag{4.4.1}$$

Note that $\hat{\beta}_n$ is the series of estimators derived for each simulated catalogue. The mean squared error for each estimate of β for a specific method is calculated. The results are added together and divided by the number of catalogues generated, or estimates found. Those close to zero are deemed to have some measure of mean squared error consistency.

In terms of simple consistency, the absolute error would have to be very small (close to zero) for a large number of estimates of β. Since the earthquake catalogues are generated with a known value of $\beta = 2.3026$, we can calculate each absolute error and count the number of times each error is sufficiently close to zero, say within 0.01 units. By dividing this number by the number of iterations, 1 000, we will obtain the probability that the absolute error is sufficiently close to zero, if this probability is close to 1, the estimator satisfies the condition for simple consistency:

$$\lim_{n\to\infty} P\left[\left|\hat{\beta}_n - \beta\right| < \varepsilon\right] = 1 \tag{4.4.2}$$

for any given $\varepsilon > 0$.

Lastly, the estimators are tested for asymptotic bias. The condition for this asymptotic unbiasedness is

$$\lim_{n\to\infty} E\left[\hat{\beta}_n\right] - \beta = 0 \ . \tag{4.4.3}$$

The sample mean of each method of estimation is calculated and compared to the actual value of β and expressed as a percentage of β by dividing the sample mean less the actual value of β by the actual value of β. Those results that are sufficiently close to zero are deemed to be asymptotically unbiased. The value obtained can then be interpreted as the average bias for the estimator over the number of catalogues investigated. The results of the test for mean squared error consistency, simple consistency and asymptotic unbiasedness are summarised in Table 4.2.

From these tests, we can conclude that all of the methods are likely to yield particularly accurate estimators for β for the particular dataset under investigation. However, since the value of β is not known when applying the methods in practice, further investigation about which kinds of results the different estimators yield will most certainly be helpful. The following section investigates the effect of changes in the underlying parameters on the properties of the estimators.

Table 4.2: Asymptotic properties of the estimators

	β_1	β_2	β_3	β_4
Asymptotic Mean Squared Error	0.008786	0.008804	0.008861	0.016118
Asymptotic Simple Consistency (10% level)	72.1%	72.3%	72.1%	53.5%
Asymptotic Bias	0.6%	1.1%	0.2%	-3.6%

4.5 Sensitivity testing of the estimators when catalogues are generated with Gaussian errors

In order to assess the robustness of the results obtained after the deterministic investigation is conducted a number of the parameters are varied, one at a time, in order to assess their relative effects on the ultimate parameter estimates and their relative asymptotic properties.

The effects of increases in the maximum possible earthquake for the catalogues that are generated are investigated, since this may provide some insight into the effects of larger earthquakes on the estimated parameters. The minimum threshold is not specifically investigated since no notable damage to buildings or infrastructure is observed for earthquakes of magnitude 3.8 or less.

Secondly, the activity rate is also varied to investigate any notable effects on the accuracy of the various parameters. Thirdly, the standard deviation of the errors is varied in order to assess the effects of the size of the errors on the estimates. Lastly, the actual value of the *b* parameter is varied in order to assess the effect of the ratio between small and large earthquakes on the accuracy of different parameters.

Figure 4.3 indicates the changes in mean squared error consistency for each sensitivity test as compared with the benchmark discussed in the previous section. We can conclude from the results that the first three estimators are all fairly mean squared error consistent since for any change in the parameters the average mean squared error remains fairly close to zero.

The average mean squared error for the estimator that includes Laplace errors is slightly less consistent in comparison for most of the parameter changes but is still acceptably low, except in the case where the value of σ is increased by 50% or to 0.3. Here the Laplace estimator seems slightly higher, however, the values of the mean squared error are still fairly low, even for the Laplace estimator at under 3.5%. For the case where the value of σ is increased by 50%, there is also a slight increase in mean squared error inconsistency for the first three estimators as well.

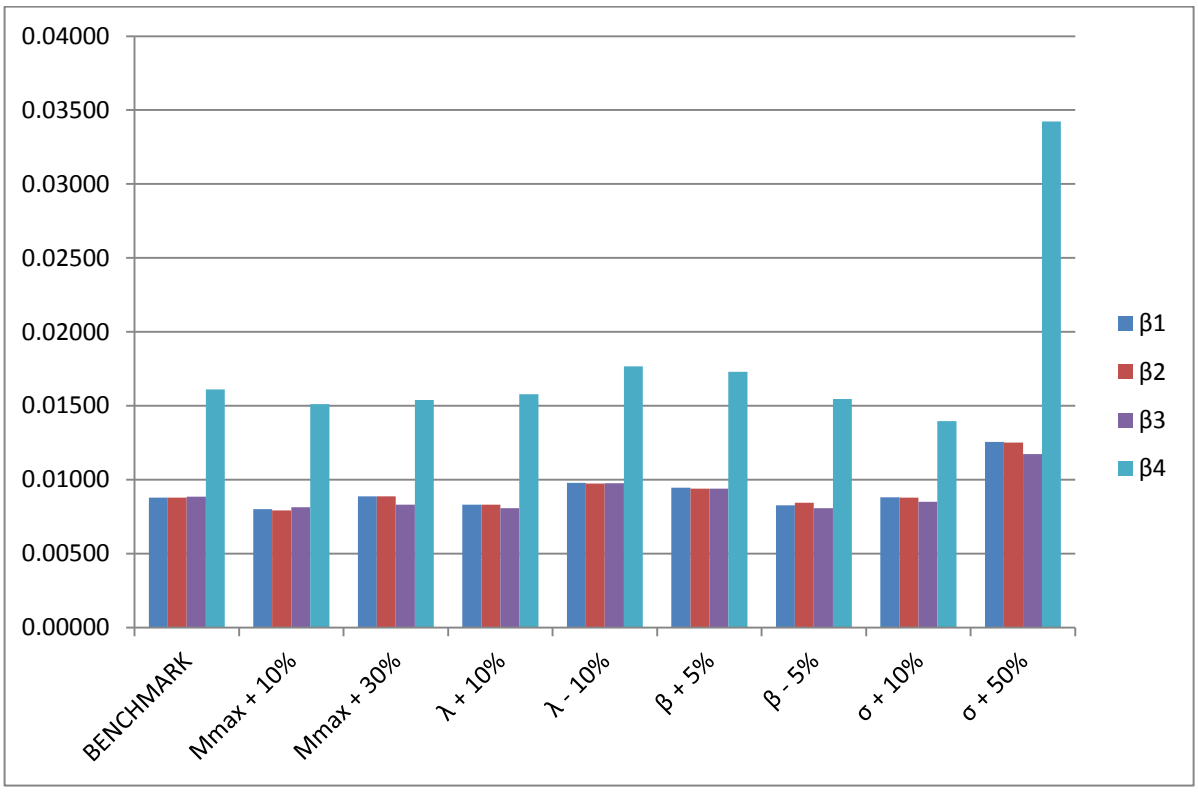

Figure 4.3: A comparison of MSE consistency – underlying Gaussian error

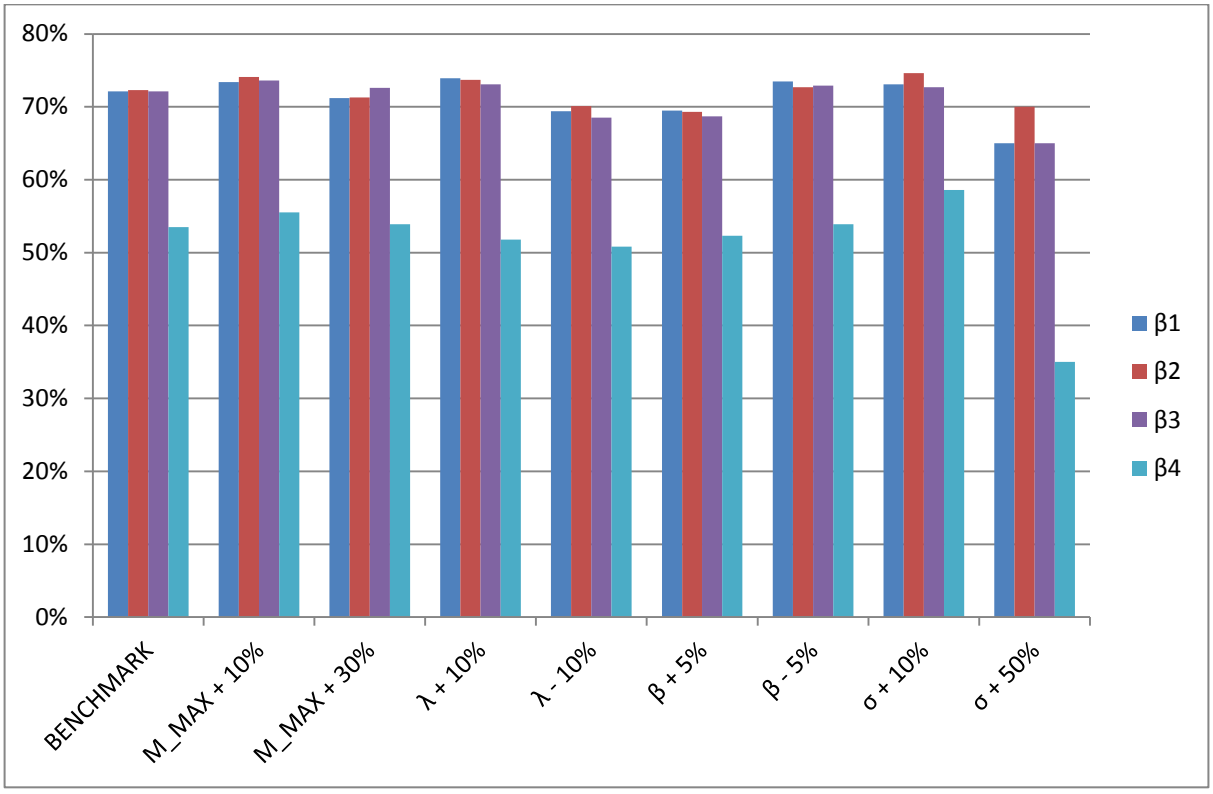

Figure 4.4: A comparison of simple consistency – underlying Gaussian error

Figure 4.4 compares how simple consistency changes with each change in the underlying parameters. Once again there is little to recommend one of the first three estimators above the other two, with all three estimators being fairly consistent indicating that around 70% of the estimates fall within 10% of the actual value of the parameter. The Laplace estimator is not as consistent, however around 55% of the estimates still fall within 10% of the actual parameter value, except for the case where the standard deviation of the errors is increased by 50% where only 35% of estimates fall within 10% of the actual parameter value.

Figure 4.5 demonstrates a comparison between the asymptotic biases of each estimator, with different underlying assumptions. From the results we can conclude that the Classic bounded estimator, β_2 and the Gaussian estimator, β_3 are the most asymptotically unbiased out the four estimators since these are closest to zero, except in the case where the maximum possible earthquake is increased by 30%, where β_1 is marginally closer to zero. The classic estimator, β_1, follows closely behind β_3 in term of lack of bias. The Laplace estimator is not particularly biased in its own right, with all scenarios underestimating the actual value of the parameter by just fewer than 4%. It should be noted that the Laplace estimator appears to become less biased as the standard deviation of the errors increases. The bias is not particularly large in any of the cases with the highest bias having an absolute value of approximately 3.5%.

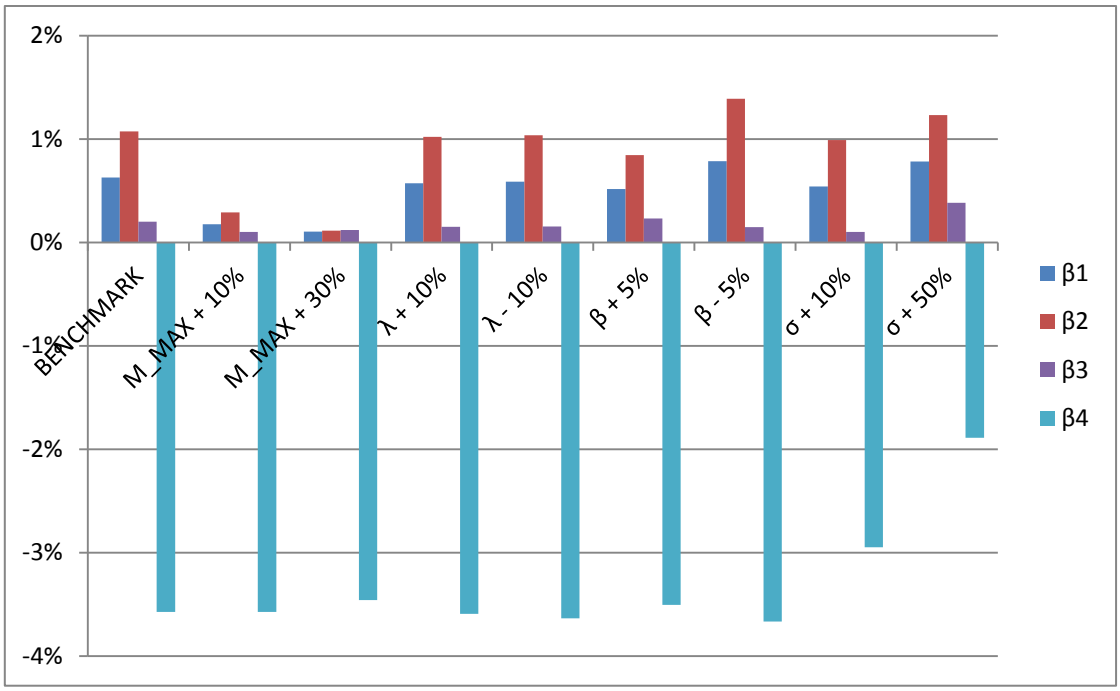

Figure 4.5: A comparison of asymptotic bias - underlying Gaussian error

While the estimator comparison study does much to recommend one estimator over another in a controlled environment, that is one where we control the underlying distributions and parameters of the data, we have to consider further implications of the changes in parameters on actual earthquake catalogues. However, we can conclude that the Laplace estimator is clearly not the best possible choice when the underlying errors cannot be characterised by a distribution with increased probabilities of large errors and decreased probabilities of smaller errors.

We need to extend the hazard analysis of the catalogue into a risk assessment pertaining to building damage. Firstly, we need to consider the case where the synthetic catalogues are perturbed by Laplace errors after which the following section examines the parameters underlying a seismic event catalogue and how changes in the parameters will result in changes in the damage to buildings.

4.6 Assessing the asymptotic properties of the methods of estimation when catalogues are generated with Laplace errors

In order to further compare the methods of estimation, the properties of each estimator needs to be established. One thousand, earthquake catalogues are generated using the same parameters, per iteration as described in Section 4.1 above but the errors are generated according to the Laplace distribution using a standard deviation of 0.2.

The various estimators are then used to calculate the sample mean and variance for each method. These sample estimates are then used to compare the methods in terms of the asymptotic properties of parameter estimates. The estimators themselves are described specifically in Table 4.2.

In Figure 4.6, the mean of the estimates are plotted for each estimator over the number of catalogues generated and compared with one another as well as the actual value of β .

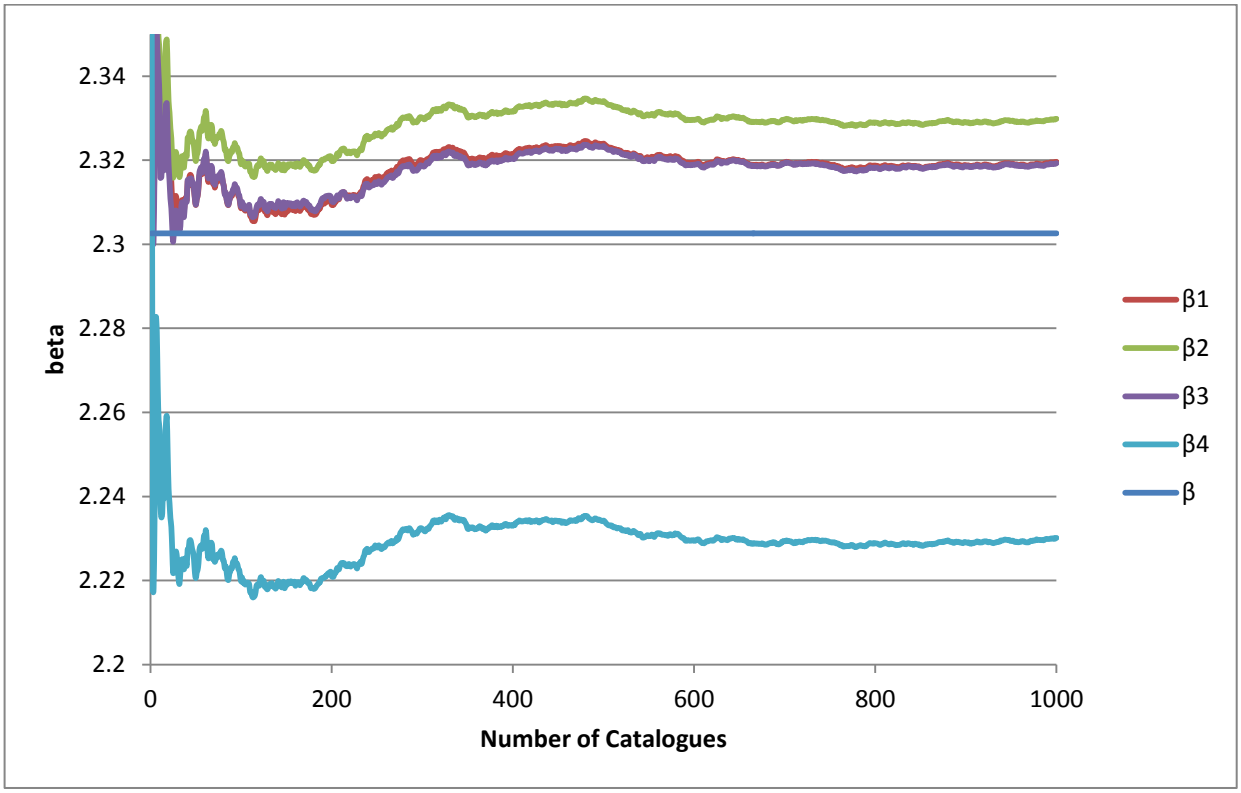

Figure 4.6: Average of estimators when catalogues are perturbed by Laplace errors

The results of the test for the asymptotic properties of the estimates for this particular set of catalogues are summarised in Table 4.3. The mean squared error, simple consistency measure and bias for each estimate of β, for a specific method, is calculated. The results are added together and divided by the number of catalogues generated.

Table 4.3: Asymptotic properties of the estimators

	β_1	β_2	β_3	β_4
Asymptotic Mean Squared Error	0.008114	0.008213	0.008259	0.013819
Asymptotic Simple Consistency (10% level)	71.4%	71.9%	71.0%	57.5%
Asymptotic Bias	0.7%	1.2%	0.7%	-3.1%

We see some fairly unintuitive results. The estimators that do not take errors into account, seem to be far more accurate, in terms of asymptotic measures, than the estimates that do take errors into account, although we would expect the opposite to be true. The classic Aki-Utsu estimator and the estimator that incorporates normal errors yield very similar results. We can better understand these results by looking at Figure 4.7. Here we can clearly see what perturbing by Laplace errors does to an earthquake catalogue.

The events at higher magnitudes are not consistent with the Gutenberg-Richter relation, but lower magnitudes are fairly consistent. It is suspected that is a result of the truncation of the errors and the assumption that the errors follow a Laplace distribution. Since we are truncating the errors that lie outside three standard deviations of the mean, we are most likely reducing a lot of the synthesised magnitudes to lie closer to the real magnitudes than what they should be.

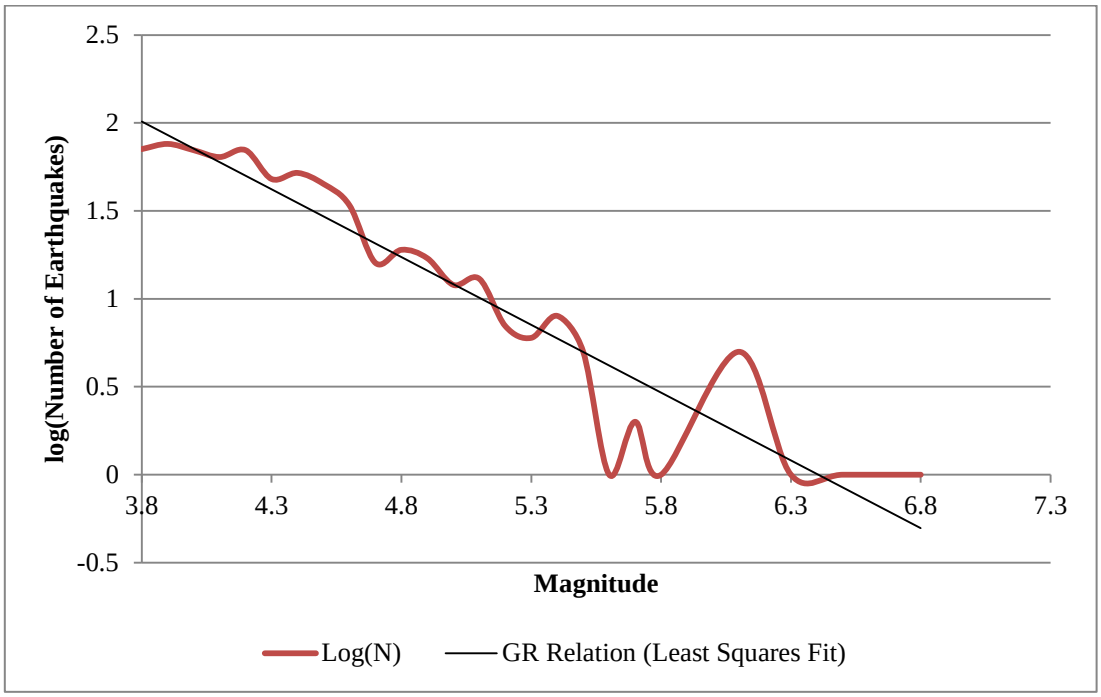

Figure 4.7: Example of a synthetic earthquake catalogue perturbed by Laplace errors

We suspect that the reason that this does not occur as much with the case where we synthesise Gaussian errors is because a much larger probability exists that we will generate an error that lies within three standard deviations of zero. Approximately 90% of all observations from a normal distribution will lie within three standard deviations of the mean. This proportion is lower for the Laplace distribution. Further investigation of the effects of the truncation of the errors on the results where we simulate underlying Laplace errors will

most likely yield more definitive answers about the results. An investigation of the effects of truncation is not included here, but proposed for future expansion of the research.

We will most likely only consider catalogues to have Laplace instead of normal errors when the data is largely historic or paleoseismic in nature. This means that there is a much bigger chance of having large errors than small ones, which is consistent with the Laplace distribution. Generally, only large earthquakes will be included in these catalogues since the events will most likely pre-date the widespread use of seismographs. So for an investigation of fairly complete catalogues that are synthesised according to parameters that are more fitting with those associated with modern catalogues will yield results that are not as expected.

From the preliminary results we can interpret that the classical Aki-Utsu estimator will likely give us accurate results, since it only includes the mean of the magnitudes in the catalogue and the minimum magnitude under consideration. This is not necessarily the case when the level of completeness is raised. We continue to compare the asymptotic properties of the various estimates for the synthesised catalogues in order to establish the sensitivity to changes in the underlying parameters in the following section.

4.7 Sensitivity testing of the estimators when catalogues are generated with Laplace errors

In order to assess the robustness of the results obtained after the deterministic investigation conducted a number of the parameters are varied, one at a time, in order to assess their relative effects on the ultimate parameter estimates and their relative asymptotic properties.

The same sensitivity analyses are conducted for the data generated assuming that the errors follow the Laplace distribution as in Section 4.5 where the errors are assumed to follow the Gaussian distribution. Figure 4.8 indicates the changes in mean squared error consistency for each sensitivity test as compared with the benchmark discussed in the previous section.

As with the previous investigation, the first three estimators are fairly consistent between one another and across different scenarios, with all the average mean squared errors being fairly close to zero. The mean squared error for the Laplace estimator also follows a very similar pattern to the previous investigation, with changes in the value of σ offering the most volatile average mean squared error. Notably, if we consider a smaller standard deviation,

there is very little difference between any of the estimators in terms of asymptotic mean squared error. Another interesting feature to take note of is that the mean squared error for the estimators that include Laplace errors are consistently lower than the mean squared errors for the same estimator in Section 4.6.

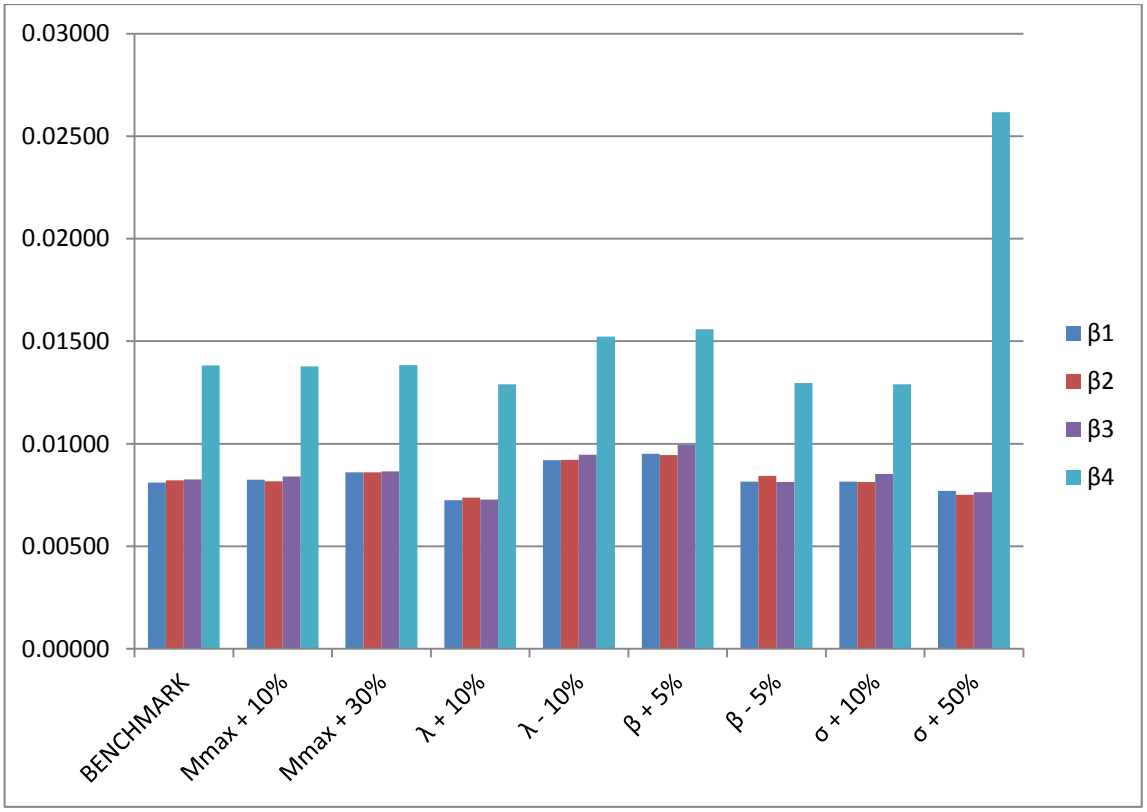

Figure 4.8: A comparison of MSE consistency - underlying Laplace error

Figure 4.9 compares how simple consistency changes with each change in the underlying parameters. The simple consistency measure also does not change significantly from the previous investigation, although all of the estimators are slightly less consistent than in the previous investigation, although the differences for the first three estimators are negligible.

For the Laplace estimator, simple consistency is similar to the previous investigation, with most falling between 50% and 60%. The most inconsistent measures are obtained when varying the value the standard deviation of the errors.

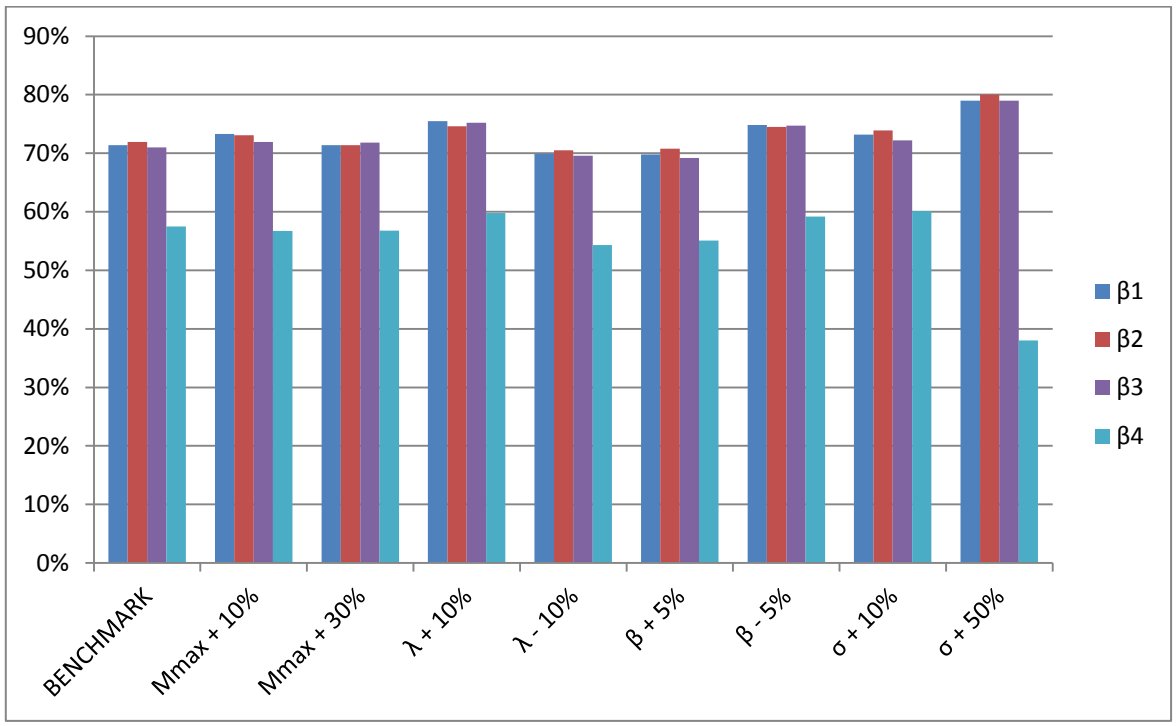

Figure 4.9: A comparison of simple consistency (10% level) - underlying Laplace error

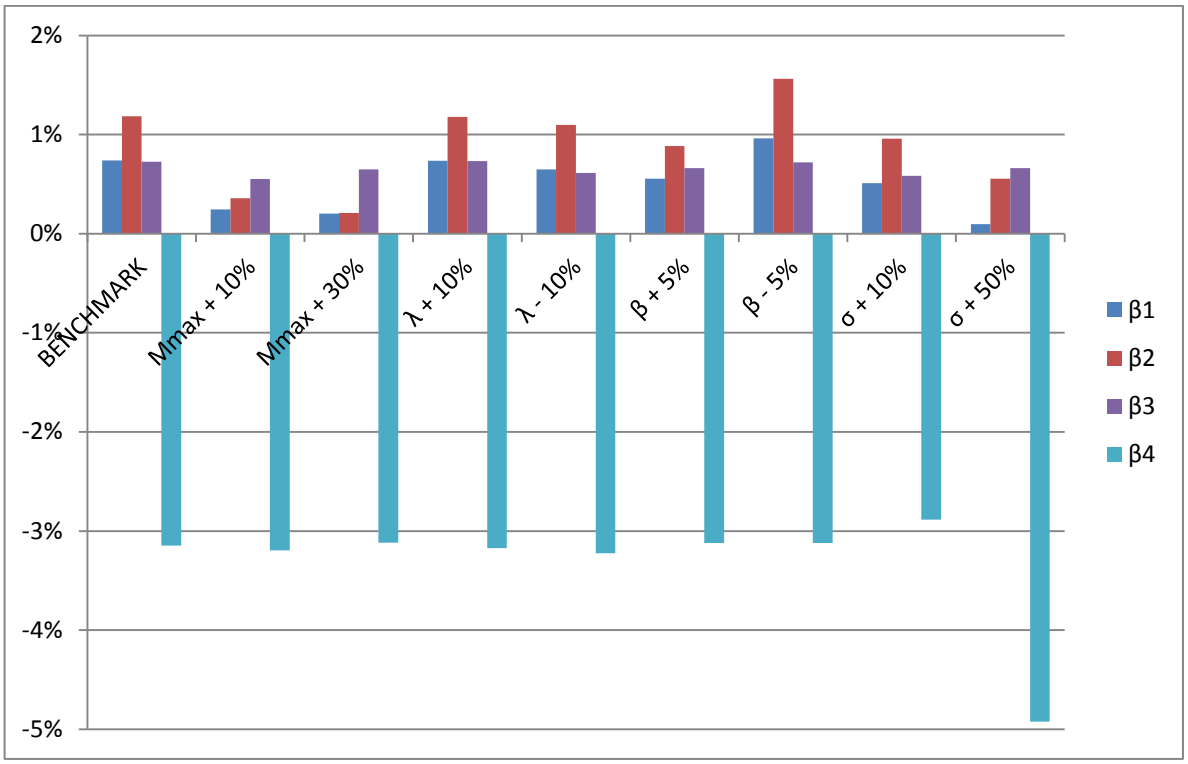

Figure 4.10: A comparison of asymptotic bias - underlying Laplace error

Figure 4.10 demonstrates a comparison between the asymptotic biases of each estimator, with different underlying assumptions. From the results we can conclude that the first three estimators are the most unbiased in the investigation, with different estimators being the most unbiased under different scenarios, but by negligible amounts. The Laplace estimator underestimates the parameter consistently by about 3%, except in the case where the standard deviation is increased by 50%, to 0.3, where the underestimation increases to almost 5%.

While the estimator comparison study does much to recommend one estimator over another in a controlled environment, that is one where we control the underlying distributions and parameters of the data, we have to consider further implications of the changes in parameters on actual earthquake catalogues. The difficulty in assuming that the errors follow a Laplace distribution is demonstrated by the sensitivity tests. We should be cautious when making this assumption for since the truncation of the errors could lead to biased results. It is also important to keep in mind that an investigation of fairly complete catalogues that are synthesised according to parameters that are more fitting with those associated with modern catalogues will yield results that are not as expected since the Laplace assumption is better suited to catalogues that only include large earthquakes.

Furthermore, we need to extend the hazard analysis of the catalogue into a risk assessment pertaining to building damage. The following section examines the parameters underlying a seismic event catalogue and how changes in the parameters will result in changes in the damage to buildings.

5 The effect of seismic parameters on insurance losses

5.1 Background: The South African seismic landscape

South Africa's seismic experience is characterised by relatively frequent small events (i.e. those smaller than magnitude 3.8), and very few large events. An overall image of the seismic hazard, as characterised by peak ground acceleration with a probability of being exceeded in 50 years of 10% is depicted in Figure 5.1. Additionally, overall seismic activity is depicted in Figure 5.2.

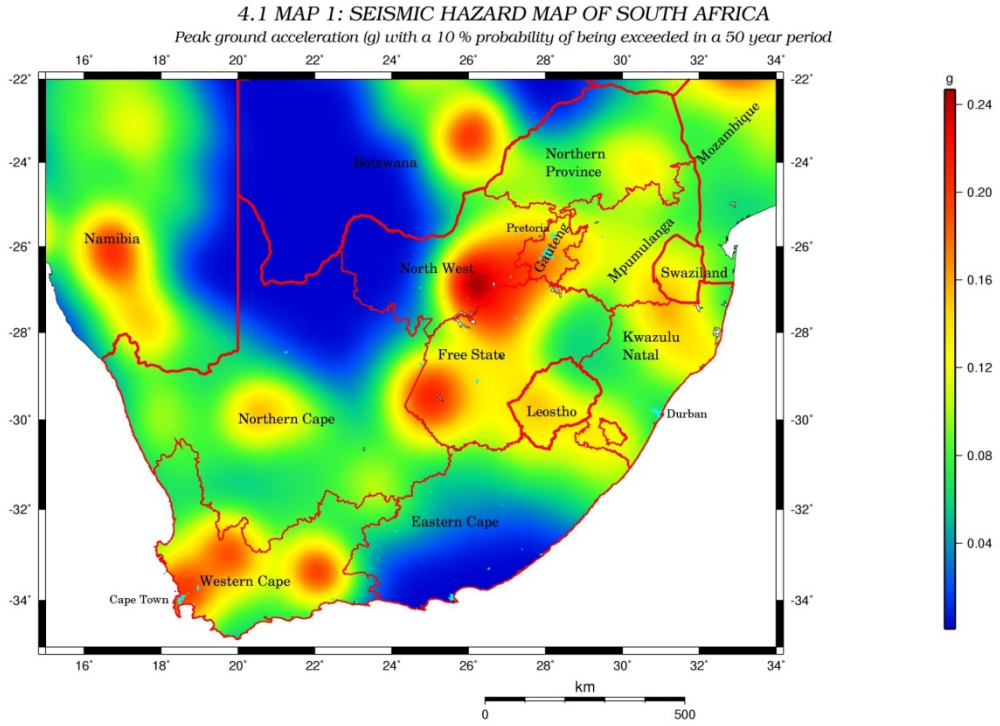

Figure 5.1: PGA probability of exceedance for South Africa (Kijko, 2008)

Seismicity in South Africa dates back to 1620, and various events have taken place. Most information has been gathered from various sources. A number of notable events have taken place in the country with three major events taking place in the latter half of the 20th century. Since 1971, a network of seismological stations has been developed in South Africa, and is called the South African Seismological Network. The network is operated by the Seismology Unit of the Council for Geoscience (Council for Geoscience, 2012).

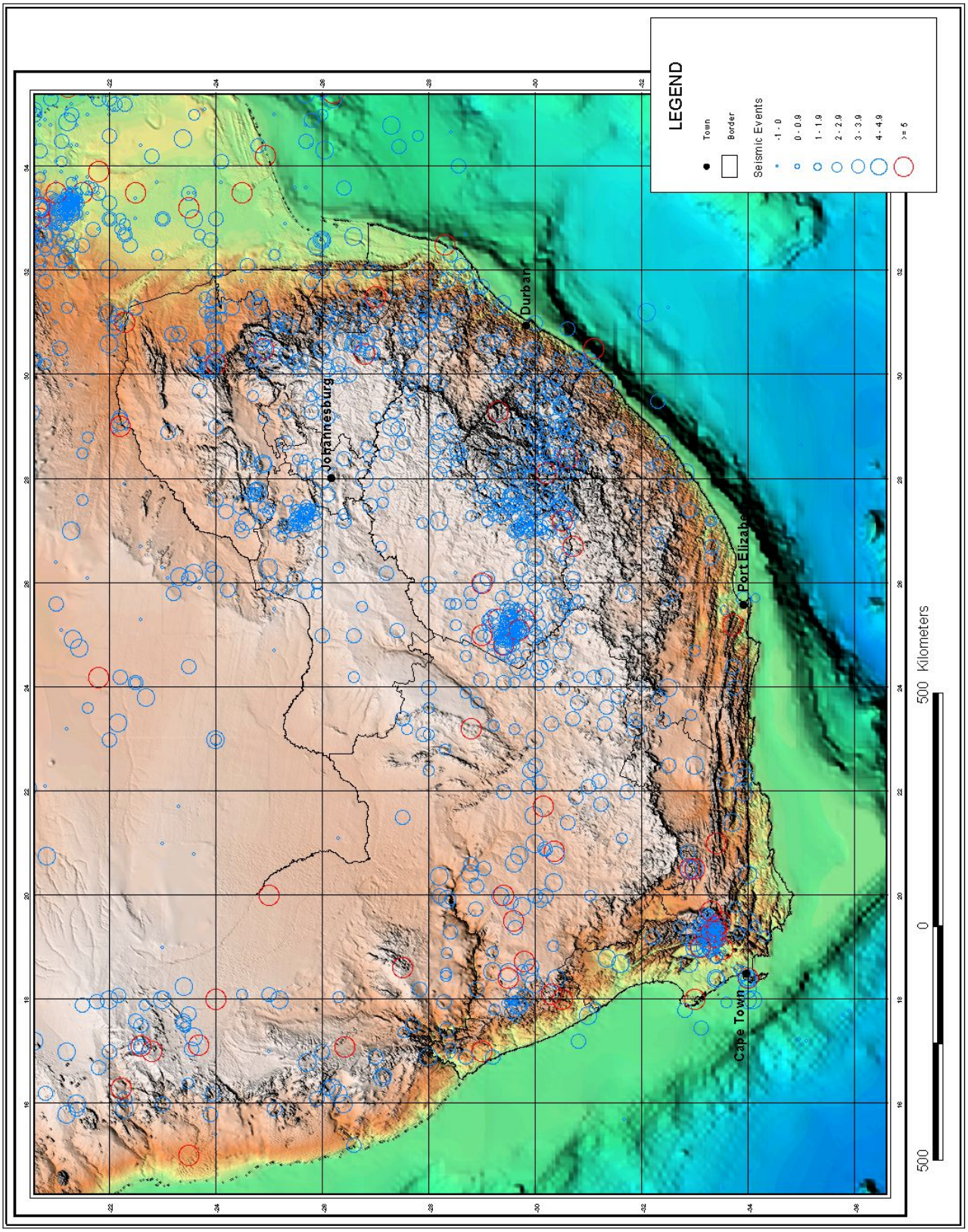

Figure 5.2: Seismic map of South Africa (Council for Geoscience, 2012)

The largest seismic event in South Africa took place in the Ceres-Tulbagh region on 29 September, 1969 which exhibited a local Richter magnitude of 6.3. The damage caused by this event is depicted in Figure 5.3, Figure 5.4 and Figure 5.5 (Kijko *et al.*, 2002, Davies and Kijko, 2003). This earthquake was followed by a number of aftershocks that lasts a considerable amount of time, the largest of which was an aftershock of local Richter magnitude 5.7 on 14 April 1970 (Kijko *et al.*, 2002).

Figure 5.3: Damage following the Ceres-Tulbagh earthquake of 1969 (ceresmuseum.co.za, 2014)

Figure 5.4: Damage following the Ceres-Tulbagh earthquake of 1969 (Cape Town Gazette)

Figure 5.5: Damage following the Ceres-Tulbagh earthquake of 1969 (ceresmuseum.co.za, 2014)

The second, notable seismic event that caused damage in South Africa, occurred in Welkom in 1971 and was recorded as having a magnitude of 5.2. Some of the damage caused by this event is illustrated in Figure 5.6. This event was attributed to mining related activity.

Figure 5.6: Damage following the Welkom earthquake of 1976 (Council for Geoscience, 2010)

A third, more recent event was also attributed to mining related activity and took place at Stilfontein mine in 2005. The event was an earthquake of magnitude 5.3, which not only caused damage on the surface, as depicted in Figure 5.7, but also caused mine operations to be suspended for several weeks following the death of two miners (Durrheim *et al.*, 2006).

Figure 5.7: Damage following the Stilfontein earthquake of 2005 (Durrheim *et al.*, 2006)

5.2 The study

In order to assess the effects of changes in the parameters that describe the seismicity of a specific area, a probabilistic seismic risk assessment can be used with good results. To compare the effect of the different estimators on property damage and consequent insurance losses, a number of PSRAs are conducted for the South African landscape.

The seismic event catalogue used in this study was compiled from several sources. After critical analysis of each of the data sources, the main contribution to pre-instrumentally recorded seismicity come from Brandt *et al.* (2005). The instrumentally recorded events are mainly selected from databases provided by the International Seismological Centre in UK. Various sensitivity tests are conducted, using this catalogue to investigate how changes in the β and λ parameters affect the results of the PSRA. The methods of estimation for β are also applied and compared.

For the purposes of the study, we consider those events with magnitudes of 3.8 or more, since these are the seismic events which will most likely cause significant damage to insured buildings (Kijko and Smit, 2012b). The largest possible earthquake is limited to a magnitude of 7, due to historical seismic activity in South Africa (Davies and Kijko, 2003). A catalogue detailing all the measurable seismic activity in South Africa between 1901 and 2013 is considered. The specific area under consideration is an area with the centre of Cape Town at

its centre and a radius of 450km around this point, as illustrated in Figure 5.8. Notably, this area included the only nuclear power station in South Africa, and the Green Point Stadium which is shown in Figure 5.9. The characteristics of the catalogue are summarised in Table 5.1 (Kijko, 2011).

None of the earthquakes are expected to exceed magnitude 7. The largest seismic event in South Africa took place in the Ceres-Tulbagh region in 1969 which exhibited a local Richter magnitude of 6.3 (Kijko *et al.*, 2002).

Figure 5.8: Map of the area under investigation in the PSRA conducted (AfriGIS (Pty) Ltd, 2014)

Figure 5.9: Image of Green Point Stadium in Cape Town, South Africa (www.woodford.co.za, 2014)

Table 5.1: Characteristics of the earthquake catalogue

Characteristic	Value
Start date	1901
End date	2013
m_{min}	3.8
m_{max}	7.0
$\bar{m}$	4.2
Number of events larger than 4.0	1307
λ	12

Four analyses are conducted in order to investigate the effects of uncertainty and the different methodologies for estimating β:

1. A sensitivity test with varying values of b, namely an assumed value of 1, and estimates of one standard deviation more, and one less than the assumed value.
2. A sensitivity test with varying values of the activity rate, namely the mean activity rate as estimated by evaluating the catalogue, as well as an activity rate of one standard deviation more than the mean rate and one less than the activity rate.
3. A sensitivity test with varying values of the maximum magnitude, as well as a maximum magnitude of 10% more and 10% less than the benchmark maximum magnitude.
4. A side-by-side comparison of the effects of the *b* values that are estimated by the different methodologies discussed in Section 2 and 3 on elements of the PSRA. For the purposes of the methodology investigation, the estimators discussed in Section 2 and 3 are derived for the specific catalogue in question and the PSRA applied and compared. The results are summarised in Table 5.2.

The specific distribution of building classes for metropolitan areas in South Africa is outlined in Table 5.3. Note that four building classes, 3, 7, 8 and 9, make up the majority of the urban structures as mentioned in Section 2. The PSRA used is coded in Matlab and was refined for the purposes of this study. The Matlab code is available on request.

Table 5.2: Estimates of the *b* value using different methods on the same catalogue

Description	Equation Number	*b* value Estimate
Aki-Utsu	(1.1.2)	1.0391
Double truncated exponential distributed magnitudes	(1.1.8)	1.0428
Double truncated exponential distributed magnitudes + Gaussian errors (σ=0.2)	(3.2.18)	1.0995
Double truncated exponential distributed magnitudes + Laplace errors (σ=0.3)	(3.2.34)	0.9855

Table 5.3: Distribution of building class types in metropolitan areas in South Africa

Class	Class Description	Class distribution (% of total replacement costs)
1	Wood frame, low rise	0.09%
2	Light metal, low rise	0.10%
3	Unreinforced masonry, with load-bearing wall, low rise	9.17%
4	Unreinforced masonry, without load-bearing wall, low rise	0.09%
5	Unreinforced masonry, with load-bearing wall, medium rise	5.06%
6	Reinforced concrete shear wall, with moment resisting frame, medium rise	5.14%
7	Reinforced concrete shear wall, with moment resisting frame, high rise	13.80%
8	Reinforced concrete shear wall, without moment resisting frame, medium rise	17.48%
9	Reinforced concrete shear wall, without moment resisting frame, high rise	46.01%
10	Braced steel frame, low rise	0.79%
11	Precast concrete, low rise	0.51%
12	Long span, low rise	0.99%

(Davies and Kijko, 2003)

For the investigations the adjusted Atkinson and Boore attenuation formulas were used as discussed in Kijko *et al.* (2002). The values of the coefficients, given in Table 5.4, describe the regression coefficients for formula (2.3.1) are used for the calculation of the PGA and the spectral acceleration for different frequencies.

Table 5.4: Regression coefficients for the attenuation formula (2.3.1)

Frequency (Hz)	c_1	c_2	c_3	c_4
0.5	-10.798	1.614	0.0042	-1.250
1.0	-9.213	1.531	0.0040	-1.237
2.0	-7.280	1.392	0.0032	-1.228
3.0	-5.927	1.276	0.0028	-1.259
5.0	-4.38	1.123	0.0021	-1.283
7.9	-3.452	1.042	0.0006	-1.279
10.0	-3.123	1.039	0.0002	-1.324
13.0	-2.749	0.982	-0.0011	-1.283
20.0	-2.346	0.968	-0.0033	-1.289
PGA	-2.682	0.980	0.0006	-1.522

(Kijko *et al.*, 2002)

5.3 Results

5.3.1 Investigation 1: Varying the *b* values

Three different permutations of the PSRA are conducted for values of *b* of 0.95, 1 and 1.05 compared to examine any notable differences. Figure 5.10 demonstrates the different distributions of the return period for a range of peak ground acceleration values.

Figure 5.10 demonstrates the relationship between the weighted mean losses of the building classes, with weights as shown in Table 5.3, against the levels of modified Mercalli intensity. Finally, Figure 5.12 demonstrates the probabilities of achieving certain levels of loss if the building classes are combined as in Table 5.3.

When considering Figure 5.10 and Figure 5.11 in terms of insurance losses, we have to consider at both figures independently. The figures imply, and reiterate the intuitive assumption, that variation in the parameters related to the Gutenberg-Richter relation will only affect the peak ground acceleration values directly and will not influence how intensity will affect losses. This relationship is defined by the building type and earthquake intensity and not by the seismic characteristics of a particular area. This means that we know that the variation in losses associated with earthquakes in this particular study is due to changes in

the parameters that define the seismicity of the region. Therefore we can draw no further inference about the differences from Figure 5.11.

From Figure 5.10 some inferences can be made regarding the peak ground acceleration. As expected, a higher *b* value will lead to a quicker acceleration of the return period. Conversely, the lower *b* value implies a much slower acceleration of the return period in terms of peak ground acceleration. It is also notable that the maximum return period for a PGA of around 0.7g is much higher that for the models with higher *b* values. Notably, deviation of the three *b* values only occurs after a peak ground acceleration of 0.3g or even 0.4g has been reached.

From consideration of Figure 5.10 and Figure 5.11 we know that the variation in Figure 5.12 is solely due to the effect of changes in the *b* value on the peak ground acceleration since there is no difference between the mean damage connected to Modified Mercalli Intensity when considering different parameter values (Kijko and Graham, 1998). This is because the same level of damage is expected for any intensity. The changes in parameters are only relevant when considering the PGA (Kijko and Graham, 1998).

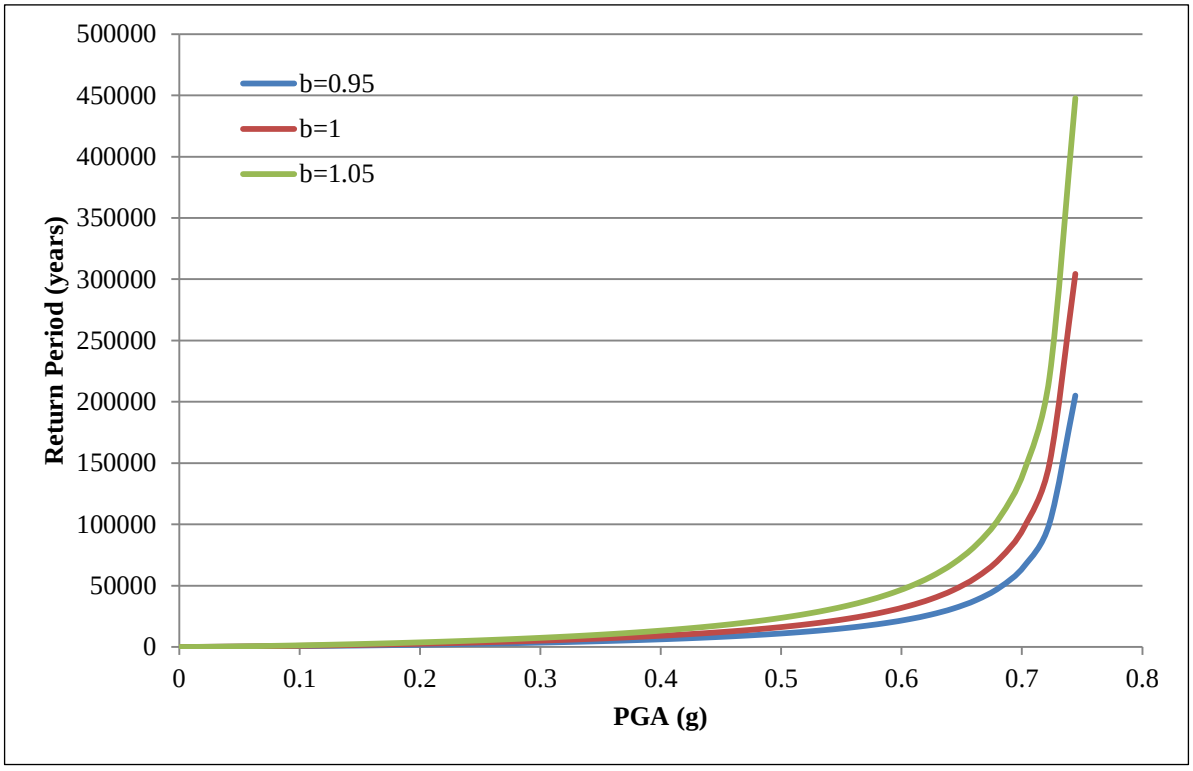

Figure 5.10: Return periods for varying *b* values for Cape Town

When considering individual building classes, the results look very similar to Figure 5.12. Therefore considering the mean damage is a good approximation of a well-balanced portfolio of insurance risks and small deviations from the mean distribution are negligible. The results depicted in Figure 5.12 also make intuitive sense.

Higher *b* values will lead to lower probabilities of damage since the ratios of small to large seismic events are larger. This implies that fewer large events will occur in relation to small events that are likely not to cause any real damage to structures. The converse argument holds for lower values of *b*. Variations in the *b* value are once again compared to the benchmark *b* value of 1.

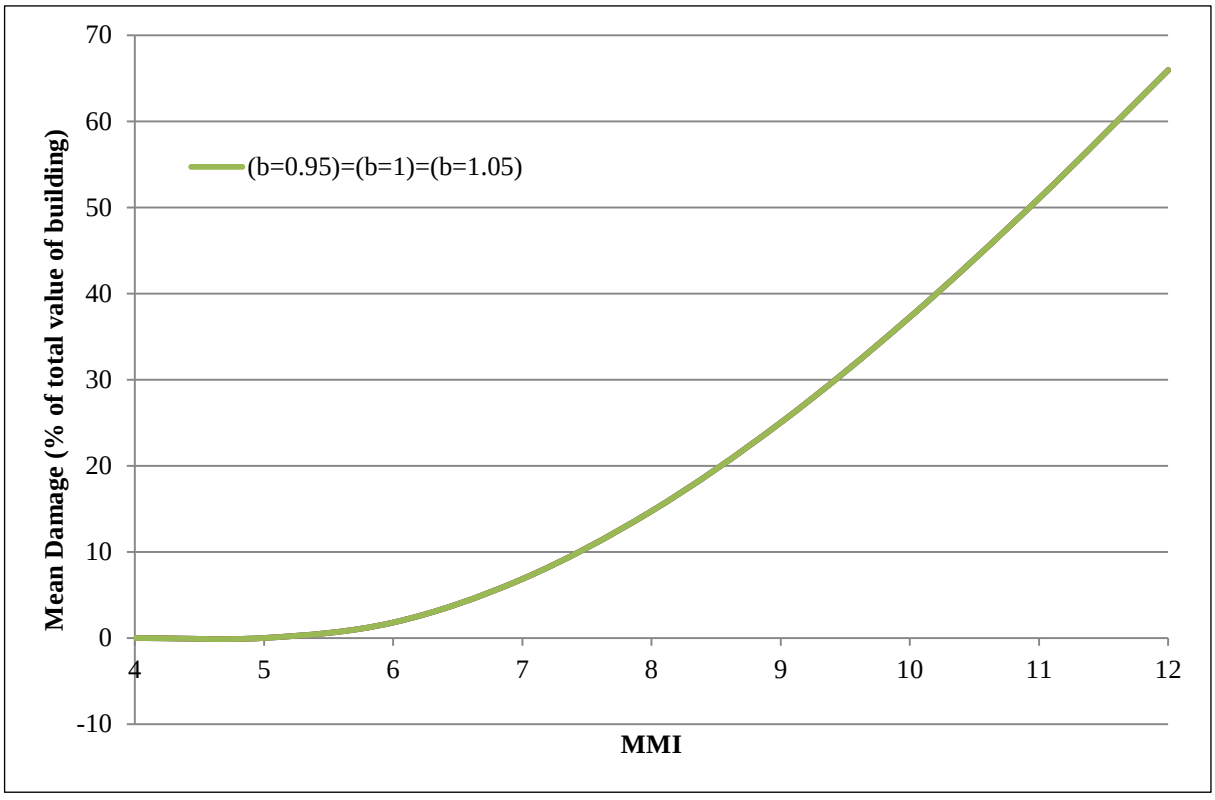

Figure 5.11: Comparison of mean damage per level of intensity for Cape Town

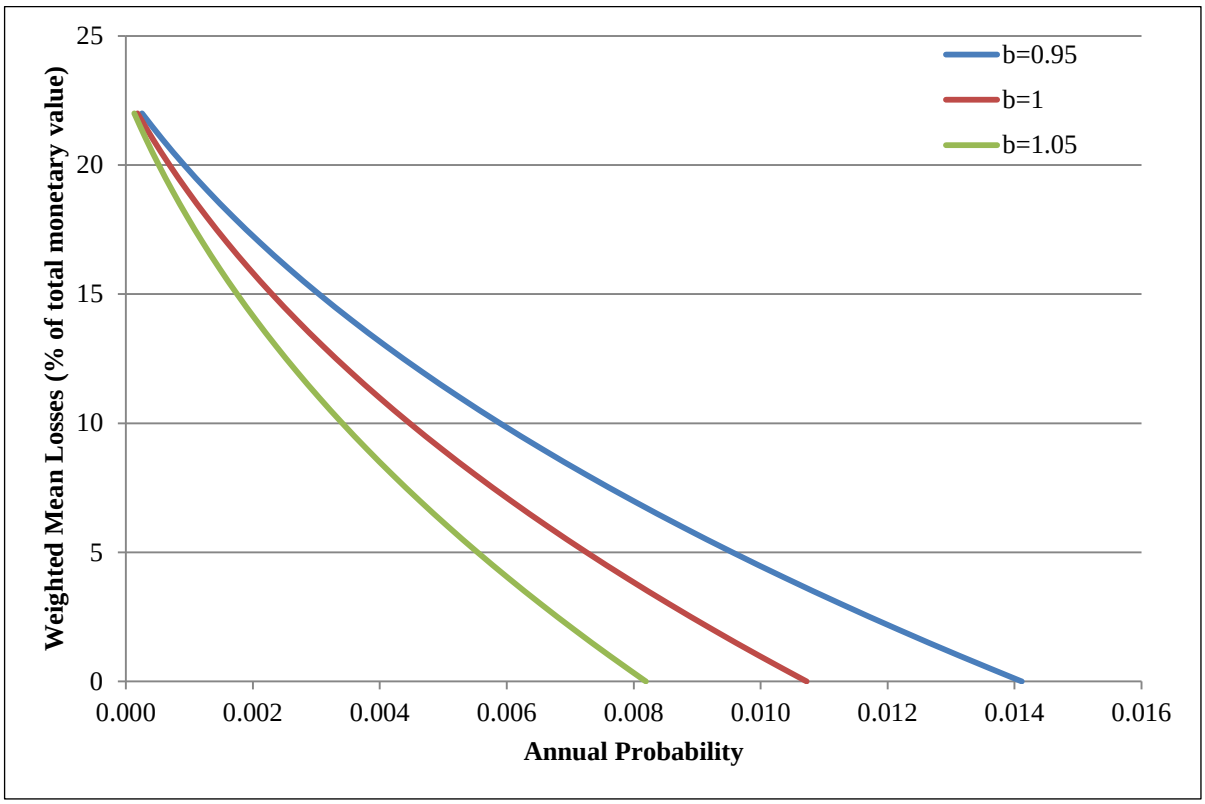

Figure 5.12: Comparison of mean losses for differing *b* values for Cape Town

5.3.2 Investigation 2: Varying the activity rate

Three different permutations of the PSRA are conducted for values of λ of 8, 12 and 16 and compared to examine any notable differences. Figure 5.13 demonstrates the different distributions of the return period for a range of peak ground acceleration values.

A graph demonstrating the relationship between the weighted mean losses of the building classes, with weights as shown in Table 5.3, against the levels of modified Mercalli intensity is not included again since there is no difference between the plots. For reference Figure 5.11 can be used and all arguments about influence of parameters follow from the interpretation of Investigation 1. Figure 5.14 demonstrates the probabilities of achieving certain levels of loss if the building classes are combined as in Table 5.3.

The relationships depicted in Figure 5.13 are consistent with our understanding of the effects of the activity rate or λ. The mean activity rate for seismic events of magnitude 3.8 or higher is calculated as 12 and has been used as the benchmark. Lower values of λ will imply a faster acceleration of the return period for lower peak ground acceleration values. The peak ground acceleration will also be lower than or equal to that of lower values but

with a higher return period. This relationship implies that lower values of λ imply less seismic activity which is exactly the case when we consider the definition of the activity rate (Kijko, 2011).

Conversely, a higher value of λ implies that earthquake activity is increased since peak ground acceleration is higher for lower return periods although acceleration is not as quick. Notably, deviation of the three values for λ only occurs after a peak ground acceleration of 0.1g has been reached.

From consideration of Figure 5.13 and Figure 5.11 we know that the variation is solely due to the effect of changes in the activity rate on the peak ground acceleration. Once again, when considering individual building classes, the results look very similar to Figure 5.14. The results make intuitive sense. Higher activity rates will lead to higher probabilities of loss since more earthquakes above magnitude 3.8 are expected to happen within a single year (Kijko, 2011). The converse argument for lower activity rates holds. Variations in the activity rate are once again compared to the benchmark value of 12. The variation in the probabilities is similar than that of Figure 5.12.

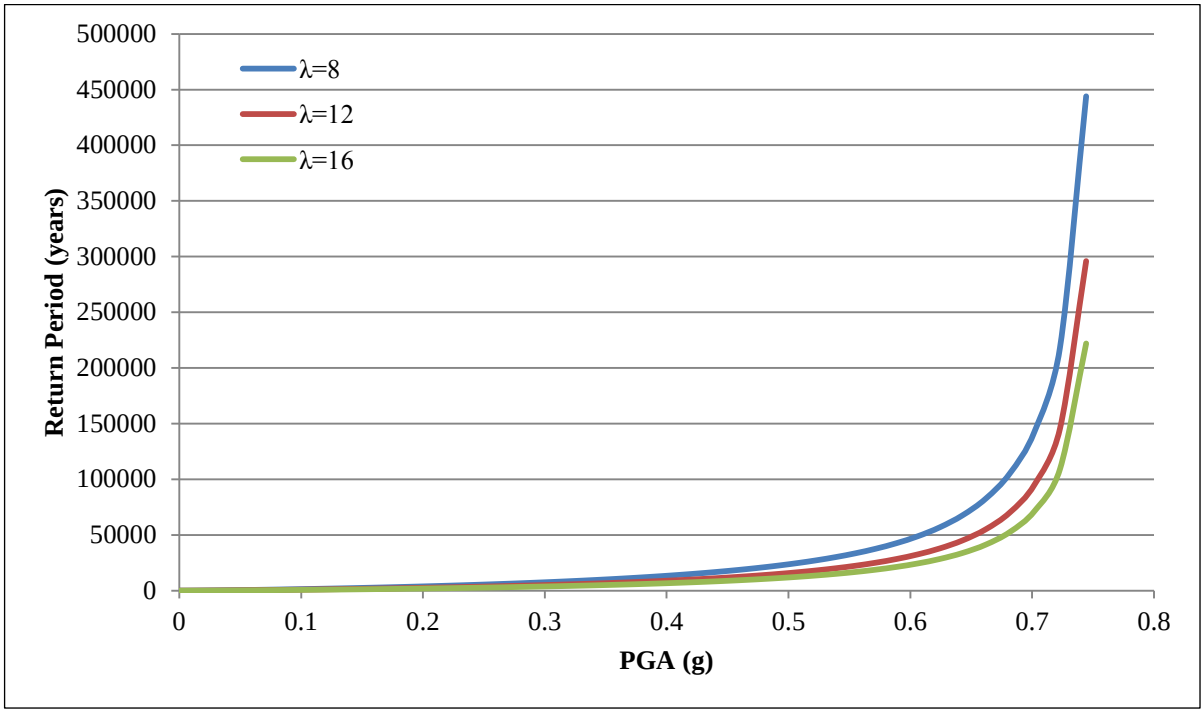

Figure 5.13: Return periods for differing activity rates for Cape Town

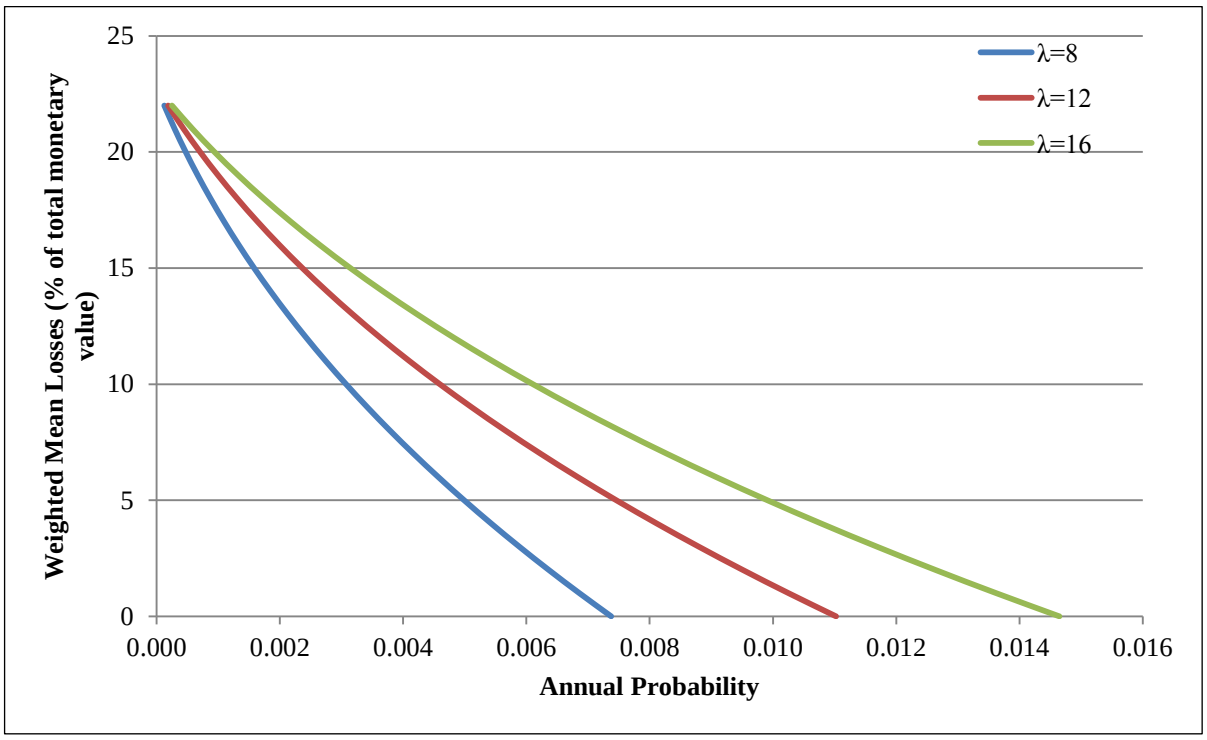

Figure 5.14: Comparison of mean losses for differing activity rates for Cape Town

5.3.3 Investigation 3: Varying the maximum possible earthquake

Three different permutations of the PSRA are conducted for values of the maximum regional magnitude of 7, 7.7 and 6.3 and compared to examine any notable differences. This is a variation of 10% above and below the actual maximum earthquake for the region of magnitude 7.

Figure 5.15 demonstrates the different distributions of the return period for a range of peak ground acceleration values. A graph demonstrating the relationship between the weighted mean losses of the building classes, with weights as shown in Table 5.3, against the levels of modified Mercalli intensity is not included again since there is no difference between the plots. For reference Figure 5.11 can be used and all arguments about influence of parameters follow from the interpretation of Investigation 1. Figure 5.16 demonstrates the probabilities of achieving certain levels of loss if the building classes are combined as in Table 5.3.

We can see here that higher maximum magnitudes values yield higher peak ground acceleration values at longer time intervals than lower maximum magnitudes. There is also very little difference between the loss estimates for varying maximum magnitudes. This is most likely because the maximum magnitude is only being varied by 10%.

If it is varied significantly more, the possible damage caused by the maximum possible earthquake will be significantly different and the loss estimates will differ, especially towards the lower probabilities and higher levels of damage.

It should be kept in mind that the loss estimate is still a function of the catalogue data, so a very large maximum magnitude will not have a significant effect on the loss estimates if there is not a similar magnitude contained in the catalogue. This could be a possible shortfall of the estimates if the catalogue is taken over a period of time that does not include large seismic events.

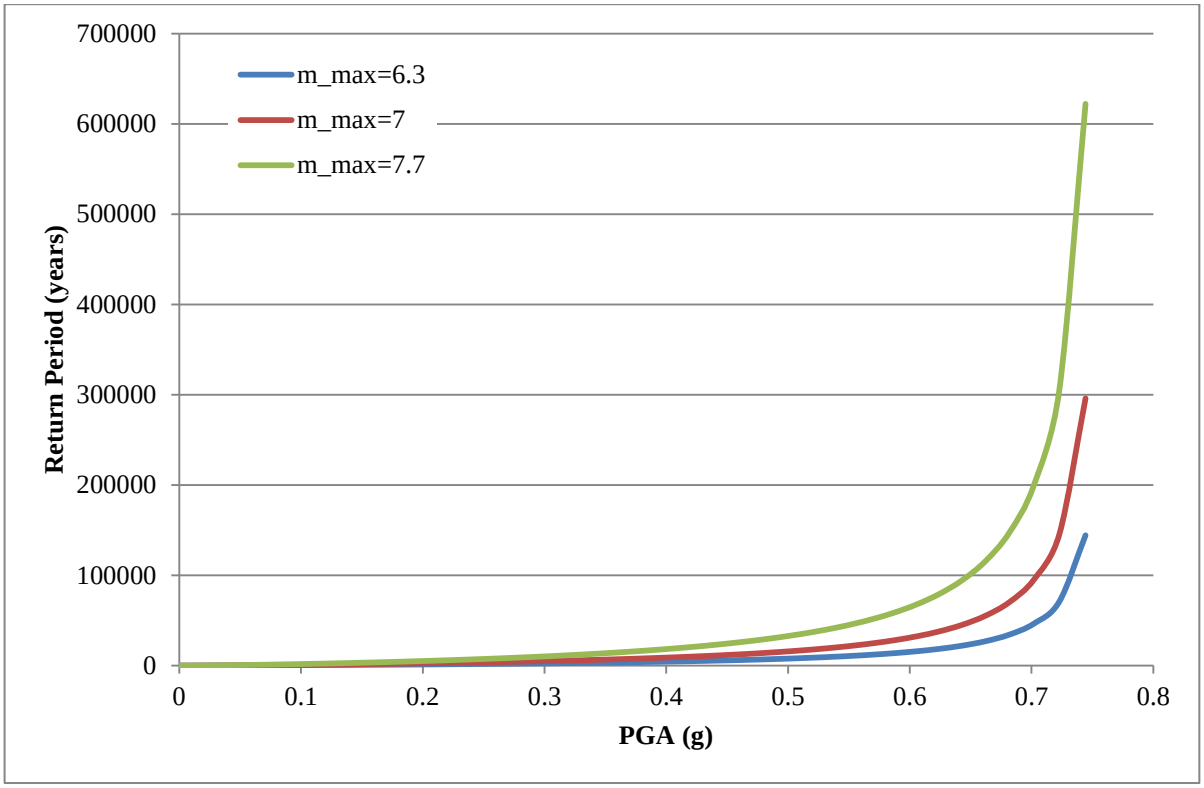

Figure 5.15: Return periods for varying m_max in Cape Town

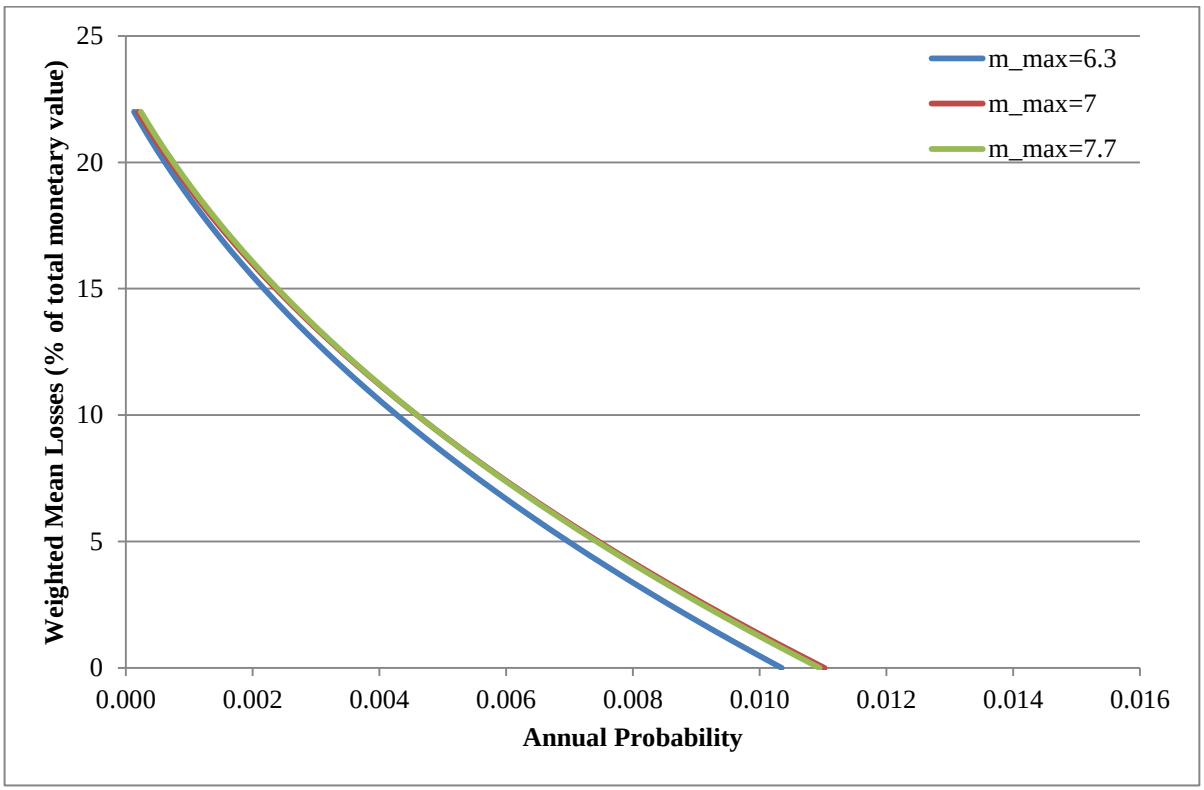

Figure 5.16: Comparison of mean losses for different m_max for Cape Town

5.3.4 Investigation 4: Estimates of the *b* value

Four different permutations of the PSRA are conducted for values of *b* as outlined in Table 5.2 compared to examine any notable differences. Figure 5.17 demonstrates the different distributions of the return period for a range of peak ground acceleration values. A graph demonstrating the relationship between the weighted mean losses of the building classes, with weights as shown in Table 5.3, against the levels of modified Mercalli intensity is not included again. For reference Figure 5.11 can be used and all arguments about influence of parameters follow from the interpretation of Investigation 1. Figure 5.19 demonstrates the probabilities of achieving certain levels of loss if the building classes are combined as in Table 5.3.

In keeping with the results from Investigation 1, lower *b* values yield higher probabilities of mean losses and higher *b* values yield lower probabilities of mean losses. The classic and bounded classic estimates yield results that are very similar. This is expected since their values are close to one another and they are based on similar methodologies. The results

show that the estimator which includes Laplace error has the shortest return periods for given levels of peak ground acceleration. The peak ground acceleration for the estimator that includes Gaussian errors has the highest return period. The differences, however, are not very significant since there is little difference between these return periods.

Interestingly, the estimator that includes Gaussian error is slightly higher than those estimates that do not include errors. The estimates that yield results in the middle of the possible loss distributions are the classical and bounded classical estimates. This is expected since their values are very close to one another. This could mean that there is an argument to be made that the classic estimator continues to be a good approximation of the underlying *b* value contained in earthquake catalogues. However, it is no great exercise to expand the estimate to include the maximum possible earthquake within the region under consideration.

The relationship of the classic estimate with other estimates could imply that the classic estimate is a reasonable estimator for areas of low seismicity, but this is largely dependent on the underlying assumptions and the data, such as the minimum and maximum earthquake values considered.

It must also be noted that the choice of method of estimation for the *b* value is largely a function of the quality of the data. For catalogues where little information is available about their origin and composition, the classic (Aki-Utsu) estimator would be a good place to start. For catalogues that consist of information from a single source, and are fairly recent, the bounded classical estimator will be a reasonable choice.

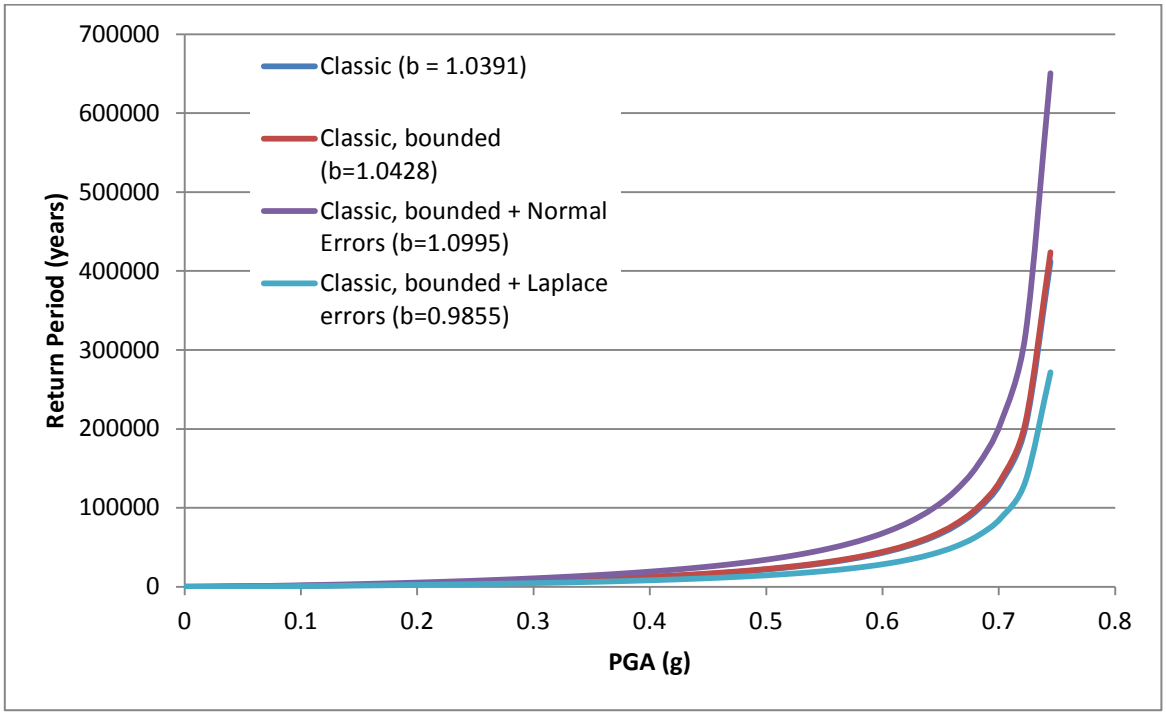

Figure 5.17: Return periods for different estimates of the *b* value for Cape Town

Figure 5.18 shows how the dataset under investigation compares with the cumulative distributions underlying each assumption for each different estimator.

From Figure 5.18 we can interpret that all of the distributions are a fairly good approximation of the actual data, although some may offer a better fit than others. It is interesting to note what the effect of not truncating the distributions that includes errors has on probabilities for magnitudes less than 3.8 and more than 7, *i.e.* those magnitudes that lie outside the bounds of the catalogue. Specifically, the probabilities of magnitude 3.8 or less is higher than zero for those distributions that include errors. These tails are larger than the tails beyond magnitude 7 since the exponential distribution is positively skewed so the resulting joint distribution will also be positively skewed. Furthermore, all of the distributions offer a fairly good visual fit to the observed data but some dominate others for parts of the observed data.

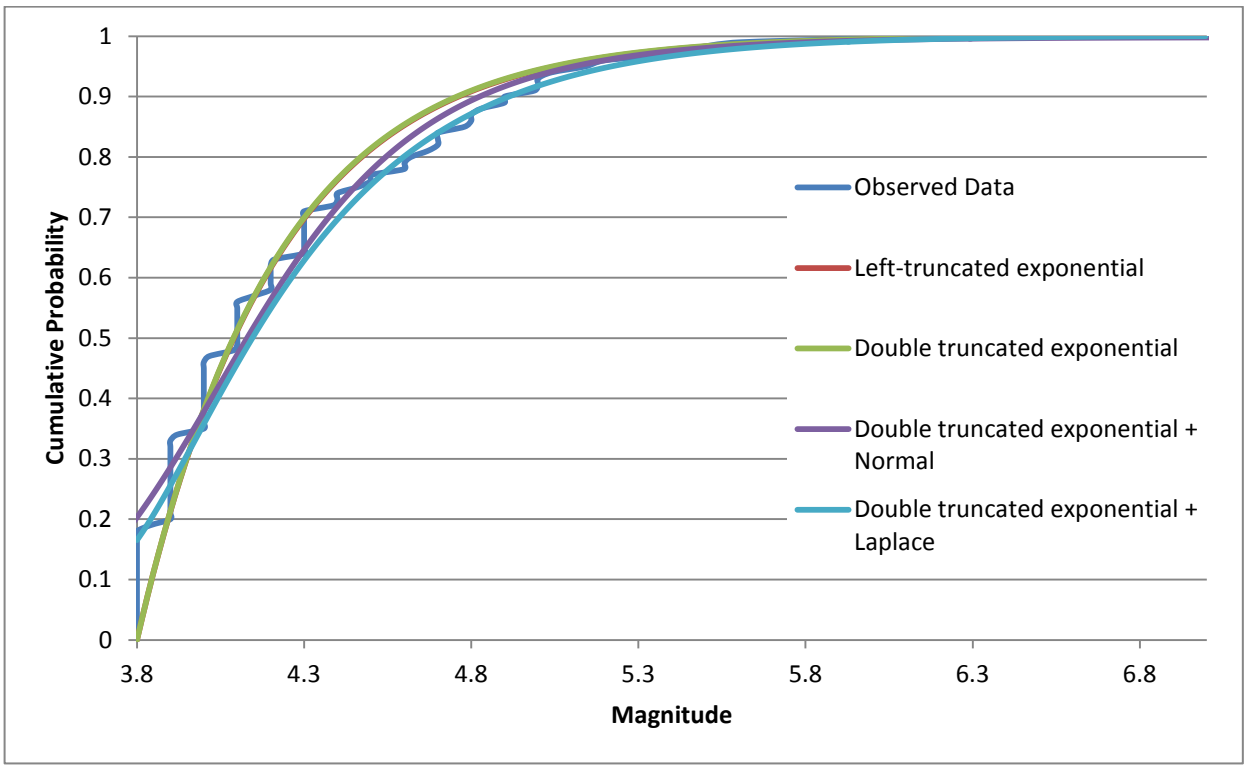

Figure 5.18: Comparison of cumulative distributions described by the estimators with actual data

The observed data seems takes a step-wise form due to the fact that considerable rounding occurs in earthquake catalogues. In this particular data set, magnitudes were only given to 1 decimal place, so it stands to reason that a plot of the cumulative probabilities increase in increments of magnitude of 0.1.

From Figure 5.19 we can conclude that there is very little difference between the probabilities of certain levels of mean losses for the classic Aki-Utsu and classic bounded estimator. This is because they are fairly close in terms of value. Mean losses indicated by the classic bounded estimate of the *b* value that includes normal errors is lower than any other. Finally, the classic bounded estimate that includes Laplace errors indicates the highest mean loss levels for given probabilities. The level of difference can be quite significant. For example, the probability for a 10% mean loss varies from a probability of occurrence of 0.00262 up to 0.00484.

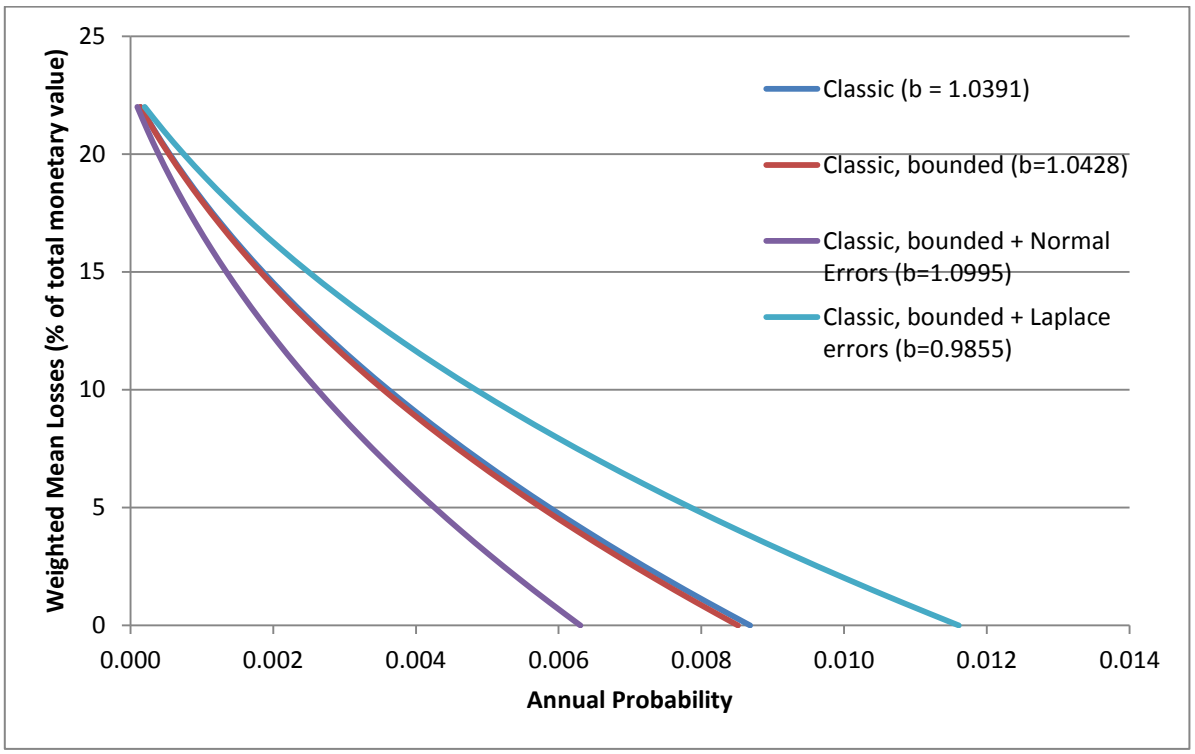

Figure 5.19: Comparison of mean losses for different estimates of the *b* value for Cape Town

When catalogues are compiled using several data sources, several data points may be used to find the best approximation for the magnitude of an earthquake. In these cases, the bounded classical estimator that includes Gaussian errors will be a good choice of method. The additional assumption that observation errors are fairly small, for example a standard deviation from the mean of 0.1 to 0.2 units of magnitude, will be reasonable.

Finally, for catalogues with large probable outliers, in particular historic catalogues, the bounded classical estimator which included Laplace errors will be a good method to employ. The reasonable assumption in such cases is that the observation errors are fairly large, i.e. that the standard deviation of these errors lies around 0.3 units of magnitude for each observation.

6 Conclusion and further research

Increasing global urbanisation means that the potential impact of a catastrophic event, such as an earthquake, is increasing. To this end, insurers are taking a more comprehensive view of managing and understanding risk. The research proposes several ideas that may aid in understanding earthquake risk in an area of low seismicity, such as South Africa.

Parameter estimates are affected by observation errors. If errors are not included in the method of estimation, the estimate is subject to bias. The nature of the errors determines the level of bias. We can therefore conclude that uncertainty in the data used in earthquake parameter estimates is largely a function of the quality of the data that is available. The inaccuracy of parameter estimates depends on the nature of the errors that are present in the data. In turn, the nature of the errors in an earthquake catalogue depends on the method of compilation of the catalogue and can vary from being negligible, for single source catalogues for an area with a sophisticated seismograph network, to fairly impactful, for historical earthquake catalogues that predate seismograph networks.

The research attempts to resolve the problem in two parts, namely, which method of estimation is the most consistent for the parameters of the earthquake model, and how these different methods of estimation, as well as other changes, in the earthquake model parameters affect the damage estimates for a specific area.

Firstly, the research investigates different methods of parameter estimation in the context of the log-linear relationship characterised by the Gutenberg-Richter relation. Traditional methods are compared to those methods that take uncertainty in the underlying data into account. Alternatives based on Bayesian statistics are also investigated briefly. The efficiency of the feasible methods is investigated by comparing the results for a large number of synthetic earthquake catalogues for which the parameters are known and errors have been incorporated into each observation.

The study only refers to the effect of changes in the activity rate as a means of testing the sensitivity of the models. The b value estimation is slightly more complex and previous investigation has not been as extensive. The a value is dependent on the b value and on λ and the assumptions for the latter parameter are not considered explicitly in this study. This research focuses on the estimation of the b value.

Sensitivity tests of the different methods of estimation based on synthetic catalogues with known parameters, indicate that for those catalogues where the underlying errors are assumed to follow a normal distribution, there is little difference between the asymptotic properties of the classic, classic bounded and classic bounded with normal errors added estimators. The asymptotic properties of these estimators are also not very sensitive to changes in the underlying parameters. The classic bounded estimator that includes Laplace errors is less desirable as an estimator under these conditions as indicated by the asymptotic properties and their sensitivity to changes in the underlying parameters. However, under the correct circumstances the classic bounded estimator that included Laplace errors could indicate the most reasonable set of assumptions. The investigations show that the Laplace estimator is not particularly biased in its own right. Additionally it should be noted that the Laplace estimator appears to become less biased as the standard deviation of the errors increases.

For sensitivity tests conducted when synthetic catalogues are perturbed by errors that follow a Laplace distribution, the results are not exactly as expected. Those estimators that do not include Laplace errors demonstrate more desirable asymptotic properties than those estimators that do take Laplace errors into account. Several reasons for these results are proposed, including the truncation of the errors at a maximum of three standard deviations from the mean, but not tested. Further investigation into this particular problem is warranted.

We will most likely only consider catalogues to have Laplace instead of normal errors when the data is largely historic or paleoseismic in nature. This means that there is a much bigger chance of having large errors than small ones, which is consistent with the Laplace distribution. Generally, only large earthquakes will be included in these catalogues since the events will most likely pre-date the widespread use of seismographs (Kijko and Dessokey, 1987). So an investigation of fairly complete catalogues that are synthesised according to parameters that are more fitting with those associated with modern catalogues will yield results that are not as expected. The sensitivity tests in the study were conducted for a catalogue with both small and large events.

In the second part of the study, the effects of changes in key parameters of the earthquake model on damage estimates are investigated. This includes an investigation of the different methods of estimation and their effect on the damage estimates. Probabilistic seismic risk assessments are utilised as a catastrophe modelling tool in order to achieve this.

Probabilistic seismic risk assessment can be used as a catastrophe modelling tool to circumvent the problem of scarce loss data in areas of low seismicity and is applied in this study for the greater Cape Town region in South Africa. The results of the risk assessment demonstrate that seemingly small changes in underlying earthquake parameters as a result of the incorporation of errors can lead to significant changes in loss estimates for buildings in an area of low seismicity.

While subjective to some degree, the PSRA is a good way of testing the potential losses related to seismic events for a particular area. The investigations conducted indicate that variability in the parameters of the Gutenberg-Richter relation influence the probabilities of potential mean losses from seismic activity. Furthermore, the investigations indicate that, for areas of weak seismicity, changes in the parameters have significant effects on loss probabilities.

It can clearly be seen from the results of the investigations that lower estimates of the *b* value and higher estimates of the activity rate lead to over-cautious loss estimates. Similarly, higher estimates of the *b* value and lower estimates of the activity rate, lead to under-cautious loss estimates. Specifically, higher *b* values will lead to lower probabilities of damage since the ratios of small to large seismic events are larger. This implies that fewer large events will occur in relation to small events that are likely not to cause any real damage to structures. The converse argument holds for lower values of *b*. Lower values of λ imply less seismic activity and consequently, lower expected levels of damage. Conversely, a higher value of λ implies that earthquake activity is increased since more earthquakes are expected to occur in a given time period and will lead to higher levels of expected damage.

Different methodologies for estimating the *b* value yield vastly different results, in particular for areas of weak seismicity, but it is vitally important to consider the nature of the catalogue when deciding on the best estimate to use. It may be a good idea to include a possible range of estimates for the parameters of the Gutenberg-Richter relation in order to draw more accurate inferences about the potential losses.

Particular care should be taken when assuming that errors within a catalogue follow a Laplace distribution since this assumption is most likely to hold only when the quality of the catalogue is particularly circumspect. The choice of methodology is dependent on the quality of the underlying data and care should be taken when making assumptions about the

distribution underlying the earthquake catalogue. The results of the risk assessment are influenced by the parameter values that characterise these distributions and damage estimates can vary significantly for different assumption as is indicated in the application of the PSRA.

The application of Bayes' theorem should be investigated further. Different assumptions or a slight variation in approach could yield interesting results. Further study should be conducted to examine the nature of errors that are not symmetrically distributed. Additionally, the tail behaviour assumptions could be strengthened, especially when considering historical earthquake catalogues, where the uncertainty is likely to be much higher than for modern catalogues.

The method for estimating the parameters over a catalogue with differing levels of the quality of data as proposed by Kijko and Dessokey (1987) could be refined when examining which time intervals to consider for which types of catalogues. Additionally, it might be possible to introduce observation errors into the estimators employed by this method. The catalogue synthesising approach for this kind of investigation will have to be adjusted to generate catalogues with varying data quality. The use of a logic tree as an additional investigation of the effect of uncertainty in the parameters could be considered in subsequent investigations but was not considered within the scope of the study.

Finally, the traditional method of incorporating errors into parameter estimates could be refined for the estimation of earthquake parameters by truncating the distribution of the errors at three standard deviations about the mean, to take the implicit assumption that is implied by the quantifiable nature of earthquake magnitudes by the damage they cause into account.

References

AfriGIS (Pty) Ltd 2014, 10/03/2014 - last update, Available: *maps.google.co.za* [2014/03/10]

Abramowitz, M. and Stegun, I. A. (Eds.). 1972, "Error Function and Fresnel Integrals." Ch.7 in *Handbook of Mathematical Functions with Formulas, Graphs, and Mathematical Tables*, 9th printing. New York: Dover, pp. 297-309.

Aki, K. 1965, "Maximum Likelihood Estimate of b in the formula logN=a-bm and its Confidence Limits", *Bulletin of the Earthquake Research Institute*, vol. 43, pp. 273-279.

Ambraseys, N. 1995, "The prediction of earthquake peak ground acceleration in Europe", *Earthquake Engineering & Structural Dynamics*, vol. 24, no. 4, pp. 467-490.

AngloGold Ashanti, 2012. *West Wits Country Report 2012*. Johannesburg, 2012.

ATC-13, Applied Technology Council 1985, *ATC 13: Earthquake Damage Evaluation Data for California*, Federal Emergency Management Agency Redwood City, CA.

Ayele, A. & Kulhánek, O. 1997, "Spatial and temporal variations of seismicity in the Horn of Africa from 1960 to 1993", *Geophysical Journal International*, vol. 130, no. 3, pp. 805-810.

Bender, F. & Bannert, D.N. 1983, Geology of Burma, Gebr. Borntraeger.

Bengoubou-Valérius, M. & Gibert, D. 2013, "Bootstrap determination of the reliability of b-values: an assessment of statistical estimators with synthetic magnitude series", *Natural Hazards*, vol. 65, no. 1, pp. 443-459.

Bommer, J.J. 2003, "Uncertainty about the uncertainty in seismic hazard analysis", *Engineering Geology*, vol. 70, no. 1, pp. 165-168.

Booker, J. 2012, *Christchurch quake third most expensive disaster ever - insurer*, 29 March 2012 edn, *The New Zealand Herald*, New Zealand, Available: http://www.nzherald.co.nz/nz/news/article.cfm?c_id=1&objectid=10795342, [26/01/2014].

Boore, D.M. & Joyner, W.B. 1982, "The empirical prediction of ground motion", *Bulletin of the Seismological Society of America*, vol. 72, no. 6B, pp. S43-S60.

Brandt, M.B.C., M. Bejaichund, E.M. Kgaswane, E. Hattingh & D.L. Roblin (2005). "Seismic history of South Africa", *Seismological Series 37*, Council for Geoscience, South Africa.

Budnitz, R.J., Senior Seismic Hazard Analysis Committee (SSHAC), US Nuclear Regulatory Commission. Office of Nuclear Regulatory Research. Division of Engineering Technology, Lawrence Livermore National Laboratory, United States. Dept. of Energy & Electric Power Research Institute 1997, Recommendations for probabilistic seismic hazard analysis: guidance on uncertainty and use of experts, US Nuclear Regulatory Commission.

Cao, T., Petersen, M.D., Cramer, C.H., Toppozada, T.R., Reichle, M.S. & Davis, J.F. 1999, "The calculation of expected loss using probabilistic seismic hazard", *Bulletin of the Seismological Society of America*, vol. 89, no. 4, pp. 867-876.

Cape Town Gazette, 29/09/2010 - last update, *Tulbagh Earthquake – 1969*, Available: http://capetowngazette.com/tulbagh-earthquake-1969-2-1726 [26/01/2014].

ceresmuseum.co.za, 26/01/2014 - last accessed, *Earthquake*, Available: http://www.ceresmuseum.co.za/?page_id=80 [26/01/2014].

Cornell, C.A. 1968, "Engineering seismic risk analysis", Bulletin of the Seismological Society of America, vol. 58, no. 5, pp. 1583-1606.

Council for Geoscience, 28/07/2010 - last updated, *Update: Earthquake Marchand Augrabies-26 July 2010*, Available: http://saweatherobserver.blogspot.com/2010/07/update-earthquake-marchand-augrabies-26.html [26/01/2014].

Council for Geoscience, 2012 – last updated, *Historical Earthquakes*, Available: http://www.geoscience.org.za/index.php?option=com_content&view=article&id=1612:historical-earthquakes&catid=138:seismology-unit-activities&Itemid=615 [03/07/2014].

Davies, N. and Kijko, A. 2003, “Seismic Risk Assessment: with an application to the South African Insurance Industry”, *South African Actuarial Journal*, vol. 3, pp. 1-28.

Dowrick, D. & Rhoades, D. 2000, "Earthquake damage and risk experience and modeling in New Zealand", *Proceedings of the 12th world conference on earthquake engineering*, Auckland.

Durrheim, R., Anderson, R., Cichowicz, A., Ebrahim-Trolloped, R., Hubert, G., Kijko, A., McGarr, A., Ortlepp, W. & Van der Merwe, N. 2006, "The risks to miners, mines, and the public posed by large seismic events in the gold mining districts of South Africa".

EMS, 1998, European Seismological Commission 1998, "European Macroseismic Scale 1998", *European Center of Geodynamics and Seismology*.

Engelhardt, B. & Bain, L. 1992, *Introduction to probability and mathematical statistics*, PWS-KENT Publishing Company.

Freeman, J.R. 1932, *Earthquake damage and earthquake insurance*, 1st edn, Mcgraw Hill Book Company, New York.

Gerstenberger, M., Wiemer, S. & Giardini, D. 2001, "A systematic test of the hypothesis that the b value varies with depth in California", *Geophysical Research Letters*, vol. 28, no. 1, pp. 57-60.

Grossi, P. & Kunreuther, H., Patel C.C. 2005, *Catastrophe modeling: A new approach to managing risk*, Springer.

Grossi, P. & Zoback, M. 2009, Catastrophe Modeling and California Earthquake Risk: A 20-year perspective, Risk Management Solutions, www.rms.com.

Gutenberg, B.R.& Richter C.F. 1954, *Seismicity of the earth and associated phenomena*.

Hanks, T.C. & Cornell, C.A. 1994, "Probabilistic seismic hazard analysis: A beginner’s guide", *Proceedings of the Fifth Symposium on Current Issues Related to Nuclear Power Plant Structures, Equipment and Piping*, pp. 1.

Kagan, Y. 1999, *"Universality of the seismic moment-frequency relation" in Seismicity Patterns, their Statistical Significance and Physical Meaning*, Springer, pp. 537-573.

Kijko, A. & Dessokey, M.M. 1987, "Application of the extreme magnitude distributions to incomplete earthquake files", *Bulletin of the Seismological Society of America*, vol. 77, no. 4, pp. 1429-1436.

Kijko, A. 1988, "Maximum likelihood estimation of Gutenberg-Richter b parameter for uncertain magnitude values", *Pure and Applied Geophysics*, vol. 127, no. 4, pp. 573-579.

Kijko, A. & Graham, G. 1998, "Parametric-historic procedure for probabilistic seismic hazard analysis Part I: estimation of maximum regional magnitude mmax", *Pure and Applied Geophysics*, vol. 152, no. 3, pp. 413-442.

Kijko, A. & Graham, G. 1999, " Parametric-historic" Procedure for Probabilistic Seismic Hazard Analysis Part II: Assessment of Seismic Hazard at Specified Site", *Pure and Applied Geophysics*, vol. 154, no. 1, pp. 1-22.

Kijko, A., 2008 Data driven probabilistic seismic hazard assessment procedure for regions with uncertain seismogenic zones. Chapter 16. “Seismic Hazard Analysis and Assessment”. E.S. Husebye (ed.), *Earthquake Monitoring and Seismic Hazard Mitigation in Balkan Countries*. © Springer 2008.

Kijko, A., Retief, S. & Graham, G. 2002, "Seismic hazard and risk assessment for Tulbagh, South Africa: Part I–assessment of seismic hazard", *Natural Hazards*, vol. 26, no. 2, pp. 175-201.

Kijko, A. 2011, "Seismic Hazard" in *Encyclopedia of Solid Earth Geophysics*, Encyclopedia of Earth Sciences Series, Springer, pp. 1107-1121.

Kijko, A. & Smit, A. 2012a, "Extension of the Aki-Utsu b-Value Estimator for Incomplete Catalogs", *Bulletin of the Seismological Society of America*, vol. 102, no. 3, pp. 1283-1287.

Kijko, A. & Smit, A. 2012b, *Probabilistic Seismic Hazard and Risk Assessment for the eThikweni Municipality*, Aon Re Africa (Pty) Limited T/A Aon Benfield, Pretoria, South Africa.

Ku, H. 1969, "Notes on the use of propagation of error formulas", *Precision Measurement and Calibration*, NBS SP 3D0, vol. 1, pp. 331-341.

Labuschagne, A., van der Merwe, A.J., van Rensburg, N.F.J. & Zietsman, L. 2006, *An introduction to numerical analysis*, 4th edn, Celtis Publisher, Pretoria.

Liechti, D., Ruettener, E., Eugster, S. & Streit, R. 2000, *"The impact of a and b value uncertainty on loss estimation in the reinsurance industry"*.

Marzocchi, W. & Sandri, L. 2003, "A review and new insights on the estimation of the b-value and its uncertainty", *Annals of geophysics*.

McGuire, R.K. 2001, "Deterministic vs. probabilistic earthquake hazards and risks", *Soil Dynamics and Earthquake Engineering*, vol. 21, no. 5, pp. 377-384.

Mertikas, S.P. 1985, *Error distributions and accuracy measures in navigation: an overview*, University of New Brunswick, Surveying Engineering Department.

news.com.au 2011, 25 February 2011 - last update 25 February 2011, *As it happened: 6.3 earthquake rocks Christchurch, New Zealand*.
Available: http://www.news.com.au/world/quake-aftershock-hits-christchurch/story-e6frfkyi-1226009960218 [2012/01/26]

Page, R. 1968, "Focal depths of aftershocks", *Journal of Geophysical Research*, vol. 73, no. 12, pp. 3897-3903.

Paine, C. 2004, *Reinsurance*, Institute of Financial Services.

Panel on Earthquake Loss Estimation Methodology 1989, Committee on Earthquake Engineering, Commission on Engineering and Technical Systems, National Research Council . *Estimating Losses from Future Earthquakes.* Panel Report, National Academy Press, Washington, DC. p 82

panoramio.com 2008, 25/10/2008 - last update, *University of Pretoria, HSB*. Available: http://www.panoramio.com/photo/15322275 [2012/12/10]

Press, W. H.; Flannery, B. P.; Teukolsky, S. A.; and Vetterling, W. T., 1992, "Secant Method, False Position Method, and Ridders' Method." Section 9.2 in *Numerical Recipes in FORTRAN: The Art of Scientific Computing*, 2nd ed. Cambridge, England: Cambridge University Press, pp. 347-352.

Rhoades, D. 1996, "Estimation of the Gutenberg-Richter relation allowing for individual earthquake magnitude uncertainties", *Tectonophysics*, vol. 258, no. 1, pp. 71-83.

Richter, C.F. 1935, "An instrumental earthquake magnitude scale", *Bulletin of the Seismological Society of America*, vol. 25, no. 1, pp. 1-32.

Rydelek, P.A. & Sacks, I.S. 1989, "Testing the completeness of earthquake catalogues and the hypothesis of self-similarity", *Nature*, vol. 337, no. 6204, pp. 251-253.

Sanchez-Silva, M. & Garcia, L. 2001, "Earthquake damage assessment based on fuzzy logic and neural networks", *Earthquake Spectra*, vol. 17, no. 1, pp. 89-112.

Sandri, L. & Marzocchi, W. 2006, "A technical note on the bias in the estimation of the b-value and its uncertainty through the least squares technique".

Schmid, E. & Schaad, W. 1995, "A database for worldwide seismicity quantification", *Natural Hazards*, vol. 12, no. 2, pp. 153-160.

Schorlemmer, D., Neri, G., Wiemer, S. & Mostaccio, A. 2003, "Stability and significance tests for b-value anomalies: Example from the Tyrrhenian Sea", Geophysical Research Letters, vol. 30, no. 16.

Shah, H., Boyle, R. & Dong, W. 1991, "Geographic information systems and artificial intelligence: an application for seismic zonation", *Proceeding of the Fourth International Conference on Seismic Zonation*, pp. 487.

Shi, Y. & Bolt, B.A. 1982, "The standard error of the magnitude-frequency b value", *Bulletin of the Seismological Society of America*, vol. 72, no. 5, pp. 1677-1687.

Solares, J.M. & Arroyo, A.L. 2004, "The great historical 1755 earthquake. Effects and damage in Spain", *Journal of Seismology*, vol. 8, no. 2, pp. 275-294.

Spence, R., Bommer, J., del Re, D., Bird, J., Aydinoğlu, N. & Tabuchi, S. 2003, "Comparing loss estimation with observed damage: a study of the 1999 Kocaeli earthquake in Turkey", *Bulletin of Earthquake Engineering*, vol. 1, no. 1, pp. 83-113.

Thiel, C.C. & Zsutty, T.C. 1987, "Earthquake characteristics and damage statistics", *Earthquake Spectra*, vol. 3, no. 4, pp. 747-792.

Tinti, S. & Mulargia, F. 1985, "Effects of magnitude uncertainties on estimating the parameters in the Gutenberg-Richter frequency-magnitude law", *Bulletin of the Seismological Society of America*, vol. 75, no. 6, pp. 1681-1697.

Trifunac, M.D. & Brady, A.G. 1975, "A study on the duration of strong earthquake ground motion", *Bulletin of the Seismological Society of America*, vol. 65, no. 3, pp. 581-626.

U.S. Geological Survey, 1989, *The Severity of an Earthquake*, U. S. Geological Survey General Interest Publication, U.S. GOVERNMENT PRINTING OFFICE: 1989-288-913.

U.S. Geological Survey 2008, 03/12/2012 - last update, *Earthquakes with 50,000 or more deaths*, Available: http://earthquake.usgs.gov/earthquakes/world/most_destructive.php [2013/12/10]

Utsu, T. 1965, "A method for determining the value of b in a formula log n= a-bM showing the magnitude-frequency relation for earthquakes", *Geophys. Bulletin. Hokkaido University*,vol. 13, pp. 99-103.

Werner, M.J. & Sornette, D. 2008, "Magnitude uncertainties impact seismic rate estimates, forecasts, and predictability experiments", J*ournal of Geophysical Research: Solid Earth (1978–2012)*, vol. 113, no. B8.

Whitman, R.V., Reed, J.W. & Hong, S. 1973, "Earthquake damage probability matrices", *Proceedings of the Fifth World conference on earthquake engineering, Rome, Italy: Palazzo Dei Congresi* , pp. 2540.

Wiemer, S. & Benoit, J.P. 1996, "Mapping the B-value anomaly at 100 km depth in the Alaska and New Zealand Subduction Zones", *Geophysical Research Letters*, vol. 23, no. 13, pp. 1557-1560.

Wiemer, S., McNutt, S.R. & Wyss, M. 1998, "Temporal and three-dimensional spatial analyses of the frequency–magnitude distribution near Long Valley Caldera, California", *Geophysical Journal International*, vol. 134, no. 2, pp. 409-421.

Woessner, J. & Wiemer, S. 2005, "Assessing the quality of earthquake catalogues: Estimating the magnitude of completeness and its uncertainty", *Bulletin of the Seismological Society of America*, vol. 95, no. 2, pp. 684-698.

www.woodford.co.za 2014 - last update, ***Cape Town Photo 1***, Available: http://www.woodford.co.za/news/cape-town-photo1.jpg [2014/03/10]

Appendix A

Description of the Modified Mercalli Intensity (Davies and Kijko, 2003)

MM I: not felt, except rarely under especially favourable circumstances. Under certain conditions, at and outside the boundary of the area in which a great shock is felt:

- sometimes birds or animals are reported to be uneasy or disturbed;
- sometimes dizziness or nausea is experienced;
- sometimes trees, structures, liquids, bodies of water, may sway, or doors may swing, very slowly.

MM II: felt indoors by few, especially on upper floors, or by sensitive, or nervous persons. Also, as in MM I, but often more noticeable:

- sometimes hanging objects may swing, especially when delicately suspended;
- sometimes trees, structures, liquids or bodies of water, may sway, or doors may swing, very slowly;
- sometimes birds or animals are reported to be uneasy or disturbed;
- sometimes dizziness or nausea is experienced.

MM III: felt indoors by several, motion usually rapid vibration.

- The event is sometimes not recognised to be an earthquake at first.
- The duration is estimated in some cases.
- Vibration is experienced like that due to the passing of light or lightly loaded trucks, or heavy trucks some distance away.
- Hanging objects may swing slightly.
- Movement may be appreciable on upper levels of tall structures.
- Standing motor cars are slightly rocked.

MM IV: felt indoors by many, outdoors by few.

- The event awakens a few, especially light sleepers.

- It frightens no one, unless apprehensive from previous experience. Vibration is experienced like that due to the passing of heavy or heavily loaded trucks. Sensations like a heavy body striking the building, or the falling of heavy objects inside, may be experienced.
- Dishes, windows and doors may rattle; glassware and crockery may clink and clash.
- The creaking of walls or the frame may be heard especially in the upper range of this grade. Hanging objects swing in numerous instances.
- Liquids in open vessels are slightly disturbed.
- Standing motor cars slightly are slightly rocked.

MM V: felt indoors by practically all, outdoors by many or most; outdoors, the direction of the event may be estimated.

- The event awakens many, or most.
- It frightens few, but slight excitement may be reported; a few may run outdoors.
- Buildings tremble throughout.
- Dishes and glassware are broken to some extent.
- Some windows may be cracked.
- Small or unstable objects are overturned occasionally falling.
- Hanging objects, doors, swing generally or considerably.
- Pictures are knocked against walls, or swung out of place.
- Doors and shutters are abruptly opened or closed.
- Pendulum clocks stop, start, or run fast, or slow.
- Small objects and furnishings are moved, the latter to a slight extent.
- Liquids are spilt in small amounts from well-filled open containers.
- Trees and bushes are shaken slightly.

MM VI: felt by all, indoors and outdoors.

- The event frightens many, excitement is general, there is some alarm, and many run outdoors. It awakens all.
- Persons are made to move unsteadily.
- Trees and bushes are shaken slightly to moderately.
- Liquid is set in strong motion.

- Small bells are rung at churches, chapels, schools etc.
- Damage is slight in poorly built buildings.
- Plaster falls in small amount.
- Plaster is somewhat cracked, especially fine cracks in chimneys in some instances.
- Dishes and glassware are broken in considerable quantity, also some windows.
- Ornaments, books and pictures fall.
- Furniture is overturned in many instances.
- Moderately heavy furnishings are moved.

MM VII: frightens all, raising general alarm, and all run outdoors.

- Some or many find it difficult to stand.
- The event is noticed by persons driving motor cars.
- Trees and bushes are shaken moderately to strongly.
- Waves form on ponds, lakes, and running water.
- Water is turbid from stirred-up mud.
- Sand or gravel stream banks cave in to some extent.
- Large church bells etc. are rung.
- Suspended objects are made to quiver.
- Damage is negligible in buildings of good design and construction, slight to moderate in well-built ordinary buildings, considerable in poorly built or badly designed buildings, abode houses, old walls (especially where laid up without mortar), spires, etc.
- Chimneys are cracked to a considerable extent, walls to some extent.
- Plaster falls in considerable to large amount, also some stucco.
- Numerous windows, and to some extent furniture, are broken.
- Loosened brickwork and tiles are shaken down.
- Weak chimneys are broken at the roof-line, sometimes damaging roofs.
- Cornices fall from towers and high buildings.
- Bricks and stones are dislodged.
- Heavy furniture is overturned, with damage from breaking.
- Damage to concrete irrigation ditches is considerable.

MM VIII: general fright; alarm approaches panic.

- Disturbs persons driving motor cars.
- Trees shaken strongly – branches, trunks, broken, especially palm trees.
- Ejected sand and mud in small amounts.
- Changes occur in the flow of springs and wells; flow is renewed in dry wells; the temperature of spring and well waters changes.
- Damage is slight in brick structures, especially those built to withstand earthquakes.
- Damage is considerable, to the extent of partial collapse, in ordinary substantial buildings; in some cases, wooden houses tumble down; panel walls are thrown out of frame structures, decayed piling is broken off. Walls topple.
- Solid stone walls are seriously cracked and broken.
- Ground is wet to some extent.
- Chimneys, columns, monuments, factory stacks and towers twist and fall.
- Very heavy furniture is conspicuously moved and overturned.

MM IX: general panic.

- Ground cracks conspicuously.
- Damage is considerable in masonry structures built especially to withstand earthquakes.
- Some wood-frame houses built especially to withstand earthquakes are thrown out of plumb.
- Substantial masonry buildings are badly damaged, some collapsing in large parts.
- Frame buildings may be wholly shifted off their foundations.
- Reservoirs are seriously damaged.
- Underground pipes are sometimes broken.

MM X: cracked ground, especially when loose and wet, up to a width of several inches; fissures up to a metre in width running parallel to canal and stream banks.

- Considerable landslides occur from river banks and steep coasts.
- Sand and mud shifts horizontally on beaches and flat land.
- The level of water in wells is changed.

- Water is thrown out on the banks of canals, lakes, rivers, etc.
- Serious damage occurs to dams, dykes and embankments.
- Well-built wooden structures and bridges are severely damaged; some are destroyed.
- Dangerous cracks develop in excellent brick walls.
- Most masonry and frame structures are destroyed, including their foundations.
- Railway lines are slightly bent.
- Underground pipe-lines are torn apart or crushed.
- Open cracks and broad wavy folds appear in cement pavements and asphalt road surfaces.

MM XI: disturbances in ground many and widespread, varying with ground material.

- Broad fissures, earth slumps, and land slips occur in soft, wet ground.
- Water is ejected in large amounts, charged with sand and mud.
- Sea-waves of significant magnitude occur.
- Wood-frame structures are severely damaged, especially near shock centres.
- Dams, dykes and embankments are severely damaged, often for long distances.
- Few, if any, masonry structures remain standing.
- Large, well-built bridges are destroyed by the wrecking of supporting piers or pillars.
- Yielding wooden bridges are less affected.
- Railway lines are severely bent.
- Underground pipe-lines are forced completely out of service.

MM XII: damage total; practically all works of construction greatly damaged or destroyed.

- Disturbances in the ground are great and varied, numerous shearing cracks appearing.
- Landslides and falls of rock are significant, and the slumping of river banks etc. is extensive.
- Large rock masses are wrenched loose and torn off.

- Fault slips develop in firm rock, with notable horizontal and vertical offset displacements.
- Water channels, both surface and underground, are disturbed and modified greatly.
- Waterfalls are produced and rivers are deflected.
- Waves are seen on ground surfaces.
- Lines of sight and level are distorted.
- Objects are thrown upward into the air.

Appendix B

Damage Probability Matrices (ATC-13, 1985)

Building Class 1: Wood Frame, Low Rise									
Damage Factor	Damage Factor Range (%)	Central Damage Factor (%)	Probability of damage (%) by MM intensity and damage state						
			VI	VII	VIII	IX	X	XI	XII
1	1	0	3.7	0.0	0.0	0.0	0.0	0.0	0.0
2	0-1	0.5	68.5	26.8	1.6	0.0	0.0	0.0	0.0
3	1-10	5	27.8	73.2	94.9	62.4	11.5	1.8	0.0
4	10-30	20	0.0	0.0	3.5	37.6	76.0	75.1	24.8
5	30-60	45	0.0	0.0	0.0	0.0	12.5	23.1	73.5
6	60-100	80	0.0	0.0	0.0	0.0	0.0	0.0	1.7
7	100	100	0.0	0.0	0.0	0.0	0.0	0.0	0.0

Building Class 2: Light Metal, Low Rise									
	Damage Factor Range (%)	Central Damage Factor (%)	Probability of damage (%) by MM intensity and damage state						
			VI	VII	VIII	IX	X	XI	XII
1	1	0	23.6	0.0	0.0	0.0	0.0	0.0	0.0
2	0-1	0.5	70.9	47.8	11.5	0.4	0.0	0.0	0.0
3	1-10	5	5.5	52.2	88.5	93.7	31.9	3.4	0.0
4	10-30	20	0.0	0.0	0.0	5.9	67.7	80.7	45.5
5	30-60	45	0.0	0.0	0.0	0.0	0.4	15.9	54.5
6	60-100	80	0.0	0.0	0.0	0.0	0.0	0.0	0.0
7	100	100	0.0	0.0	0.0	0.0	0.0	0.0	0.0

Building Class 3: Unreinforced Masonry, bearing wall, low rise									
Damage Factor	Damage Factor Range (%)	Central Damage Factor (%)	Probability of damage (%) by MM intensity and damage state						
			VI	VII	VIII	IX	X	XI	XII
1	1	0	0.0	0.0	0.0	0.0	0.0	0.0	0.0
2	0-1	0.5	9.1	0.6	0.0	0.0	0.0	0.0	0.0
3	1-10	5	90.5	55.5	10.9	0.5	0.0	0.0	0.0
4	10-30	20	0.4	43.4	66.0	22.4	2.0	0.1	0.1
5	30-60	45	0.0	0.5	22.9	65.9	35.0	10.1	3.4
6	60-100	80	0.0	0.0	0.2	11.2	62.5	83.1	50.4
7	100	100	0.0	0.0	0.0	0.0	0.5	6.7	46.1

Building Class 4: Unreinforced Masonry, bearing wall, medium rise									
Damage Factor	Damage Factor Range (%)	Central Damage Factor (%)	Probability of damage (%) by MM intensity and damage state						
			VI	VII	VIII	IX	X	XI	XII
1	1	0	5.2	0.0	0.0	0.0	0.0	0.0	0.0
2	0-1	0.5	38.8	3.2	0.7	0.0	0.0	0.0	0.0
3	1-10	5	55.9	84.1	37.9	5.5	0.8	0.2	0.1
4	10-30	20	0.1	12.7	55.4	52.6	20.6	6.9	2.5
5	30-60	45	0.0	0.0	6.0	40.4	60.8	40.2	17.7
6	60-100	80	0.0	0.0	0.0	1.5	17.8	51.7	62.8
7	100	100	0.0	0.0	0.0	0.0	0.0	1.0	16.9

Building Class 5: Unreinforced Masonry, load bearing frame, medium rise									
Damage Factor	Damage Factor Range (%)	Central Damage Factor (%)	Probability of damage (%) by MM intensity and damage state						
			VI	VII	VIII	IX	X	XI	XII
1	1	0	0.5	0.0	0.0	0.0	0.0	0.0	0.0
2	0-1	0.5	15.3	2.9	0.0	0.0	0.0	0.0	0.0
3	1-10	5	81.2	66.6	13.5	1.9	0.3	0.0	0.0
4	10-30	20	3.0	30.1	69.3	40.6	14.1	2.0	0.2
5	30-60	45	0.0	0.4	17.2	54.4	63.4	28.4	8.5
6	60-100	80	0.0	0.0	0.0	3.1	22.2	67.5	78.8
7	100	100	0.0	0.0	0.0	0.0	0.0	2.1	12.5

Building Class 6: Reinforced concrete shear wall, with moment resisting frame, medium rise									
Damage Factor	Damage Factor Range (%)	Central Damage Factor (%)	Probability of damage (%) by MM intensity and damage state						
			VI	VII	VIII	IX	X	XI	XII
1	1	0	20.4	0.0	0.0	0.0	0.0	0.0	0.0
2	0-1	0.5	70.3	15.5	0.0	0.0	0.0	0.0	0.0
3	1-10	5	9.3	84.5	88.4	28.9	1.4	0.0	0.0
4	10-30	20	0.0	0.0	11.6	71.1	81.6	38.7	3.8
5	30-60	45	0.0	0.0	0.0	0.0	17.0	61.3	88.7
6	60-100	80	0.0	0.0	0.0	0.0	0.0	0.0	7.5
7	100	100	0.0	0.0	0.0	0.0	0.0	0.0	0.0

Building Class 7: Reinforced concrete shear wall, with moment resisting frame, high rise									
Damage Factor	Damage Factor Range (%)	Central Damage Factor (%)	Probability of damage (%) by MM intensity and damage state						
			VI	VII	VIII	IX	X	XI	XII
1	1	0	19.1	0.0	0.0	0.0	0.0	0.0	0.0
2	0-1	0.5	62.9	7.2	0.2	0.0	0.0	0.0	0.0
3	1-10	5	18.0	92.2	83.4	17.6	0.6	0.0	0.0
4	10-30	20	0.0	0.6	16.4	81.9	70.1	6.2	0.7
5	30-60	45	0.0	0.0	0.0	0.5	29.3	86.5	59.2
6	60-100	80	0.0	0.0	0.0	0.0	0.0	7.3	40.1
7	100	100	0.0	0.0	0.0	0.0	0.0	0.0	0.0

Building Class 8: Reinforced Concrete Shear Wall, without moment resisting frame, medium rise									
Damage Factor	Damage Factor Range (%)	Central Damage Factor (%)	Probability of damage (%) by MM intensity and damage state						
			VI	VII	VIII	IX	X	XI	XII
1	1	0	2.5	0.0	0.0	0.0	0.0	0.0	0.0
2	0-1	0.5	59.0	8.6	0.0	0.0	0.0	0.0	0.0
3	1-10	5	38.5	89.2	66.4	11.7	0.4	0.0	0.0
4	10-30	20	0.0	2.2	33.6	83.9	56.9	19.7	3.7
5	30-60	45	0.0	0.0	0.0	4.4	42.7	77.0	77.6
6	60-100	80	0.0	0.0	0.0	0.0	0.0	3.3	18.7
7	100	100	0.0	0.0	0.0	0.0	0.0	0.0	0.0

Building Class 9: Reinforced concrete shear wall, without moment resisting frame, high rise									
Damage Factor	Damage Factor Range (%)	Central Damage Factor (%)	Probability of damage (%) by MM intensity and damage state						
			VI	VII	VIII	IX	X	XI	XII
1	1	0	2.8	0.0	0.0	0.0	0.0	0.0	0.0
2	0-1	0.5	49.9	2.5	0.0	0.0	0.0	0.0	0.0
3	1-10	5	47.3	86.8	42.3	2.8	0.4	0.0	0.0
4	10-30	20	0.0	10.7	57.3	70.8	19.3	1.8	0.3
5	30-60	45	0.0	0.0	0.4	26.4	80.0	67.2	27.3
6	60-100	80	0.0	0.0	0.0	0.0	0.7	31.0	72.4
7	100	100	0.0	0.0	0.0	0.0	0.0	0.0	0.0

Building Class 10: Braced Steel Frame, Low rise									
Damage Factor	Damage Factor Range (%)	Central Damage Factor (%)	Probability of damage (%) by MM intensity and damage state						
			VI	VII	VIII	IX	X	XI	XII
1	1	0	18.9	0.6	0.0	0.0	0.0	0.0	0.0
2	0-1	0.5	60.4	29.2	2.6	0.0	0.0	0.0	0.0
3	1-10	5	20.7	70.2	90.3	54.4	15.5	1.2	0.0
4	10-30	20	0.0	0.0	7.1	45.6	82.9	64.1	20.4
5	30-60	45	0.0	0.0	0.0	0.0	1.6	34.7	77.3
6	60-100	80	0.0	0.0	0.0	0.0	0.0	0.0	2.3
7	100	100	0.0	0.0	0.0	0.0	0.0	0.0	0.0

Building Class 11: Precast Concrete, low rise									
Damage Factor	Damage Factor Range (%)	Central Damage Factor (%)	Probability of damage (%) by MM intensity and damage state						
			VI	VII	VIII	IX	X	XI	XII
1	1	0	9.8	0.0	0.0	0.0	0.0	0.0	0.0
2	0-1	0.5	49.6	12.8	0.3	0.0	0.0	0.0	0.0
3	1-10	5	40.6	86.8	72.4	1.8	0.2	0.0	0.0
4	10-30	20	0.0	0.4	27.3	80.7	27.0	8.2	3.3
5	30-60	45	0.0	0.0	0.0	17.5	69.6	71.1	44.9
6	60-100	80	0.0	0.0	0.0	0.0	3.2	20.7	51.6
7	100	100	0.0	0.0	0.0	0.0	0.0	0.0	0.2

Building Class 12: Long span, low rise									
Damage Factor	Damage Factor Range (%)	Central Damage Factor (%)	Probability of damage (%) by MM intensity and damage state						
			VI	VII	VIII	IX	X	XI	XII
1	1	0	37.4	5.2	0.0	0.0	0.0	0.0	0.0
2	0-1	0.5	56.7	52.0	7.7	0.0	0.0	0.0	0.0
3	1-10	5	5.9	42.8	89.1	64.7	18.7	0.4	0.0
4	10-30	20	0.0	0.0	3.2	35.2	77.9	53.2	6.9
5	30-60	45	0.0	0.0	0.0	0.1	3.4	46.3	83.8
6	60-100	80	0.0	0.0	0.0	0.0	0.0	0.1	9.3
7	100	100	0.0	0.0	0.0	0.0	0.0	0.0	0.0

Appendix C

Matlab code for testing asymptotic properties of estimators

```
% Program Mult_Cat
% ======================================================================

% The program will generate a specified number of synthetic earthquake
% catalogues with specified parameters and then calculates beta using
% different estimators in order to compare them.

clear;

%% INPUT PARAMETERS
iterations = 100;
iter = 0;
m_min = 3.8;
m_max = 7;
sd_mag = 0.2;
bvalue = 1;
year_begin = 1900;
year_end = 2010;
lambda = 7;
est_b = zeros(iterations,5);
est_beta = zeros(iterations,5);

% END OF INPUT PARAMETERS



% ======================================================================

% Further calculations related to input data

beta = bvalue/(log10(exp(1)));
time_span = year_end - year_begin;



% Loop estimates  a number of times to obtain a sample set of estimates


while (iter < iterations)


% Reset catalogue inputs
time = 0.0;
nr_eq_total1 = 0;
sum_mag = 0;
sd_mag3 = sd_mag * 3.0;


%% CATALOGUE COMPUTATIONS ----------------------------------------
while (time < time_span)
```

```
  eps3 = 3.0 * eps;
  r_n = rand;

  if r_n < eps3
     r_n = eps3;
  end;

  if (1.0 - r_n) < eps3;
      r_n = 1.0 - eps3;
  end;

  int = -log(1.0 - r_n) / lambda;    % RANDOM TIME INTERVAL [Y]
                                     % CORRESPONDING TO LAMBDA

  time = time + int;

  nr_eq_total1 = nr_eq_total1 + 1; % NR OF EQ-s STARTING FROM m_min

  a1  = exp(-beta * m_min);
  a2  = exp(-beta * m_max);
  a12 = a1 - a2;

  r_n1 = rand;

% Calculate d_mag if errors follow the Gaussian distribution
  d_mag = randn * sd_mag;

% Calculate d_mag if errors follow the laplacian distribution
% nu_c = sqrt((sd_mag^2)/2);
% r_n2 = rand - (0.5);
% d_mag = -nu_c * sign(r_n2) * log(1-2*abs(r_n2));

 % Truncate the errors
  if abs(d_mag) > sd_mag3
     if d_mag > 0
        d_mag = sd_mag3;
     else
        d_mag = -sd_mag3;
     end;
  end;

  % Simulate the real magnitude
  rmag = -log(a1 - r_n1 * a12) / beta;      % G-R MAGNITUDE

  % Add the real magnitude and error
  mag = rmag + d_mag;                % APPARENT G-R MAGNITUDE

  mag = .01 * round(100 * mag);

  % Write to the catalogue
  M(nr_eq_total1,iter+1) = mag;
  %cat(nr_eq_total1,iter+1) = mag;  % removed for laplace run
  sum_mag = sum_mag + mag; % added for laplace run

end;
count2 = nr_eq_total1;
```

```
% Exclude magnitudes below m_min % this causes the programme to fail and
% the estimates to become distorted

%count1 =0;
%count2 =0;
%while count1 < nr_eq_total1
    %if cat(count1+1,iter+1)<m_min
%       count1 = count1 + 1;
        %M(count2+1,iter+1) = m_min;
        %count2 = count2 + 1;
        %sum_mag = sum_mag + M(count2,iter+1);
    %else
%       M(count2+1,iter+1) = cat(count1+1,iter+1);
%       count2 = count2 + 1;
       %count1 = count1 + 1;
 %      sum_mag = sum_mag + M(count2,iter+1);
    %end;
%end;


nr_eq_total = count2;

mean_mag = sum_mag / nr_eq_total;


%% Calculate estimators

 if nr_eq_total > 0

   %% Calculate b1 (Classic)

  beta1 = 1/(mean_mag-m_min);
  b1 = log10(exp(1))*beta1;
  %b1 = 0.01 * round(100 * b1);




   %% Calculate b2 (Classic-bounded) using the Regula falsi/ False
position method

   % Bounds
  a = beta-0.5;
  b = beta+0.5;
  flag = 1;
  maxerr = 0.00001;

   % First iteration
  fa3 = 1/a - mean_mag + m_min + ((m_max)*exp(-a*(m_max-m_min)))/(1-exp(-
a*(m_max-m_min)));
  fb3 = 1/b - mean_mag + m_min + ((m_max)*exp(-b*(m_max-m_min)))/(1-exp(-
b*(m_max-m_min)));

  % Ensure fa and fb have differing signs:
  while sign(fa3) == sign(fb3)
      a = a + 0.001;
```

```
      b = b + 0.001;
      fa3 = 1/a - mean_mag + m_min + ((m_max)*exp(-a*(m_max-m_min)))/(1-
exp(-a*(m_max-m_min)));
      fb3 = 1/b - mean_mag + m_min + ((m_max)*exp(-b*(m_max-m_min)))/(1-
exp(-b*(m_max-m_min)));
  end;

  c = b - (fb3*(b-a))/(fb3-fa3);
  %c = (a*fb3 - b*fa3)/(fb3-fa3);

  fc = 1/c - mean_mag + m_min + ((m_max)*exp(-c*(m_max-m_min)))/(1-exp(-
c*(m_max-m_min)));
  fa = fa3;


  % Subsequent iterations
  while abs(fc) > maxerr
      if sign(fa) == sign(fc)
          a = c;
      else
          b = c;
      end;
      fa = 1/a - mean_mag + m_min + ((m_max)*exp(-a*(m_max-m_min)))/(1-
exp(-a*(m_max-m_min)));
      fb = 1/b - mean_mag + m_min + ((m_max)*exp(-b*(m_max-m_min)))/(1-
exp(-b*(m_max-m_min)));
      c = b - (fb*(b-a))/(fb-fa);
      %c = (a*fb - b*fa)/(fb-fa);
      fc = 1/c - mean_mag + m_min + ((m_max)*exp(-c*(m_max-m_min)))/(1-
exp(-c*(m_max-m_min)));
      flag = flag +1;
      if (flag == 1000)
            break;
      end;
  end;
  beta2 = c;
  b2 = log10(exp(1))*beta2;
  %b3 = 0.01 * round(100 * b3);

  %% Calculate b3 (Classic-bounded + normal error) using the Regula
falsi/false position method

     % Bounds
  a = beta-0.5;
  b = beta+0.5;
  flag4 = 1;
  maxerr = 0.00001;
  sd_err = sd_mag;

   % First iteration
  calc_a4 = 0;
  for i = 1:nr_eq_total
      y1 = (m_max+a*sd_err^2-M(i,iter+1))/(sqrt(2*sd_err^2));
      y2 = (m_min+a*sd_err^2-M(i,iter+1))/(sqrt(2*sd_err^2));
      num = exp(-(y1^2))-exp(-(y2^2));
      den = erf(y1) - erf(y2);
      calc_a4 = calc_a4 + num/den;
  end;
```

```
  fa4 = 1/a - mean_mag + (m_max*exp(m_min*a)-
m_min*exp(m_max*a))/(exp(m_min*a)-exp(m_max*a)) + a*(sd_err^2) +
calc_a4*((sqrt(2)*sd_err)/(nr_eq_total*sqrt(pi)));

  calc_b4 = 0;
  for i = 1:nr_eq_total
      y1 = (m_max+b*sd_err^2-M(i,iter+1))/(sqrt(2*sd_err^2));
      y2 = (m_min+b*sd_err^2-M(i,iter+1))/(sqrt(2*sd_err^2));
      num = exp(-(y1^2))-exp(-(y2^2));
      den = erf(y1) - erf(y2);
      calc_b4 = calc_b4 + num/den;
  end;
  fb4 = 1/b - mean_mag + (m_max*exp(m_min*b)-
m_min*exp(m_max*b))/(exp(m_min*b)-exp(m_max*b)) + b*(sd_err^2) +
calc_b4*((sqrt(2)*sd_err)/(nr_eq_total*sqrt(pi)));

  % Ensure fa and fb have differing signs:

  while sign(fa4) == sign(fb4)

      a = a+0.001;
      calc_a4 = 0;
      for i = 1:nr_eq_total
          y1 = (m_max+a*sd_err^2-M(i,iter+1))/(sqrt(2*sd_err^2));
          y2 = (m_min+a*sd_err^2-M(i,iter+1))/(sqrt(2*sd_err^2));
          num = exp(-(y1^2))-exp(-(y2^2));
          den = erf(y1) - erf(y2);
          calc_a4 = calc_a4 + num/den;
      end;
      fa4 = 1/a - mean_mag + (m_max*exp(m_min*a)-
m_min*exp(m_max*a))/(exp(m_min*a)-exp(m_max*a)) + a*(sd_err^2) +
calc_a4*((sqrt(2)*sd_err)/(nr_eq_total*sqrt(pi)));

      b = b + 0.001;
      calc_b4 = 0;
      for i = 1:nr_eq_total
          y1 = (m_max+b*sd_err^2-M(i,iter+1))/(sqrt(2*sd_err^2));
          y2 = (m_min+b*sd_err^2-M(i,iter+1))/(sqrt(2*sd_err^2));
          num = exp(-(y1^2))-exp(-(y2^2));
          den = erf(y1) - erf(y2);
          calc_b4 = calc_b4 + num/den;
      end;
      fb4 = 1/b - mean_mag + (m_max*exp(m_min*b)-
m_min*exp(m_max*b))/(exp(m_min*b)-exp(m_max*b)) + b*(sd_err^2) +
calc_b4*((sqrt(2)*sd_err)/(nr_eq_total*sqrt(pi)));
  end;

  c = b - (fb4*(b-a))/(fb4-fa4);


  calc_c4 = 0;
  for i = 1:nr_eq_total
      y1 = (m_max+c*sd_err^2-M(i,iter+1))/(sqrt(2*sd_err^2));
      y2 = (m_min+c*sd_err^2-M(i,iter+1))/(sqrt(2*sd_err^2));
      num = exp(-(y1^2))-exp(-(y2^2));
      den = erf(y1) - erf(y2);
      calc_c4 = calc_c4 + num/den;
  end;
```

```
  fc = 1/c - mean_mag + (m_max*exp(m_min*c)-
m_min*exp(m_max*c))/(exp(m_min*c)-exp(m_max*c)) + c*(sd_err^2) +
calc_c4*((sqrt(2)*sd_err)/(nr_eq_total*sqrt(pi)));

  fa = fa4;

  % Subsequent iterations
  while abs(fc) > maxerr
      if sign(fa) == sign(fc)
          a = c;
      else
          b = c;
      end;

  calc_a = 0;
  for i = 1:nr_eq_total
      y1 = (m_max+a*sd_err^2-M(i,iter+1))/(sqrt(2*sd_err^2));
      y2 = (m_min+a*sd_err^2-M(i,iter+1))/(sqrt(2*sd_err^2));
      num = exp(-(y1^2))-exp(-(y2^2));
      den = erf(y1) - erf(y2);
      calc_a = calc_a + num/den;
  end;
  fa = 1/a - mean_mag + (m_max*exp(m_min*a)-
m_min*exp(m_max*a))/(exp(m_min*a)-exp(m_max*a)) + a*(sd_err^2) +
calc_a*((sqrt(2)*sd_err)/(nr_eq_total*sqrt(pi)));

  calc_b = 0;
  for i = 1:nr_eq_total
      y1 = (m_max+b*sd_err^2-M(i,iter+1))/(sqrt(2*sd_err^2));
      y2 = (m_min+b*sd_err^2-M(i,iter+1))/(sqrt(2*sd_err^2));
      num = exp(-(y1^2))-exp(-(y2^2));
      den = erf(y1) - erf(y2);
      calc_b = calc_b + num/den;
  end;
  fb = 1/b - mean_mag + (m_max*exp(m_min*b)-
m_min*exp(m_max*b))/(exp(m_min*b)-exp(m_max*b)) + b*(sd_err^2) +
calc_b*((sqrt(2)*sd_err)/(nr_eq_total*sqrt(pi)));

  c = b - (fb*(b-a))/(fb-fa);


  calc_c = 0;
  for i = 1:nr_eq_total
      y1 = (m_max+c*sd_err^2-M(i,iter+1))/(sqrt(2*sd_err^2));
      y2 = (m_min+c*sd_err^2-M(i,iter+1))/(sqrt(2*sd_err^2));
      num = exp(-(y1^2))-exp(-(y2^2));
      den = erf(y1) - erf(y2);
      calc_c = calc_c + num/den;
  end;
  fc = 1/c - mean_mag + (m_max*exp(m_min*c)-
m_min*exp(m_max*c))/(exp(m_min*c)-exp(m_max*c)) + c*(sd_err^2) +
calc_c*((sqrt(2)*sd_err)/(nr_eq_total*sqrt(pi)));

  flag4 = flag4 +1;
      if (flag4 == 1000)
            break;
      end;
  end;
```

```
  beta3 = c;
  b3 = log10(exp(1))*beta3;
  %b4 = 0.01 * round(100 * b4);

  %% Calculate b4 (Classic-bounded + Laplace error) using the Regula
falsi/False position method

  nu_c = sqrt((sd_mag^2)/2);
  % Bounds
  a = beta-0.5;
  b = beta+0.5;
  flag = 1;
  maxerr = 0.00001;

   % First iteration

   y=a;
   calc = 0;
   z1 = (2*(nu_c)^2*y)/((nu_c^2)*y^2-1);
   z11 = (y*nu_c-1);
   z12 = (y*nu_c+1);
   for i = 1:nr_eq_total
      y1 = exp(((M(i,iter+1)-m_min)*z11)/nu_c);
      y2 = exp(((M(i,iter+1)-m_max)*z12)/nu_c);
      x1 = nu_c + (M(i,iter+1)-m_min)*z12;
      x2 = nu_c + (M(i,iter+1)-m_max)*z11;
      num = x1*y1-x2*y2;
      den = -z12*y1+z11*y2+2;
      calc = calc + num/den;
   end;
   fa5 = 1/y - mean_mag + (m_max*exp(m_min*y)-
m_min*exp(m_max*y))/(exp(m_min*y)-exp(m_max*y)) + z1 + calc/nr_eq_total;

   y=b;
   calc = 0;
   z1 = (2*(nu_c)^2*y)/((nu_c^2)*y^2-1);
   z11 = (y*nu_c-1);
   z12 = (y*nu_c+1);
  for i = 1:nr_eq_total
      y1 = exp(((M(i,iter+1)-m_min)*z11)/nu_c);
      y2 = exp(((M(i,iter+1)-m_max)*z12)/nu_c);
      x1 = nu_c + (M(i,iter+1)-m_min)*z12;
      x2 = nu_c + (M(i,iter+1)-m_max)*z11;
      num = x1*y1-x2*y2;
      den = -z12*y1+z11*y2+2;
      calc = calc + num/den;
   end;
   fb5 = 1/y - mean_mag + (m_max*exp(m_min*y)-
m_min*exp(m_max*y))/(exp(m_min*y)-exp(m_max*y)) + z1 + calc/nr_eq_total;

   fa5_1 = fa5;
   fb5_1 = fb5;

  % Ensure fa and fb have differing signs:
  while sign(fa5_1) == sign(fb5_1)
      %    a = a + 0.001;

      %    y=a;
      %    calc = 0;
```

```
      %    z1 = (2*(nu_c)^2*y)/((nu_c^2)*y^2-1);
      %    z11 = (y*nu_c-1);
      %    z12 = (y*nu_c+1);

      %for i = 1:nr_eq_total
      %y1 = exp(((M(i,iter+1)-m_min)*z11)/nu_c);
      %y2 = exp(((M(i,iter+1)-m_max)*z12)/nu_c);
      %x1 = nu_c + (M(i,iter+1)-m_min)*z12;
      %x2 = nu_c + (M(i,iter+1)-m_max)*z11;
      %num = x1*y1-x2*y2;
      %den = -z12*y1+z11*y2+2;
      %calc = calc + num/den;
   %end;

         %fa5_1 = 1/y - mean_mag + (m_max*exp(m_min*y)-
m_min*exp(m_max*y))/(exp(m_min*y)-exp(m_max*y)) + z1 + calc/nr_eq_total;

         b = b + 0.000001;

         y=b;
         calc = 0;
         z1 = (2*(nu_c)^2*y)/((nu_c^2)*y^2-1);
         z11 = (y*nu_c-1);
         z12 = (y*nu_c+1);

     for i = 1:nr_eq_total
      y1 = exp(((M(i,iter+1)-m_min)*z11)/nu_c);
      y2 = exp(((M(i,iter+1)-m_max)*z12)/nu_c);
      x1 = nu_c + (M(i,iter+1)-m_min)*z12;
      x2 = nu_c + (M(i,iter+1)-m_max)*z11;
      num = x1*y1-x2*y2;
      den = -z12*y1+z11*y2+2;
      calc = calc + num/den;
   end;
      fb5_1 = 1/y - mean_mag + (m_max*exp(m_min*y)-
m_min*exp(m_max*y))/(exp(m_min*y)-exp(m_max*y)) + z1 + calc/nr_eq_total;

      end;


      c = b - (fb5_1*(b-a))/(fb5_1-fa5_1);


   y=c;
   calc = 0;
   z1 = (2*(nu_c)^2*y)/((nu_c^2)*y^2-1);
   z11 = (y*nu_c-1);
   z12 = (y*nu_c+1);

   for i = 1:nr_eq_total
      y1 = exp(((M(i,iter+1)-m_min)*z11)/nu_c);
      y2 = exp(((M(i,iter+1)-m_max)*z12)/nu_c);
      x1 = nu_c + (M(i,iter+1)-m_min)*z12;
      x2 = nu_c + (M(i,iter+1)-m_max)*z11;
      num = x1*y1-x2*y2;
      den = -z12*y1+z11*y2+2;
      calc = calc + num/den;
   end;
```

```
  fc = 1/y - mean_mag + (m_max*exp(m_min*y)-
m_min*exp(m_max*y))/(exp(m_min*y)-exp(m_max*y)) + z1 + calc/nr_eq_total;

  fa = fa5_1;

  % Subsequent iterations
  while abs(fc) > maxerr

      if sign(fa) == sign(fc)
          a = c;
      else
          b = c;
      end;

   y=a;
   calc = 0;
   z1 = (2*(nu_c)^2*y)/((nu_c^2)*y^2-1);
   z11 = (y*nu_c-1);
   z12 = (y*nu_c+1);

   for i = 1:nr_eq_total
      y1 = exp(((M(i,iter+1)-m_min)*z11)/nu_c);
      y2 = exp(((M(i,iter+1)-m_max)*z12)/nu_c);
      x1 = nu_c + (M(i,iter+1)-m_min)*z12;
      x2 = nu_c + (M(i,iter+1)-m_max)*z11;
      num = x1*y1-x2*y2;
      den = -z12*y1+z11*y2+2;
      calc = calc + num/den;
   end;
   fa = 1/y - mean_mag + (m_max*exp(m_min*y)-
m_min*exp(m_max*y))/(exp(m_min*y)-exp(m_max*y)) + z1 + calc/nr_eq_total;


   y=b;
   calc = 0;
   z1 = (2*(nu_c)^2*y)/((nu_c^2)*y^2-1);
   z11 = (y*nu_c-1);
   z12 = (y*nu_c+1);

    for i = 1:nr_eq_total
      y1 = exp(((M(i,iter+1)-m_min)*z11)/nu_c);
      y2 = exp(((M(i,iter+1)-m_max)*z12)/nu_c);
      x1 = nu_c + (M(i,iter+1)-m_min)*z12;
      x2 = nu_c + (M(i,iter+1)-m_max)*z11;
      num = x1*y1-x2*y2;
      den = -z12*y1+z11*y2+2;
      calc = calc + num/den;
   end;
   fb = 1/y - mean_mag + (m_max*exp(m_min*y)-
m_min*exp(m_max*y))/(exp(m_min*y)-exp(m_max*y)) + z1 + calc/nr_eq_total;

   c = b - (fb*(b-a))/(fb-fa);

   y=c;
   calc = 0;
   z1 = (2*(nu_c)^2*y)/((nu_c^2)*y^2-1);
   z11 = (y*nu_c-1);
   z12 = (y*nu_c+1);
```

```
    for i = 1:nr_eq_total
      y1 = exp(((M(i,iter+1)-m_min)*z11)/nu_c);
      y2 = exp(((M(i,iter+1)-m_max)*z12)/nu_c);
      x1 = nu_c + (M(i,iter+1)-m_min)*z12;
      x2 = nu_c + (M(i,iter+1)-m_max)*z11;
      num = x1*y1-x2*y2;
      den = -z12*y1+z11*y2+2;
      calc = calc + num/den;
   end;
   fc = 1/y - mean_mag + (m_max*exp(m_min*y)-
m_min*exp(m_max*y))/(exp(m_min*y)-exp(m_max*y)) + z1 + calc/nr_eq_total;

      flag = flag +1;

      if (flag == 20000)
            break;
      end;

  end;

  beta4 = c;
  b4 = log10(exp(1))*beta4;
  %b5 = 0.01 * round(100 * b5);


  %% Write estimates to data set
  est_beta(iter+1,1) = beta1;
  est_beta(iter+1,2) = beta2;
  est_beta(iter+1,3) = beta3;
  est_beta(iter+1,4) = beta4;


  est_b(iter+1,1) = b1;
  est_b(iter+1,2) = b2;
  est_b(iter+1,3) = b3;
  est_b(iter+1,4) = b4;


end;

iter = iter +1;

end;

% END OF CATALOGUE AND ESTIMATE CALCULATIONS ============================

%% ASYMPTOTIC PROPERTY CALCULATIONS

MSE = zeros(iterations,4); % Mean squared error
AE = zeros(iterations,4);  % Absolute error
count = zeros(1,4); % Number of absolute errors below a certain threshold

iter1 = 0;

while iter1 < iterations
    for i = 1:4
        MSE(iter1+1,i) = (est_beta(iter1+1,i)-beta)^2;
```

```
        AE(iter1+1,i) = abs(est_beta(iter1+1,i)-beta);
        if AE(iter1+1,i) < 0.1
            count(1,i) = count(1,i)+1;
        end;
    end;
    iter1 = iter1 + 1;
end;

asymp_est = zeros(3,4);

for j = 1:4
    asymp_est(1,j) = nansum(MSE(1:iterations,j))/iterations;
    asymp_est(2,j) = count(1,j)/iterations;
    asymp_est(3,j) = (nansum(est_beta(1:iterations,j))/iterations-
beta)/beta;
end;

% END OF PROGRAM: mult_cat ================================================
```